

**FORECASTING THE MATERIAL AND MANUFACTURING COSTS OF LITHIUM-ION BATTERIES
FOR ELECTRIC VEHICLES WITH COMMODITY PRICE FEEDBACK**

Nathan Murray

31st August 2018

Supervised by:

Dr Ajay Gambhir

Oliver Schmidt

James Whiteside

Dr Adam Hawkes

A thesis presented to Imperial College London in partial fulfilment of the requirements for the degree of *Master of Science in Sustainable Energy Futures* and for the *Diploma of Imperial College*

Energy Futures Lab
Imperial College London
SW7 2AZ

List of Abbreviations

ANL	– Argonne National Laboratory
BatPaC	– Battery Performance and cost
BCM	– Battery commodity model
BEV	– Battery Electric Vehicle
BMS	– Battery Management System
BNEF	– Bloomberg New Energy Finance
BOL	– Beginning-of-life
CCS	– Carbon Constrained Scenario
CSG	– Coated Spherical Graphite
CSPV	– Crystalline silicon photovoltaic
DMC	– Dimethyl Carbonate
DoD	– Depth of discharge
DOE	– Department of Energy
DRC	– Democratic Republic of Congo
EC	– Ethylene Carbonate
E-buses	– Electric Buses
EERE	– Energy Efficiency and Renewable Energy
EES	– Electrical energy storage
EOL	– End-of-life
EV	– Electric Vehicle
GHG	– Greenhouse Gas
ICEV	– Internal combustion engine vehicle
IEA	– International Energy Agency
kWh	– Kilowatt-hour
LCE	– Lithium Carbonate Equivalent
LIB	– Lithium-ion batteries
LFP	– Lithium-iron-phosphate
LME	– London Metals Exchange
LMO	– Lithium manganese oxide
LMR	– Lithium and manganese-rich
LR	– Learning rate
LTO	– Lithium-titanate
NCA	– Nickel cobalt aluminium
NMC	– Nickel manganese cobalt
NPS	– New Policies Scenario
PHEV	– Plug-in Hybrid Electric Vehicle
SoC	– State of Charge
TCO	– Total cost of ownership
TWh	– Terra-watt-hour
US	– United States
USGS	– United States Geological Survey
VTO	– Vehicle Technology Office
YoY	– Year over year
WM	– Wood Mackenzie

Abstract

Electric vehicles are an important tool to decarbonise transportation and are expected to grow rapidly over the next decade. The market for battery electric vehicles and plug-in hybrid vehicles doubled in the five years between 2012 to 2017 and may double again in another five. The cost of the lithium-ion batteries that are critical for these vehicles has fallen by 70% over the same five-year period, improving their affordability and putting them in closer reach of the mass-market. The supply chain of metals that are crucial for commercial lithium-ion batteries will be similarly affected by accelerating demand in electric vehicles.

This thesis studies the supply and cost of commodities that make up the functional material in lithium-ion batteries. Commercial battery cells commonly use lithium, nickel, cobalt, and graphite. If high levels of electric vehicle demand occur, the supply for elements such as lithium and cobalt will primarily be supplied for lithium-ion batteries. Despite predictions of lower costs of lithium-ion battery technology through innovation and learning, commodity prices for these metals may not be relied upon to hold firm.

Scenarios of electric vehicle demand are used to estimate battery demand in terms of energy capacity and feedstock mass informed by technological modelling. Projections for the markets of lithium, cobalt, and nickel are analysed with thesis co-supervisor Wood Mackenzie, an energy research consultancy based in London. Wood Mackenzie's metals and mining team publishes a battery raw material service as well as intelligence in specific commodity markets. Through collaboration on this thesis, long-term incentive prices for critical elements are forecast.

An experience curve model is used to inform future cost improvements in lithium-ion batteries based on previous prices and projected manufactured capacity by scenario. The experience curves are calculated by isolating the commodity cost from the value-added cost and projecting industrial learning only on the value-added cost. This way, commodity price forecasts can act as a floor on the cost of a lithium-ion battery.

This thesis finds that neither lithium, nickel, nor cobalt appears to be a showstopper for lithium-ion batteries, but also that a significant increase in production will need to occur over the next decade. The experience curve analysis suggests that higher commodity prices could offset any acceleration in battery cost reductions. Therefore, this thesis finds that an analysis of the growth of EVs should consider fluctuations in the price of commodities.

Acknowledgements

I would like to dedicate this thesis to my beautiful and brilliant wife, Alice. Thank you for supporting my transition from the working world to that of a mature student. I am incredibly proud of your accomplishments, and I look forward to the rest of our life together.

I would also like to dedicate this thesis to my advisors: Ajay, Oliver, James, and Adam. It has been a pleasure researching battery technology and mineral pricing with you. I hope that we can work together again in the future.

Table of Contents

LIST OF ABBREVIATIONS	2
ABSTRACT	3
ACKNOWLEDGEMENTS	4
TABLE OF CONTENTS	5
LIST OF FIGURES	8
LIST OF TABLES	10
1. INTRODUCTION	11
1.1 THE IMPORTANCE OF ELECTRIC VEHICLES ON THE CLIMATE	11
1.2 GROWING DEMAND FOR ELECTRIC VEHICLES	13
1.3 OVERVIEW ON EV COSTS	15
1.4 SUPPLY CHAIN CONCERNS FOR EVS	16
1.5 PROJECT JUSTIFICATION	18
2. REVIEW ON EV TECHNOLOGY AND LITHIUM-ION BATTERIES	20
2.1 CATEGORIES OF EVS	20
2.2 COSTS FOR EV BATTERIES	21
2.3 LITHIUM-ION BATTERY PRINCIPLES	22
2.4 LIB CHEMISTRY DETAILS AND SHORT-TERM DEVELOPMENTS	24
2.4.1 CATHODE	24
2.4.2 ANODE	25
2.4.3 ELECTROLYTE & SEPARATOR	27
3. EV BATTERY DEMAND FORECASTS TO 2030 (PHASE I)	28
3.1 EV MARKET PROJECTIONS FROM THE IEA	28
3.2 COMPARISON TO NON-IEA SCENARIOS (BNEF, 2018)	31

3.2.1	WOOD MACKENZIE	31
3.2.2	BLOOMBERG NEW ENERGY FINANCE	32
3.2.3	OTHER EV FORECASTS	33
3.3	DEMAND BY APPLICATION (BEV OR PHEV)	34
3.4	DEMAND BY CHEMISTRY	36
3.4.1	LITHIUM MANGANESE OXIDE (LMO)	37
3.4.2	LITHIUM-IRON-PHOSPHATE (LFP)	38
3.4.3	NICKEL MANGANESE COBALT (NMC)	39
3.4.4	NICKEL COBALT ALUMINIUM (NCA)	40
3.5	THESIS DEMAND SCENARIOS	40
3.6	ELECTRIC BUSES	42
4.	<u>THE BATTERY COMMODITY MODEL (PHASE II)</u>	43
4.1	BOTTOM-UP COST MODELLING OVERVIEW	43
4.2	THE BATPAC MODEL	43
4.3	THE BATTERY COMMODITY MODEL	44
4.4	FORECASTING LIB COMMODITY DEMAND	47
4.5	LIB MATERIAL FORECASTS BY COMMODITY	51
5.	<u>SUPPLY AND DEMAND FOR LIB MATERIALS (PHASE III)</u>	53
5.1	COMMODITY REVIEW	53
5.1.1	LITHIUM	53
5.1.2	COBALT	55
5.1.3	GRAPHITE	56
5.1.4	NICKEL	57
5.2	LIB CELL COMMODITY COSTS BY CHEMISTRY	58
5.3	SUPPLY-DEMAND BALANCE FOR LIB MATERIALS	59
5.3.1	LITHIUM	61
5.3.2	NICKEL	62
5.3.3	COBALT	63
5.4	LIB COMMODITY PRICE FORECASTS BY SCENARIOS	64
6.	<u>LIB COST FORECASTING WITH COMMODITY PRICE FLOORS (PHASE IV)</u>	66

6.1	FORECASTING WITH EXPERIENCE	66
6.2	LEARNING RATES APPLIED TO LIBS	67
6.3	RE-CALCULATING EXPERIENCE CURVES	69
6.4	COMPARING EXPERIENCE COST FORECASTS FOR DIFFERENT SCENARIOS	72
7.	DISCUSSION	74
7.1	RESULTS OF THE THESIS	74
7.2	LESSONS FROM THE POLYSILICON SHORTAGE	76
8.	CONCLUSIONS	79
	APPENDIX I: GLOBAL EV SALES IN 2017	80
	APPENDIX II: EV BATTERY DEMAND BY SCENARIO	81
	APPENDIX III: EV LIB CATHODE MARKET SHARE ASSUMPTIONS	82
	APPENDIX IV: EV LIB COMMODITY PRICE FORECASTS BY SCENARIO	83
	APPENDIX V: LIB COST FORECAST BY SCENARIO	84
	REFERENCES	85

List of Figures

Figure 1.1 Global sales of BEV and PHEVs (EV-Sales, 2018, IEA, 2018)	14
Figure 1.2 EV sales "base case" forecasts for 2018 to 2025 from consultancy and bank analysts (BMO, 2018, BNEF, 2018, Deutsche Bank, 2016, IEA, 2018, McKinsey, 2017, UBS, 2017, Wood Mackenzie, 2017a)	15
Figure 1.3 Chevy Bolt electric powertrain cost estimates in USD. Source: (UBS, 2017)	16
Figure 1.4 Element intensity of common LIB active materials (C, Ni, Co, Mn, Li, and Al) in kg/kWh. "Other" represents mostly oxygen as well as carbon and binder in the NMC/NCA and phosphorus and iron in LFP. Each cathode is paired with a graphite anode.	18
Figure 2.1 Charge and discharge of a Lithium Cobalt Oxide / Graphite cell demonstrating lithium intercalation between the anode, electrolyte, and cathode. Reprinted from: Thackeray, Wolverton, and Isaacs (2012). Copyright 2012.	23
Figure 3.1 IEA EV Forecast Comparison (IEA, 2018)	29
Figure 3.2 Comparison of Paris paths and NPS to 2030 - Stock View	30
Figure 3.3 Comparison of Paris paths and NPS to 2030 - Market View	30
Figure 3.4 Wood Mackenzie EV comparison to IEA inspired thesis scenarios	31
Figure 3.5 Comparison of thesis and BNEF EV scenarios (BNEF, 2018)	32
Figure 3.6 EV sales "base case" forecasts for 2018 to 2025 from consultancy and bank analysts (BMO, 2018, BNEF, 2018, Deutsche Bank, 2016, IEA, 2018, McKinsey, 2017, UBS, 2017, Wood Mackenzie, 2017a)	34
Figure 3.7 Energy Density for Commercial Cathode Chemistries (Nitta et al., 2015, Schmuch et al., 2018)	37
Figure 3.8 Comparison of PHEV and BEV battery chemistry market share of vehicles sold from 2016-2018. Source: (EV-Sales, 2018, EV-Volumes.com, 2018, watter2buy.com, 2018) & manufacturer reports	37
Figure 3.9 Consensus on cathode chemistry characteristics from independent reviews. (BCG, 2010, Cluzel & Douglas, 2012, IRENA, 2017, McKinsey, 2017, O'Donovan, 2017, Perner & Vetter, 2015)	38
Figure 3.10 The relationship between NMC discharge capacity and thermal stability with nickel intensity. Reprinted from Noh et al. (2013). Copyright 2013.	39
Figure 3.11 Forecasted battery demand across the NPS, "2022 Action" and "Early Action" scenarios	41
Figure 4.1 Process to determine the quantity of active material necessary in a LIB	46
Figure 4.2 Early Action EV Sales split by application from 2018 -2030. BEV share slowly increases to 70%	47
Figure 4.3 Early Action EV battery demand (GWh) by application from 2018 – 2030	48
Figure 4.4 "Early Action" scenario EV LIB demand by LIB Chemistry	48
Figure 4.5 NMC Demand by Variant (333, 622, or 811) from 2018 – 2030	49
Figure 4.6 "Early Action" Metal Demand for LIBs 2017-2029 (kTons)	50
Figure 4.7 Early Action Change in EV Metal Demand 2017-2029	50
Figure 4.8 change in LCE Demand from 2017 to 2029	51
Figure 4.9 Change in nickel demand from 2017 - 2029	51
Figure 4.10 Change in cobalt demand from 2017 – 2029	52
Figure 4.11 Change in graphite demand from 2017 - 2029	52

Figure 5.1 LIB Commodity prices in USD per kg from 2008 to 2018 (Bloomberg, 2018)	53
Figure 5.2 Comparison of nickel sulfate and nickel metal spot prices from the LME (Bloomberg, 2018)	58
Figure 5.3 Commodity costs for NMC cathode chemistries from 2008 to 2018 (Bloomberg, 2018)	59
Figure 5.4 Theoretical incentive price curve (Speirs et al., 2014)	60
Figure 5.5 Lithium supply-demand balance from 2017 to 2030 (Wood Mackenzie, 2018a)	61
Figure 5.6 LCE long-term incentive prices (Wood Mackenzie, 2018a)	61
Figure 5.7 Nickel supply-demand balance from 2018 – 2030 (Wood Mackenzie, 2018a)	62
Figure 5.8 Long-term Ni incentive prices (Wood Mackenzie, 2018a)	63
Figure 5.9 Cobalt supply-demand balance from 2018 to 2030 (Wood Mackenzie, 2018a)	64
Figure 5.10 Long-term cobalt incentive prices (Wood Mackenzie, 2018a)	64
Figure 5.11 LIB commodity price forecasts through the Base, Base Plus, and Early Action scenarios	65
Figure 6.1 Log experience curve of LIB prices out to 2030. Source: (Frith, 2017)	68
Figure 6.2 Historical LIB commodity price index (\$/kWh) (Bloomberg, 2018)	68
Figure 6.3 Commodity and Value-Add Components for Lithium-Ion Batteries. Source: (Frith, 2017)	69
Figure 6.4 LIB experience curve modelled with a best-fit method across two endpoints and by considering the entire pack price	71
Figure 6.5 “Base Plus” scenario yearly LIB pack price calculated by the least-squares commodity floor method compared with the share of pack price for commodities.	71
Figure 6.6 LIB "Value-Add" price forecast compared by scenario from 2018 to 2030	72
Figure 6.7 Total LIB pack price forecast by scenario with commodity price feedback from 2018 to 2030 using the least-squares method	73
Figure 6.8 Total LIB pack price forecast by scenario with commodity price feedback from 2018 to 2030 using the endpoint method	73
Figure 7.1 Comparison of comparable EV and ICEV powertrain costs in 2017 and 2030 (BofAML, 2017, UBS, 2017)	75
Figure 7.2 CSPV cost improvement by cumulative production projected versus actual 1979 to 2010. Reprinted from Swanson (2011)	77

List of Tables

Table 1.1 Well-to-wheel emissions savings of BEV vs gasoline ICE in France, China, and Europe for 2015 and 2030 (IEA, 2017)	12
Table 1.2 Comparison of LIB elements by global production, reserves, and depletion ratio (USGS, 2018). Share of 2017 EV market demand from own calculations assuming one year of demand lag.	17
Table 2.1 Comparison of Electric Vehicle Segments	20
Table 2.2 Comparison of NMC-333 and LMO cathode chemistries (Nelson et al., 2012)	24
Table 3.1 Comparison of BNEF and NPS 2030 EV battery demand (BNEF, 2018)	33
Table 3.2 Global Sales for top 10 BEV models ranked by battery demand. Source: (EV-Sales, 2018, EV-Volumes.com, 2018, watev2buy.com, 2018) and manufacturer reports.	35
Table 3.3 Global sales for top 10 PHEV models ranked by battery demand. Source: (EV-Sales, 2018, EV-Volumes.com, 2018, watev2buy.com, 2018) and manufacturer reports.	36
Table 3.4 Average battery size for BEV and PHEV vehicles. Source: (EV-Sales, 2018, EV-Volumes.com, 2018, watev2buy.com, 2018) and manufacturer reports.	36
Table 4.1 Cathode Chemistry properties. OCV and Current Capacity from Nelson et al. (2012)	45
Table 4.2 Comparison of anode chemistry properties (Dash & Pannala, 2016, Nelson et al., 2012)	45
Table 4.3 Material Intensity by commercial cathode/anode combinations	49
Table 5.1 Lithium reserves by the top 4 countries in terms of production (USGS, 2018)	54
Table 5.2 Cobalt production, resources, and reserves (USGS, 2018)	55
Table 5.3 Bloomberg commodity tickers and metal intensity for battery cell commodity cost analysis.	59
Table 6.1 Calculated learning rates for LIB pack prices using a whole pack and commodity floor methods	70
Table 6.2 Calculated R-squared fit of LIB pack learning rates of whole pack and commodity floor methods	70
Table 7.1 ICEV and EV fuel cost comparison (BofAML, 2017, UBS, 2017)	76

1. Introduction

As demand for electric vehicles (EVs) grow, two significant trends become clear. First, as an emerging technology, EVs become less expensive as economies of scale develop and industrial learning diffuses. Second, as demand for lithium-ion batteries grows, so do the markets for the metal elements that form lithium-ion batteries. While decreasing EV costs accelerate EV demand, their cost reduction may be limited by bottlenecks in the material supply chain. Studying the relationship between EV demand and the price of primary metals that compose lithium-ion batteries are essential to studying the question: “When will electric vehicles become cost competitive with internal combustion engine vehicles?”

Section 1.2 reviews the historical evidence for demand in EVs. Section 1.1 describes the greenhouse gas (GHG) benefits of EV technology. Concerns about the supply of valuable metal commodities necessary to enable high growth EV forecasts are summarised in section 1.2. Finally, this introduction concludes with a justification of the work proposed for the research of this masters’ thesis.

1.1 The Importance of Electric Vehicles on the Climate

The Paris Agreement defined an internationally agreed pathway to limiting global average temperature rise to 2° above pre-industrial levels (UNFCCC, 2015). To reach this goal, broad sectors such as energy production, transportation, agriculture, industry and buildings should move toward deep decarbonisation. In 2010, transportation contributed 14% to annual anthropogenic GHG emissions, of which 72% is attributed to road transportation (IPCC, 2014). The global warming impact arising from transportation can be abstractly summarised as follows:

$$Impact = Activity * \frac{Energy}{Activity} * \frac{Emissions}{Energy} * \frac{Damage}{Emissions}$$

Equation 1.1: Components that influence the environmental impact of transportation. (Stettler, 2018)

Equation 1.1 details four main levers to minimising the impact of transportation. The variables can be applied to climate change as follows:

Activity: The quantity of transportation (e.g. km travelled via road transport methods)

Energy/Activity: The amount of energy required to complete the activity.

Emissions/Energy: The by-product of vehicle energy consumption (e.g. CO₂ or NOX)

Damage/Emissions: The global warming potential, or health consequences of emissions.

A promising tool to mitigate GHG emissions in the transportation sector is the electrification of road transportation. While EVs release no emissions during operation (including greenhouse and noxious gases), the electricity supplied to charge their batteries is commonly produced from power stations which burn fossil fuels and vent most of the resulting gases into the atmosphere, although not at the point of use.

EVs primarily act on the **Energy/Activity** and **Emissions/Energy** variables by converting electrical energy very efficiently and preventing local emissions (Equation 1.1). Traditional internal combustion engine vehicles (ICEVs) only transfer ~25% of the energy they burn into useful motion while EVs powered by electric motors are ~75% efficient (Helms, Kämper & Lambrecht, 2015). A complete well-to-wheel energy efficiency analysis should also compare the energy efficiency of extracting and refining fossil fuels to the generation of electricity.

Economies with plentiful low-carbon electricity generation, such as nuclear-powered France, will show a significant GHG reduction from the use of EVs, but countries where electricity is generated from high-carbon sources, such as China, will not (IEA, 2017). The IEA notes that as electricity generation continues to decarbonise through to 2030, the relative savings in switching to EVs grow even despite improvements in ICEV engine efficiency. The data in Table 1.1 considers improvements to electricity generation in a base-case reference technology scenario (RTS) which considers technologies that are likely to commercialise without the impetus from a climate-constrained beyond two degrees scenario (B2DS).

	France 2015	France 2030	China 2015	China 2030	Europe 2015	Europe 2030
Absolute CO₂ savings (gCO₂/km)	151	105	17	15	99	75
Relative CO₂ savings (%)	88.32%	90.40%	6.79%	9.44%	57.94%	66.43%

Table 1.1 Well-to-wheel emissions savings of BEV vs gasoline ICE in France, China, and Europe for 2015 and 2030 (IEA, 2017)

Ford showed in a lifecycle analysis that EVs currently accrue a carbon debt of around 2 tonnes of CO₂-eq during the manufacturing stage when compared to an equivalent ICEV (or around 140 kg-CO₂/kWh-battery-capacity) (Kim et al., 2016). The batteries for plug-in hybrid electric vehicles (PHEVs) are smaller than battery electric vehicles (BEVs) and hence undertake smaller carbon debts. A study by the Fraunhofer Institute and KIT used real driving data from PHEVs and BEVs to compare their relative CO₂ impacts and found that while PHEVs showed positive climate impacts in less than four years, BEVs only show a positive GHG impact versus ICEVs after seven years (Plötz et al., 2017). The effect of vehicle life on climate impacts suggests that fleet longevity is just as essential a metric as energy-efficiency.

If EVs are incautiously used as a tool against climate change, there can still be risks. For example, drivers may prefer to travel more if the marginal cost of travel is reduced such as is the case with low-cost electricity versus petrol or diesel. Therefore, if the electrification of light-duty vehicles leads to increased travel, there is a possibility that overall energy use would increase despite the higher efficiency of EVs (US EIA, 2018).

EVs provide societal benefits beyond the reduction in GHG emissions. No local road emissions also mean that EVs contribute less to urban smog and dangerous nitrous oxide emissions. However, in the pursuit of minimising GHG emissions after the signing of the Kyoto protocol in the nineties, Europe promoted diesel technology while the US and Japan promoted hybrids (Vidal, 2015). While diesel vehicles reduce GHG emissions, they also contribute more to nitrous oxide emissions than their gasoline counterparts. Due to the aftermath of the “Dieselgate” scandal, where automakers were found to have deceived regulators and the public on the severity of the emissions from their diesel vehicles, cities such as Paris have announced plans to ban ICEV vehicles from the year 2030 (Zimmermann, 2018).

1.2 Growing Demand for Electric Vehicles

Since 2010, global sales of plug-in electric vehicles expanded from seven thousand to over one million vehicles per year in 2017, as shown in Figure 1.1 (IEA, 2018). Plug-in electric vehicles include plug-in hybrid electric vehicles (PHEVs) and battery electric vehicles (BEVs) which can both be recharged from electricity at a wall socket or faster electric charging stations. However, the category of plug-in electric vehicles excludes hybrid electric vehicles which cannot be charged from an electric power source and rely upon liquid gasoline or diesel for fuel. Although hybrid electric vehicles and plug-in electric vehicles both use high-capacity

batteries which internal combustion vehicles do not, the batteries for plug-in vehicles tend to be much larger. An in-depth review of EV technology is discussed in Chapter 2.

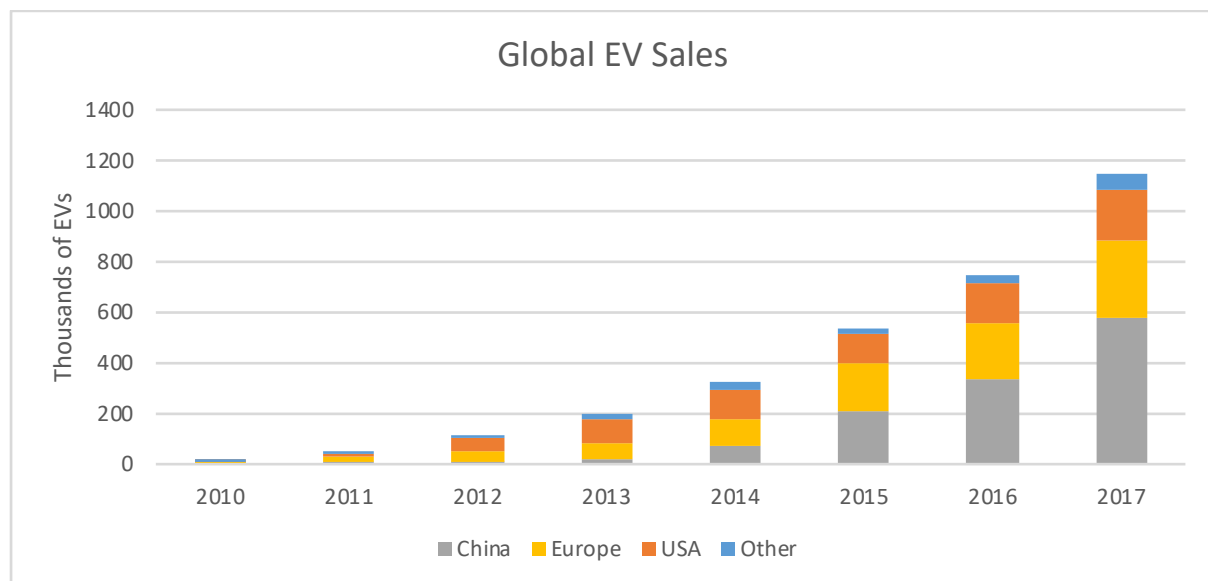


Figure 1.1 Global sales of BEV and PHEVs (EV-Sales, 2018, IEA, 2018)

Most EVs are currently sold in China, Europe or the USA. While the USA and Europe purchased more than 80% of the EVs before 2014, China has since rapidly acted to stimulate domestic EV sales and manufacturing. In 2017, every second EV was sold in China.

Three factors can explain the sharp growth in the EV market. First, government policies in the US and China reduce the cost of purchasing an EV through direct subsidy or income tax credit. Second, EVs are generally more energy efficient and produce less local gaseous as well as acoustic emissions than ICEVs. Simpler electric motors do not require oil changes, and EVs generally contain fewer moving parts than their ICEV counterparts which lead to more reliable operation. Third, EV manufacturers such as Tesla have seized upon a strategy which not only promotes their EVs as an economical alternative to reduce fuel costs but highlight features which provide a more pleasurable and high-tech driving experience than alternative options. Seizing upon the opportunity to develop a new car drivetrain from scratch, Tesla promotes features such as semi-autonomous driving and a simplified computer human-machine interface to sell to customers as an additional benefit to fully-electrified transportation.

A survey of various intergovernmental organisations such as the IEA and energy-focused consultancies such as Wood Mackenzie and Bloomberg New Energy Finance projects a consensus for accelerating growth in the market for PHEVs (Figure 1.2). The most

conservative forecast considered in the selection of reports predicts a market growth of 900,000 EVs in 2025, a change in market demand larger than the entire EV market in 2016.

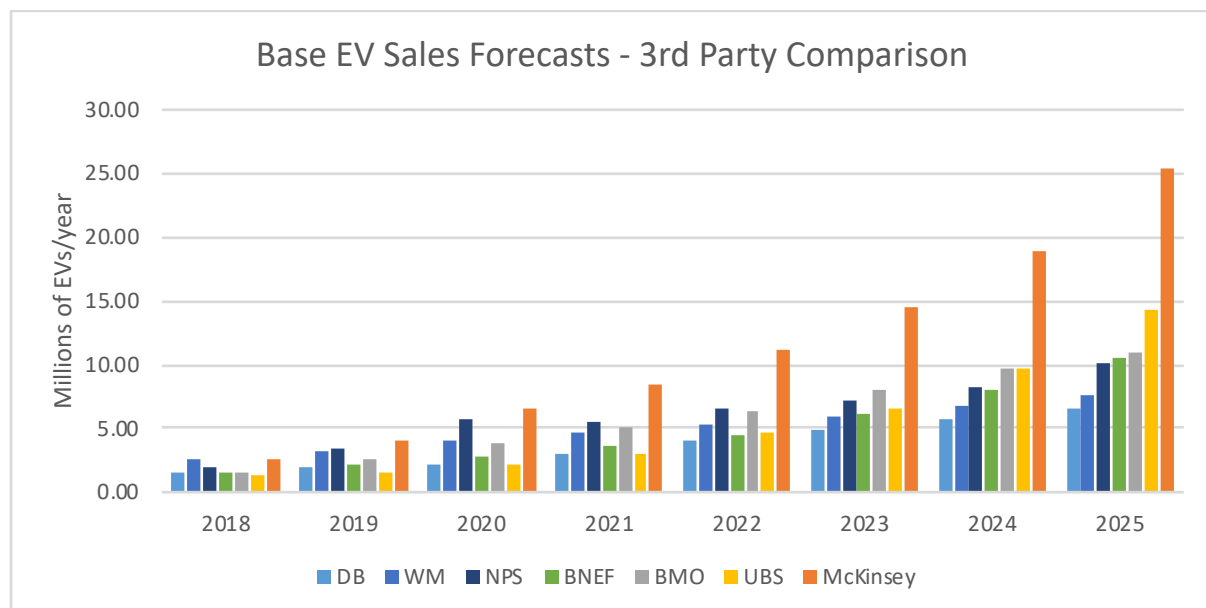


Figure 1.2 EV sales "base case" forecasts for 2018 to 2025 from consultancy and bank analysts (BMO, 2018, BNEF, 2018, Deutsche Bank, 2016, IEA, 2018, McKinsey, 2017, UBS, 2017, Wood Mackenzie, 2017a)

1.3 Overview on EV Costs

The primary difference between an ICEV and an EV is the lack of combustion engine, exhaust and fuel system in an EV. Instead, an EV is propelled by an electric motor which uses a LIB as a mobile store of electrical energy. The complete LIB pack contains battery cells, a battery management system, housing, and wiring.

A vehicle teardown by Munro associates in Figure 1.3 found that the Chevy Bolt's battery assumed three-quarters of the cost of the entire EV powertrain (UBS, 2017). Over half of the powertrain's cost was the lithium-ion cells. UBS (2017) also compared the cost of a comparable VW Golf ICEV and found that the Bolt's powertrain costs (excluding the battery pack) were 16% less than the Golf's.

Over the next decade costs for EVs and ICEVs will likely diverge. Stricter emissions standards for ICEVs will probably mean that powertrain costs will rise in Europe and the US (BofAML, 2017). Petrol powertrains may rise by 3% per year adding 30% to their cost by 2030. Meanwhile, LIB prices have fallen rapidly from 1,000 \$/kWh in 2010 to just over 200 \$/kWh in 2017 (Frith, 2017), and are expected to decline further over the next decade with

consultancies such as Bloomberg New Energy Finance predicting battery cross \$100/kWh by 2026. In the Chevy Bolt example, a battery pack price of 100\$/kWh would suggest a reduction in vehicle production cost of 6,000 USD for a vehicle that currently sells for 36,600 USD.

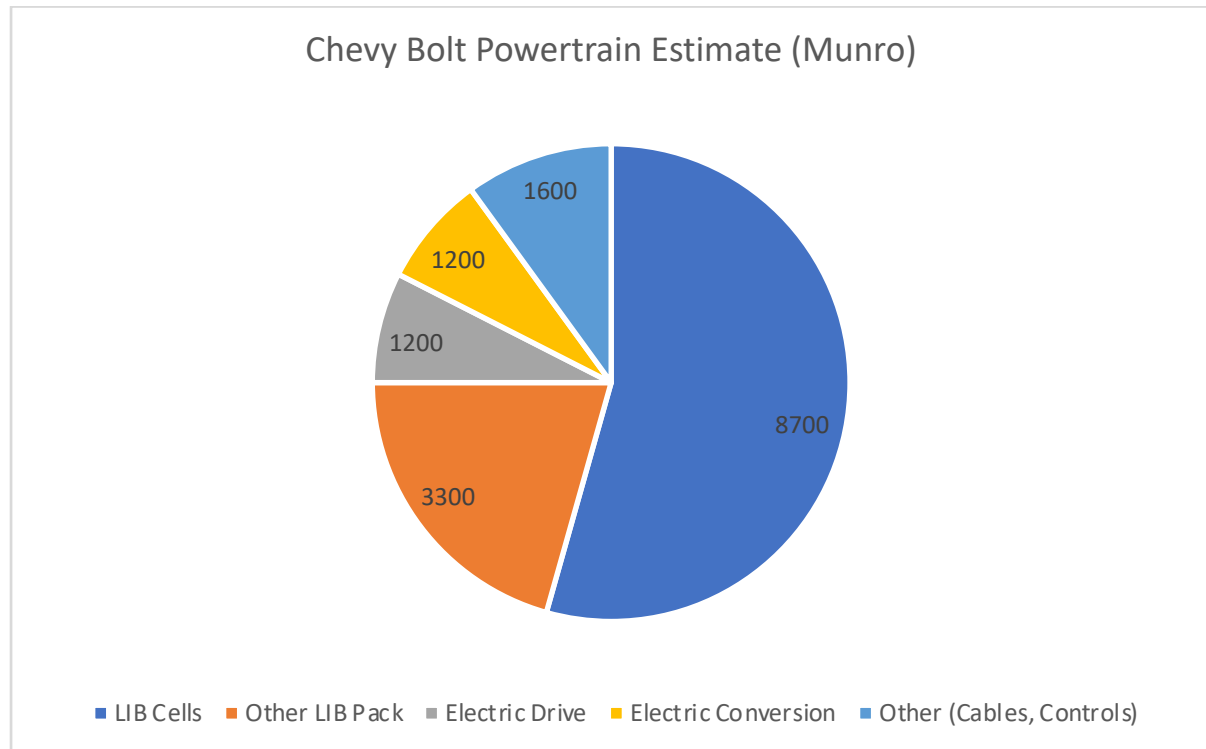


Figure 1.3 Chevy Bolt electric powertrain cost estimates in USD. Source: (UBS, 2017)

1.4 Supply Chain Concerns for EVs

Section 1.2 demonstrated that electric vehicle manufacturing is expected to grow five to twenty-five times 2017 levels by 2025. Fast growth in LIB manufacturing assumes that demand for materials required for LIB production grows by the same amount and that the supply is available to satisfy demand. If future material supply lags demand, then prices could theoretically rise until they incentivise new production. A primary goal of this thesis is to understand better whether such price rises or supply bottlenecks could be significant or likely.

Nickel, cobalt, manganese, lithium, and carbon (graphite) are typically found in LIB active materials, especially the materials which are focused on in this thesis (NMC, NCA, and LFP) (Figure 1.4). Magnesium, lithium, cobalt and graphite are elements which demonstrate high production concentration of over 60% supplied by just three countries each (Olivetti et al., 2017). Global production statistics from the United States Geological Survey (USGS) suggest

that while LIBs contain mostly carbon and nickel by weight, nickel is the element with the lowest depletion ratio, which is measured by global reserves normalised by annual production.

Element	Annual Production (ktons)	Global Reserves (ktons)	Depletion Ratio (years)	% Demand by EVs
Nickel	2,100	74,000	35	~ 1%
Cobalt	110	7,100	65	~ 10 %
Manganese	16,000	680,000	43	< 0.1%
Lithium	43	16,000	372	~ 15%
Graphite (Carbon)	1,200	270,000	225	~ 5 %

Table 1.2 Comparison of LIB elements by global production, reserves, and depletion ratio (USGS, 2018). Share of 2017 EV market demand from own calculations assuming one year of demand lag.

Lithium is already heavily linked to EV demand growth, with around 15% of 2017 supply already consumed by demand from EVs. However, lithium has the most extended depletion ratio of the elements studied since it is under-utilised compared to known reserves.

Cobalt is also heavily linked to the EV market but has a much smaller depletion ratio than lithium. Therefore, cobalt’s depletion ratio could be heavily impacted by rapid growth in the EV market. Cobalt also experienced high price volatility in 2017-2018, and many manufacturers are searching for methods and materials to omit the expensive metal (King, 2018).

Manganese is the most abundant LIB commodity by production weight and has a low depletion ratio but does not show much impact from the EV market. As LIB cathodes progress towards high nickel NMC varieties (Figure 1.4), manganese will play an ever-decreasing role in the share of LIB cathodes.

Nickel is second most abundantly mined commodity for LIB cathodes, and currently shows a relatively small demand by the EV sector. However, nickel has the smallest depletion ratio (35 years) and will assume growing importance in LIB active materials as the industry shifts toward energy-dense high-nickel cathode chemistries such as NCA or NMC-811.

Natural Graphite is carbon that has been formed under the earth with high pressures to create highly ordered structures. While is ubiquitous in LIBs as the sole component of the anode material, natural graphite can be substituted with higher-quality **synthetic graphite**.

Synthetic graphite can be created by heating petroleum coke and coal-tar pitch above 2000°C (Jäger et al., 2012).

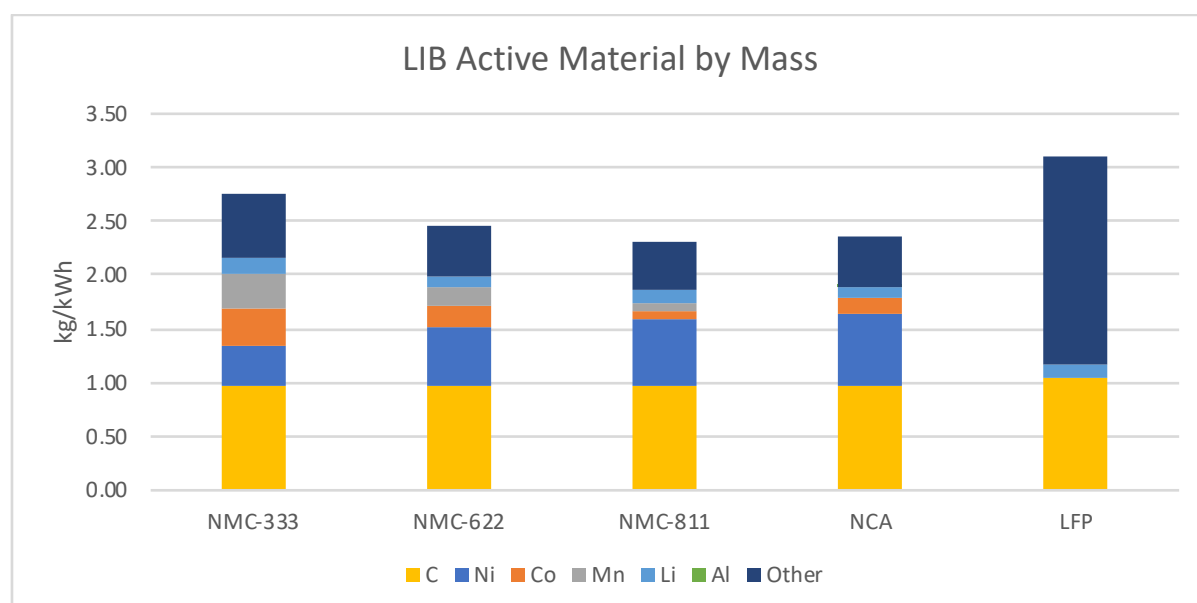


Figure 1.4 Element intensity of common LIB active materials (C, Ni, Co, Mn, Li, and Al) in kg/kWh. “Other” represents mostly oxygen as well as carbon and binder in the NMC/NCA and phosphorus and iron in LFP. Each cathode is paired with a graphite anode.

The trends that describe the metal intensity for each of the LIB chemistries in Figure 1.4 are explored in Chapter 4. Graphite has the highest intensity because the LIB anode is typically composed of carbon. However, silicon could enable the reduced use of graphite in the future. Nickel will show an increasing intensity over time as battery manufacturers prefer energy-dense NMC-811 and NCA chemistries to build large-capacity batteries for light-duty vehicles. Cobalt shows an inverse relationship to nickel because nickel is being designed to substitute for cobalt in the LIB cathode. Lithium is an invariable in LIB designs and will show reduced intensity as chemistry technologies improve and become more energy-dense.

1.5 Project Justification

The mass uptake of EVs is a vital pathway to decarbonise transportation. EVs are relatively more energy efficient and lead to less lifecycle GHG emissions than ICEVs. Ignoring the effects of transportation demand modulation by urbanisation, globalisation, and autonomous driving, the complete electrification of the existing global road transportation system will most likely occur if: (1) there are enough materials to manufacture vehicles to replace the existing fleet and; (2) the cost associated with mining these materials and manufacturing EVs is economical compared with maintaining or purchasing ICEVs. A literature review conducted in

the initial stages of this thesis identified that there is a lack of bottom-up cost analyses regarding commodity feedback effects for LIBs.

This thesis project has been completed in the following phases.

Phase I: This phase develops scenarios for EV adoption out to 2030. These scenarios give projections on EV adoption by battery chemistry and quantity (in kWh).

Phase II: Developing and applying a bottom-up cost model called the Battery Commodity Model (BCM). It will be based on the BatPaC model developed by Argonne National Lab. The goals of this model will be to (a) simplify BatPaC; (b) explicitly model cathode cost; (c) expand temporal effects (2020-2030) (d) expand model for detailed commodity price input (e) informs material inputs in kg/kWh terms for popular LIB chemistries.

The expanded model will apply the EV scenarios to project manufacturing cost by applying learning rates on EV battery quantity. It will also apply battery chemistry and quantity to project annual demand for battery commodities such as lithium, cobalt, nickel, and graphite.

Phase III: The results of the detailed battery demand scenarios for commodities are supplemented by Wood Mackenzie's knowledge of dynamic mineral commodity supply curves. Projections for incremental EV metal demand will be compared with future supply to determine long-term forecasts for relevant LIB commodity prices.

Phase VI: Experience curves are used as a tool to approximate the cost reductions in lithium-ion batteries as a function of cumulative capacity. Historical and projected commodity prices are then considered as a cost floor to calculate appropriate learning rates on the non-commodity portion of LIB pack prices.

This thesis will assess the majority of battery chemistries that are likely to dominate EV supply chains until 2030. While there are a variety of chemistries that have already been applied for Electric Vehicles (Cathodes: LCO, LMO, NMC, NCA, LFP; Anodes: Graphite, LTO) and which are possible candidates for Advanced-LI and Beyond-LI Batteries (HE-NMC, Si alloy anodes, Solid-State Lithium-Ion and Lithium-Air), this thesis will focus on those that have been selected for mass production by automakers in large-scale operations.

2. Review on EV Technology and Lithium-Ion Batteries

This chapter reviews the technical background for EV LIBs starting with an overview of the technology in different EVs in section 2.1. Next, cost forecasts for EVs are reviewed in section 2.2 with a particular analysis on a levelised cost per kilowatt-hour which can help EVs become cost competitive with ICEVs. Section 2.3 describes the fundamental working principles of a LIB and categorises popular active materials. Section 2.4 analyses the sub-components of a LIB cell and describes near-term improvements that can increase LIB performance or lead to greater cost-competitiveness.

2.1 Categories of EVs

EVs are distinguished into two main categories. Plug-in hybrid electric vehicles (PHEVs) have internal combustion engines that run a generator when the battery runs low. These vehicles have the option to refuel with both electricity and liquid fuels which can be advantageous when trying to refuel quickly over long trips. The other more popular option is the battery electric vehicle (BEV) which solely supports electric charging. BEVs generally offer larger batteries than PHEVs.

	Battery Electric Vehicle (BEV)	Plug-In Hybrid Electric Vehicle (PHEV)	Hybrid Electric Vehicle (HEV)
Electric Motor	○	○	○
Combustion Engine	✗	○	○
Battery Size (kWh)	20 – 100	10 – 20	< 6
Battery Technology	Lithium-Ion	Lithium-Ion	Nickel Metal Hydride or Lithium-Ion
Plug	○	○	✗
Example	Nissan Leaf	Chevy Volt	Toyota Prius

Table 2.1 Comparison of Electric Vehicle Segments

2.2 Costs for EV Batteries

Cost is currently a barrier to the mass uptake of EVs. BNEF (2017) has determined that a BEV in the medium segment is currently \$10,000 more expensive than a comparable ICEV and nearly all of the cost difference can be explained by the cost of the battery. The total cost of ownership (TCO) of an EV is lower than for comparable ICEVs in Europe due to the high gap between petrol and electricity costs as well as reduced maintenance costs. A teardown by UBS found that the Chevy EV had 24 moving parts in its powertrain versus 149 in the comparable VW Golf (UBS, 2017). However, further cost reductions are necessary for TCO parity to be reached in regions with cheap petrol and diesel prices such as the United States (UBS, 2017).

LIB costs can be described in different contexts. It is common to normalise the total cost of a LIB to its capacity (i.e. USD/kWh). However, it is essential to clarify whether total LIB capacity or usable LIB capacity is referenced. Many vehicle manufacturers will advertise the usable capacity of an EV battery since that is the most relevant specification for the consumer.

It is uncommon to discharge a LIB to its real physical energy capacity since a full discharge can negatively affect future capacity retention. A battery's lifetime is an essential trait in applying them to transportation since vehicles are designed to be used for eight years or longer. BatPaC, a bottom-up cost model for LIBs referenced later in this thesis, utilises a depth-of-discharge (DoD) ratio for BEVs, defined by the ratio of the usable capacity by the total capacity, of 85% (Nelson et al., 2012).

The U.S. Department of Energy (DOE) has criticised nontechnical media for occasionally confusing the LIB costs for the cell level and pack level (US DOE, 2017). The battery cell is the smallest subcomponent of a LIB pack and contains the electrodes, active materials, and electrolyte. The battery pack contains a set of cells connected to a battery management system (BMS), physical housing, and thermal management system. Therefore, pack level costs will always be higher than cell level costs.

Nykvist & Nilsson (2015) published a highly cited review of LIB costs in *Nature Climate Change* which considered \$150/kWh to be the target for EVs to be competitive with ICEVs. To support this target, Nykvist & Nilsson cite a study by a US DOE study from 2000 (Gaines & Cuenca, 2000). However, a recent review from the US National Renewable Energy Lab (NREL) considers the target of \$150 a poorly documented artefact from the US Advanced

Batteries Consortium's goals from the early 90s (Neubauer, 2013). The target preferred by private analysts and NREL is \$100/kWh on the pack level (BMO, 2018, Frith, 2017, McKinsey, 2017, Neubauer et al., 2014).

A key finding from the review by Nykvist & Nilsson is that costs for LIBs are falling at a faster rate than many peer-reviewed academics and analysts have anticipated. They highlight that since 2012, peer-reviewed academic literature has underestimated battery prices while even the most optimistic forecast (published by McKinsey) predicted \$200/kWh by 2020 (Nykvist & Nilsson, 2015). Recent reviews by UBS (2017) and BNEF (2017) have reported prices of 205-209 \$/kWh at the pack level for 2017.

2.3 Lithium-Ion Battery Principles

A LIB has four main components: the anode, cathode, electrolyte, and the circuit (Figure 2.1). The anode is the "negative" end of the battery. "Negative" can either mean it is electron-rich when the battery is charged, or that it is the reference to which voltage potential is measured to the cathode. The cathode is the "positive" end of the battery and contains most of the lithium ions when the battery is discharged. Both the anode and cathode contain active material which holds charge and allows lithium-ion intercalation during the charge and discharge processes.

The active material for the anode is typically graphite, and the active material for the cathode is either a lithium-based phosphate or oxide with a transition metal. The morphology of the active cathode material determines the direction the lithium-ions can move (Yoshino, 2014):

1-Directional: Olivines. Examples: Lithium-Iron-Phosphate (LFP) LiFePO_4 .

2-Directional: Layered Rock Salts. General form: LMO_2 where M is an element such as M=Cobalt in LiCoO_2 or a transition metal alloy as in Nickel-Manganese-Cobalt (NMC) $\text{Li}_{1.05}(\text{Ni}_{0.33}\text{Mn}_{0.33}\text{Co}_{0.33})_{0.95}\text{O}_2$. Other examples are M = Nickel or M = Nickel-Cobalt-Aluminium.

3-Directional: Spinel: Example: Lithium Manganese Oxide (LMO) LiMn_2O_4 .

The active material is bonded to a current collecting metal foil to conduct electrons to the circuit. Typically, aluminium is favoured for its low cost. However, when handling anodes with very low potentials versus lithium (graphite, lithium, silicon), copper is used to prevent lithium from plating on the current collector (Vaalma et al., 2018).

The circuit is a critical component of a LIB because it provides a path for the electrons to flow. Similarly, the electrolyte provides a path for the positive lithium ions to flow as the battery is operated. In LIB designs with a liquid electrolyte, a separator divides the “positive” and “negative” ends of the cell into two half-cells each with separate chemistry and half-cell potential.

The separator is designed to allow positive ions to pass through and block electrons selectively. The separator is critical in ensuring that the electrons flow through the circuit as intended. If electrons conduct internally in the cell between the anode and cathode, a short-circuit can occur which can have dangerous implications if the cell temperature rises above thermally stable levels.

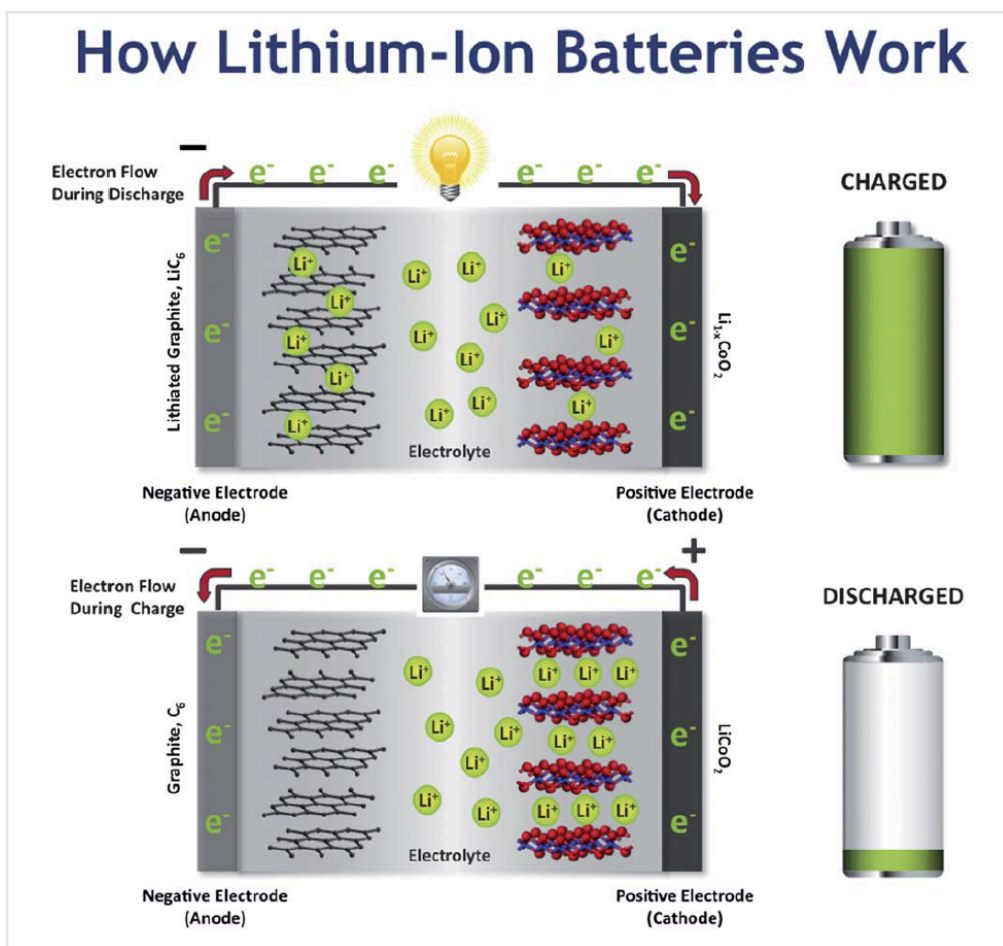


Figure 2.1 Charge and discharge of a Lithium Cobalt Oxide / Graphite cell demonstrating lithium intercalation between the anode, electrolyte, and cathode. Reprinted from: Thackeray, Wolverton, and Isaacs (2012). Copyright 2012.

2.4 LIB Chemistry Details and Short-Term Developments

The purpose of this section is to break out the battery cell into its main sub-components and discuss their design goals and developmental status. Recent trends in LIB technology will be overviewed to give a sense of likely near-term improvements for the cathode, anode, electrolyte and separator.

2.4.1 Cathode

Selecting the proper cathode material can have significant implications for cost and performance of an EV LIB pack. For example, in the case of a selection between NMC and LMO chemistries, NMC has nearly twice the energy density of LMO. Even though NMC includes cobalt, an expensive metal, a LIB would utilise less mass of NMC for the same battery energy despite LMO's lower cost per unit mass and higher open-circuit voltage (Table 2.2 Comparison of NMC-333 and LMO cathode chemistries (Nelson et al., 2012)

). Since a battery with NMC would use less active-material, the general effect is that the pack becomes both lighter and less expensive (Vaalma et al., 2018). This example highlights an acceptable trade-off between energy density and material cost with today's commodity prices.

Characteristic	NMC-333	LMO
Positive active material per cell (g)	364	523
Negative active material per cell (g)	206	184
Voltage 50% SoC (V)	3.67	3.95
Capacity per Cell (Ah)	56	52
Battery Size (kWh)	60	60
# of Cells	290	290

Table 2.2 Comparison of NMC-333 and LMO cathode chemistries (Nelson et al., 2012)

EV manufacturers are starting to favour the layered material NMC for its higher operating voltages, energy density, and lifetime. NMC is being developed to compose of increasing amounts of nickel and decreasing amounts of cobalt. There are two driving forces for this change. First, nickel improves the cathode current carrying capacity which enables more energy-dense batteries that offer more range for the same weight. Second, cobalt is identified as a potentially risky commodity, due to volatile prices and concentrated supply from regions with claims of human rights violations (BMO, 2018).

Aside from improving charge capacity in the active materials, increasing cell voltage is a second route to improving energy density in batteries. To further improve cathode

performance, research is also dedicated to finding a stable high-voltage NMC variant (Howell, 2017). However, high-voltages tend to lead to capacity fade or even electrolyte instability.

A candidate for high discharge capacity cathode material includes lithium and manganese-rich (LMR) NMC with the chemistry $x\text{Li}_2\text{MnO}_3 \cdot (1-x)\text{LiNi}_a\text{Co}_b\text{Mn}_c\text{O}_2$ ($a+b+c = 1$). Layered LMR-NMC is similar to spinel-based LMO in that it contains high quantities of low-cost manganese but differs in that it retains energy-dense characteristics of NMC (Erickson et al., 2017). The technology is currently being developed to avoid a voltage-fade problem which leads to significant energy capacity reduction after cycling (Erickson et al., 2017). LMR-NMC has been used blended with spinel LMO and has been incorporated in early EVs such as the Chevy Volt (Thackeray, Wolverton & Isaacs, 2012).

A second technique to create energy-dense cathode materials is by developing nanoparticles with nickel-rich cores and manganese-rich shells (Schmuck et al., 2018). The advantage of this design would be that unstable capacity contributing materials (nickel) would be buffered from the electrolyte with a shell of stabilising material (manganese). Laboratory experiments suggest that such a particle could have higher capacity and retention characteristics than NCA (Lim et al., 2016), which is a leading material utilised by Panasonic and Tesla.

2.4.2 Anode

With the exception of lithium titanate (LTO) (an expensive but highly cyclable and efficient anode material), graphite is nearly universally applied as an active material for LIB anodes because it is abundant, low-cost, and has a low-lithiation potential versus lithium which allows for greater cell voltage potentials (Nitta et al., 2015). The portable electronics industry first adopted graphite due to it having a flatter discharge profile than hard carbon (Yoshino, 2014).

Future materials for the anode will still include graphite and will increase its current capacity by introducing small portions of alloying materials such as silicon (Patel, 2015). Since graphene can only hold one lithium ion per graphene unit (Graphene = C_6 ; Mass = 72 grams), and lithium metal alloys can hold four lithium ions per metal unit (Si mass = 28 grams), these metal alloy anodes will be much more energy-dense than graphene (Thackeray, Wolverton & Isaacs, 2012).

The challenge in adopting high proportions of alloying materials is that they increase in volume 27x greater than graphite under lithiation and degrade the battery's lifetime (Nitta et al., 2015).

Tesla is suspected to have started using small quantities of silicon in the anode for the Model 3 for their NCA battery redesign (Schmuck et al., 2018). The Wall Street Journal recently reported that BMW might start using Si/C anodes by 2023, and Tesla may have already started mixing small amounts of Silicon into their graphite anodes for their domestic Powerwall EES product (Mims, 2018).

Another option is to use Lithium Titanate (LTO) in place of graphite. LTO has a very high cycle life and can lead to a low total-cost-of-ownership when used with a low-cost cathode such as Lithium-Iron-Phosphate (LFP) (Vaalma et al., 2018). LTO exhibits long lifetime due to “zero-strain” intercalation that swells 50x less than Graphite (Nitta et al., 2015). Experts interviewed in a study conducted by Few (2018) suggested that there may be other chemistries that can give the lifecycle benefits of LTO without its drawbacks of increased cost and reduced energy density.

Aside from specific current capacity (mAh/g), the volumetric density (g/L) of the anode helps determine the amount of electrolyte required in a battery’s design. A high-density anode will absorb less electrolyte. This second order effect implies that volumetric density, as well as energy density, are crucial to driving electrolyte and total cell and pack costs down (Vaalma et al., 2018). Specifically, Si-C with 20% Si and Li Metal have similar volumetric capacities which are around 3x the volumetric capacity of graphite (Schmuck et al., 2018).

Lithium metal anodes are a future developmental goal for LIBs. Inherently, lithium has a 0V discharge potential versus Li/Li⁺ (Schmuck et al., 2018). However, the lithium charge cycle leads to safety issues since lithium deposition upon charging can cause dendrite formation can short-circuit the cell. Therefore, the goal of utilising energy-dense lithium metal is driving the development of safer polymer electrolytes which can also act as a physical barrier to dendrite formation (Jürgen & Zeier, 2016).

Even if polymer electrolytes are developed to pair with lithium metal anodes, it may be costly to manufacture lithium metal thin enough to provide material cost and energy density benefits to LIB anodes (Schmuck et al., 2018). However, there are stackable benefits if lithium metal can be applied to LIB anodes. For example, it may be possible to eliminate costly copper foil as a current collector and use lithium directly instead without copper or aluminium (Albertus et al., 2018)

2.4.3 Electrolyte & Separator

The electrolyte most commonly used in LIBs is lithium phosphate tetra-fluoride (LiPF_6), an organic non-aqueous electrolyte salt, which is dissolved in a blended liquid solvent such as ethylene carbonate (EC) mixed with dimethyl carbonate (DMC) (Nelson et al., 2012). Current issues with common LIB electrolytes are that LiPF_6 is corrosive and that the organic solvents are flammable, both of which contribute to limiting the LIB potential to below 4.2V (Thackeray, Wolverton & Isaacs, 2012). Batteries are built with robust enclosures to prevent the corrosive electrolyte from leaking (Cluzel & Douglas, 2012).

The separator in the battery is typically made from a polyethene or polypropylene plastic material which is porous to allow the lithium ions to cross (Nelson & Gallagher, 2014). If the cathode and anode ever come into contact, a runaway condition caused by a short-circuit could occur which would be dangerous with a flammable electrolyte. The plastic separator can prevent dendrites, which can form over the battery's operation, from crossing across both half-cells. It can also be designed to melt at sufficiently high temperatures, effectively blocking lithium ion transport and downregulating a runaway reaction (Nelson & Gallagher, 2014).

Next generation electrolytes may contain a polymer or solid material, which are sometimes referred to as solid-state batteries. Solid electrolytes would be less prone to leak or combust, and in the case of an inorganic solid, provide a higher voltage window in which to operate (Cluzel & Douglas, 2012). PEO polymer or LiPON thin-film are two examples of solid-state electrolytes that can conduct lithium ions but also have the added benefit of dual-acting as the battery separator (Manthiram, Yu & Wang, 2017).

3. EV Battery Demand Forecasts to 2030 (Phase I)

This chapter will discuss EV market projections from non-governmental organisations and independent consultancies. An analysis of EV sales data will assess past battery demand by quantity (GWh) and chemistry (NMC, NCA, or LFP). The functional differences between the most popular cathode chemistries for LIBs in EV applications will also be reviewed with a brief overview of short-term developmental goals for the cathode, anode, and electrolyte. A bottom-up model developed in chapter 4 will translate these projections into material demands for a commodity supply-demand analysis.

Sections 3.1 & 3.2 discuss forecasts of EV adoption from the International Energy Agency (IEA) and other consultancies. The following sections break down battery demand by application (3.3) and chemistry (3.4). In section 3.5, this thesis introduces two broad scenarios to cover status-quo and aggressive action on carbon targets with for EV markets. Finally, this chapter ends with a review of electric buses.

3.1 EV Market Projections From the IEA

The IEA is a global energy think tank that is run by OECD member countries. The IEA publishes its annual Global Electric Vehicle Outlook (GEVO) to track the adoption of EVs and predict the scenarios to meet global climate targets. This thesis will consider three scenarios inspired by the IEA report to define pathways of EV adoption and the necessary battery and material demand. In 2018, the IEA revised two scenarios illustrating projected and potential EV adoption based on existing policies and country commitments.

The New Policies Scenario (NPS) is the IEA's base case forecast on EV sales based on existing policies and sales trends (IEA, 2018). The IEA revised this policy upward in 2017 in part due to 100% zero emission vehicle sales mandates or ICE sales bans across some European countries including France, Norway and the United Kingdom.

The IEA cautions that global climate targets agreed to in the Paris Climate Agreement will not be met by existing policies. Therefore, the IEA also publishes a scenario based on its EV30@30 campaign, which represents commitments by Paris signatories to accelerate EV market growth to reach 30% of all vehicle sales and a stock of 220M EVs by 2030 (IEA, 2018). However, the EV30@30 considers the case that all countries join the EV30@30 campaign and not just the existing members which already cover 60% of global electric car stock

(Canada, China, Finland, France, India, Japan, Mexico, the Netherlands, Norway, and Sweden) (CEM-EVI, 2017).

The EV30@30 scenario also requires the following changes in the market relative to the NPS scenario to be Paris compliant (IEA, 2018):

- Increase of electric vehicle market share from 30% to 60% for BEVs (versus PHEVs);
- Electricity generation carbon emissions fall 50%;
- The total number of light-duty vehicles is 12% less than the NPS; and
- The proportion of electric-only mileage for a PHEV increases from 30% in 2017 to 80% in 2030 (versus 65% in the NPS case).

An analysis of the two scenarios reveals the necessary number of EVs that must be sold each year to confirm each pathway. NPS requires the EV market to average 3.5M vehicles/year from 2018-2020 while the 30@30 scenario requires the EV market to average 8.9M vehicles/year. In 2017, 1.1M EVs were sold, and the market grew above 50% per year. For the market to grow and meet market goals in 2020, the NPS requires a growth rate of 70% a year, and the 30@30 scenario requires a growth rate of 100% a year to 2020. The IEA base case lines up more favourably with recent historical sales trends.

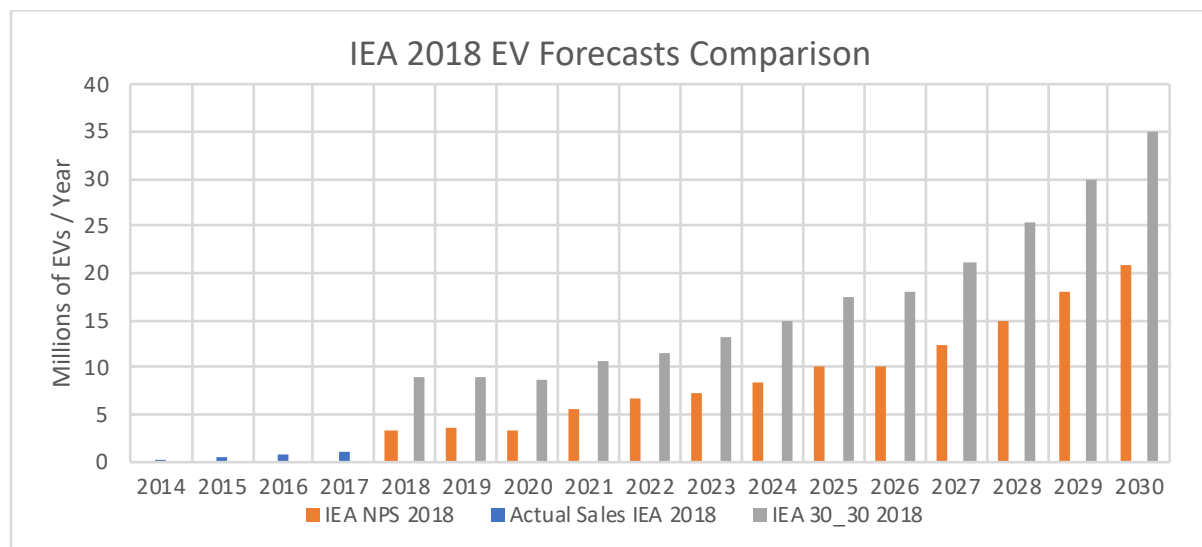


Figure 3.1 IEA EV Forecast Comparison (IEA, 2018)

This thesis will study three different EV market scenarios. The first, called the “base case,” will forecast the EV market with existing government policies and market forces. The second, “base plus,” will forecast the same number of vehicles but will modify the type of battery sold over time. The final scenario, called “early action,” will be a climate-constrained aspirational

scenario which meets the Paris Climate Agreement and will be inspired by the IEA 30@30 scenario.

It is necessary to understand how LIB supply chains will be affected if global action is taken to place the transportation sector on a path of decarbonisation by 2030. The IEA 30@30 scenario requires market growth to reach 800% in 2018, which is much higher than the 50% average growth between 2015-2017. It will also place pressure on EV battery manufacturing over the next decade.

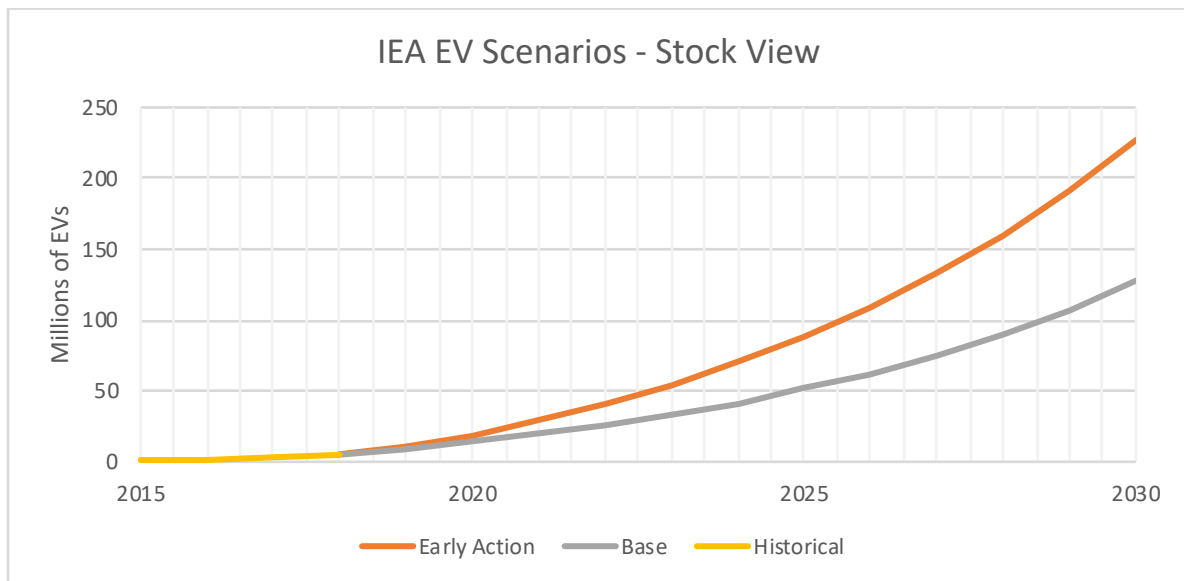


Figure 3.2 Comparison of Paris paths and NPS to 2030 - Stock View

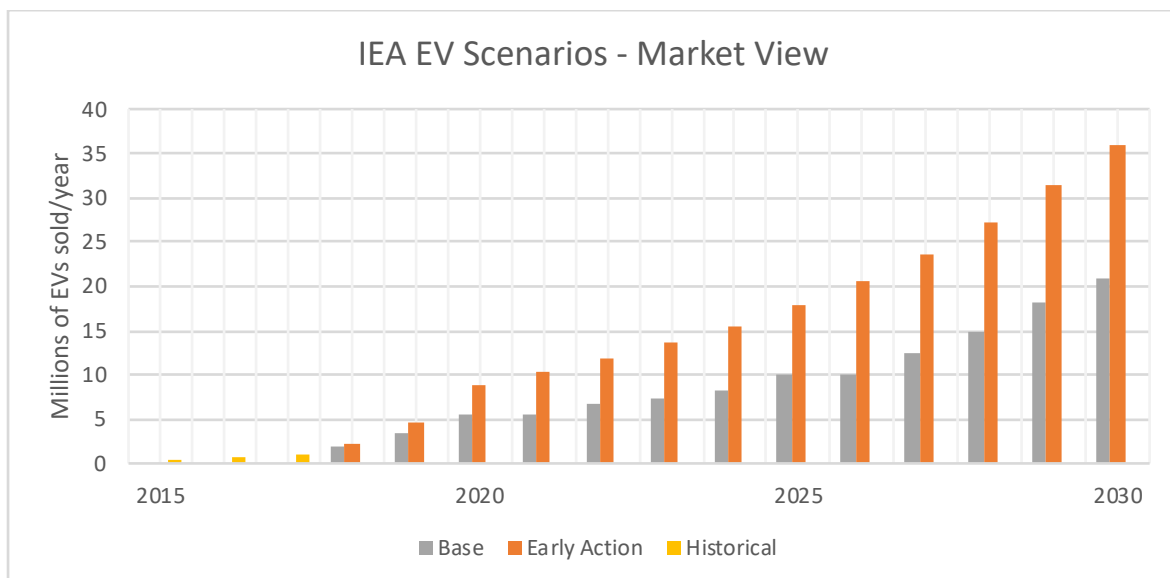


Figure 3.3 Comparison of Paris paths and NPS to 2030 - Market View

3.2 Comparison to Non-IEA Scenarios (BNEF, 2018)

While the IEA is a respected international organisation, it, along with any player in the prediction business, can be prone to mistakes. Indeed, the IEA has been criticised for underestimating the growth of PV technology since 2002 (Mackenzie, 2017). This section will compare the IEA-inspired EV scenarios developed for this thesis with current scenarios and forecasts published by research consultancies and banks. The scenarios modelled by this thesis compare favourably to those completed by consultancies such as Wood Mackenzie, Bloomberg New Energy Finance (BNEF), and McKinsey.

3.2.1 Wood Mackenzie

Wood Mackenzie is an energy-focused research consultancy. They have published two EV forecasts which line up closely with the IEA-based forecasts in this thesis. The first is a base case forecast from their “Battery Raw Materials Service” published in the first half of 2018 which is aligned with the IEA New Policies Scenario (Wood Mackenzie, 2018a). The second is a Paris aligned “Carbon Constrained Scenario” (CCS) which is designed as a pathway to meet international climate targets (Wood Mackenzie, 2018c).

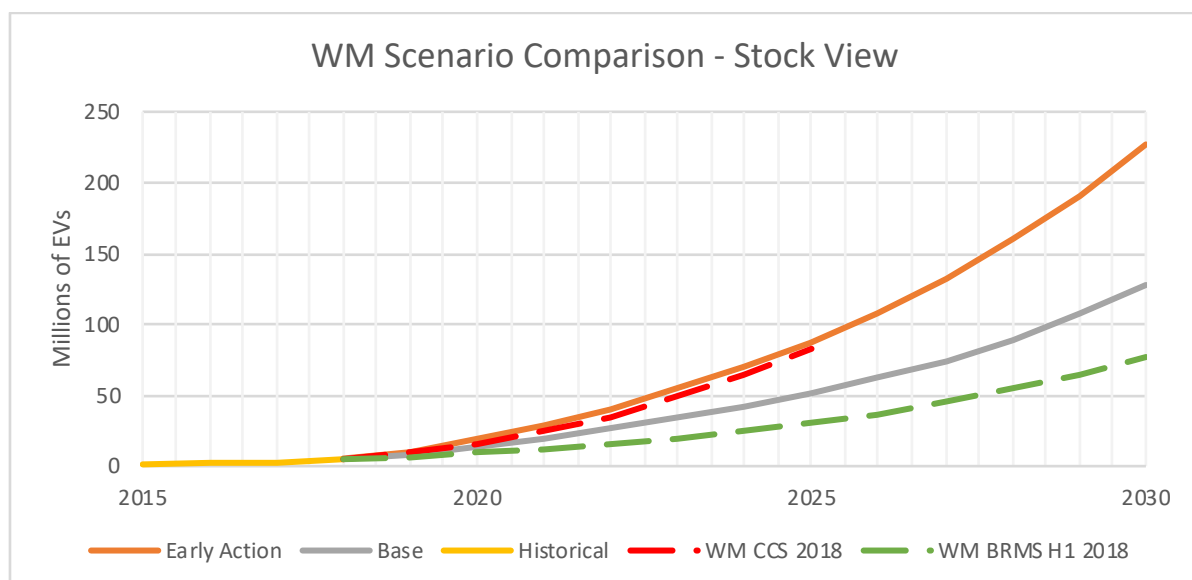


Figure 3.4 Wood Mackenzie EV comparison to IEA inspired thesis scenarios

While Wood Mackenzie’s base case relatively underestimates EV stock compared to the IEA and BNEF scenarios, EV stock is defined in Figure 3.4 as the sum of PHEV and BEV sales and does not include hybrid vehicle sales. Wood Mackenzie’s scenarios place a high

emphasis on non-pluggable HEV growth, which they project to be the favourite among passenger vehicles outselling PEVs by 2 to 1 in 2025 and by 3 to 2 in 2030. Additionally, the Wood Mackenzie scenario has a high BEV ratio of 65% which translates battery demand projections in 2030 closer to the climate constrained scenarios than the IEA base scenario.

3.2.2 Bloomberg New Energy Finance

Each year BNEF, a research consultancy focused on the clean energy transition, publishes an electric vehicle outlook. The forecast for EV stocks shown in Figure 3.5 aligns very closely with the NPS scenario from the IEA and predicts a stock of 147 million EVs in 2030, which is close to the 127 million predicted by the NPS (BNEF, 2018). The difficulty with only considering the stock of all EVs is that it is incomplete to predict battery demand.

Relative to the IEA base case, BNEF is less optimistic on the market before 2026 and relatively optimistic after. This could be a consideration of a prediction for the cost parity of LIB powered vehicles or the commercialisation of advanced-lithium-ion or beyond-LIB technologies at that time. Indeed, BNEF predicts that EVs will start to become purchase price competitive in the mid-2020s because the cost per kWh of EV LIBs reach a target cost of \$100/kWh around 2025 (Frith, 2017).

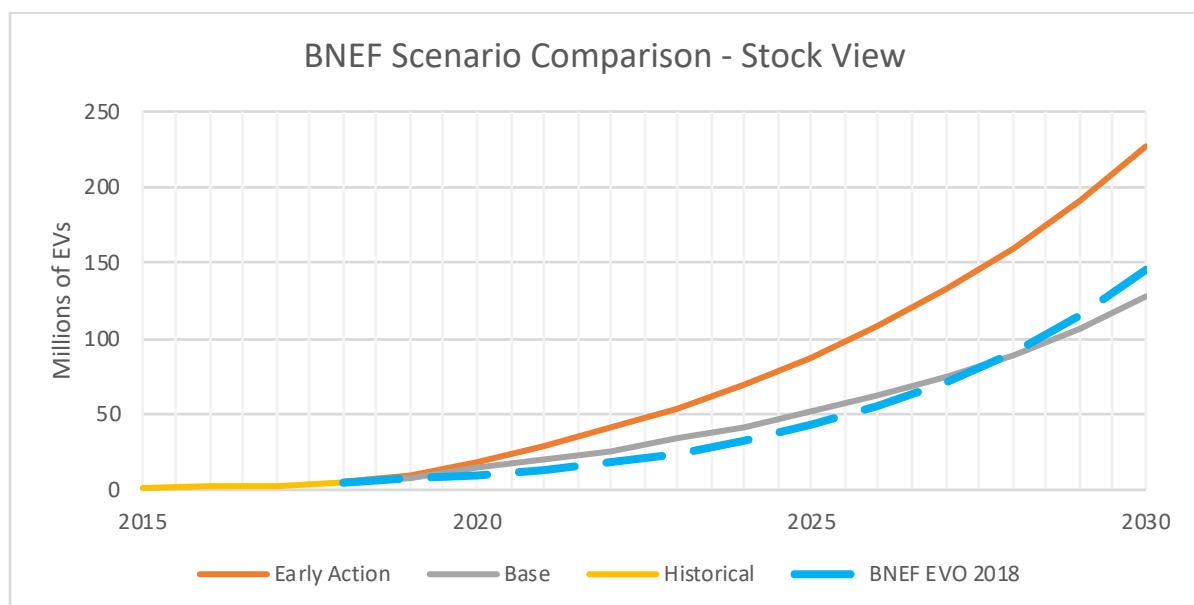


Figure 3.5 Comparison of thesis and BNEF EV scenarios (BNEF, 2018)

BNEF has written that battery demand for electric passenger vehicles will exceed 1500 GWh in 2030. Despite having very similar predictions for vehicle stock, the NPS scenario only

predicts a battery demand of less than 450 GWh in 2030 (Table 3.1). The discrepancy can be attributed to differences in how batteries are modelled: First, BNEF predicts accelerating sales at the end of the next decade with 29.5 M EVs sold per year vs the base case's 20M. Second, the proportion of BEVs sold (79%) is above most optimistic IEA predictions (70%). Finally, BNEF projects that the average BEV battery sold also increases by 50% from 41.5 kWh today to roughly 60 kWh in 2030.

These assumptions in the BNEF model show that the number of vehicles sold is only partially relevant in determining necessary battery manufacturing capacity. It is possible to have moderate EV stock projections and exceed the battery manufacturing capacity predicted in other more seemingly aggressive scenarios such as the Early Action scenario used in this thesis (Table 3.1). Therefore, it is critical to determine both the BEV powertrain share of EV sales as well as the average BEV battery sold since BEVs can command the plurality of demand for EV LIBs.

There is uncertainty in this analysis of the BNEF scenario since BNEF does not explicitly publish their assumptions for the size of the average BEV and PHEV batteries sold. However, Table 3.1 extrapolates reasonable assumptions regarding PHEV batteries and demonstrates that increasing the average PHEV battery sold from 12 to 20 kWh does little to affect the necessary size of the average BEV battery sold to predict a market demand of 1500 GWh.

Scenarios in 2030	BEV Sales (M)	PHEV Sales (M)	BEV %	Total Demand (GWh)	Avg. PHEV Size (kWh)	BEV Demand (GWh)	Avg. BEV Size (kWh)
BNEF 2018	23.3	6.1	79%	1,500	12-20	1427 - 1378	61.3 - 59.2
NPS (thesis)	6.2	14.5	30%	434	12	258	41.5
Mid Case (thesis)	14.5	6.2	70%	834	14.7	743	51
Early Action (thesis)	23.3	10.8	70%	1,106	12	976	41.5

Table 3.1 Comparison of BNEF and NPS 2030 EV battery demand (BNEF, 2018)

3.2.3 Other EV Forecasts

Analysis of base forecasts from various other banks and consultancies shows a wide range of variance for near-term EV sales forecasts (including both BEVs and PHEVs and excluding hybrids). At the low end, a report from Deutsche Bank (2016) predicted EV sales to reach 6.5

million by 2025. At the high end, McKinsey forecasts over 25 million vehicles with more than 50% BEV powertrain share (McKinsey, 2017). Interestingly, McKinsey’s base case is even more aggressive than the IEA EV30@30 Paris-aligned scenario. The other projections featured previously (IEA, BNEF, WM) are the median views in this sample.

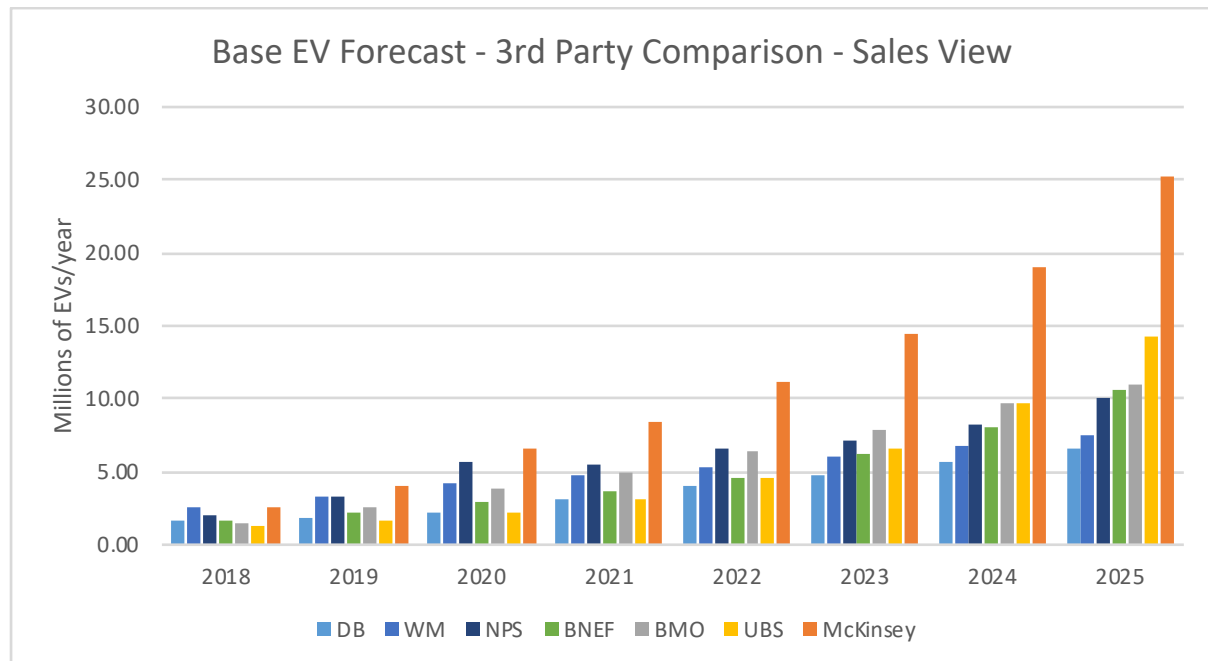


Figure 3.6 EV sales "base case" forecasts for 2018 to 2025 from consultancy and bank analysts (BMO, 2018, BNEF, 2018, Deutsche Bank, 2016, IEA, 2018, McKinsey, 2017, UBS, 2017, Wood Mackenzie, 2017a)

3.3 Demand by Application (BEV or PHEV)

The size of a battery installed in an EV is typically measured in kilowatt-hours (kWhs), which describes the amount of energy the battery can supply over a full charge or discharge cycle. Two metrics can be cited to distinguish the relevant characteristics of a battery design. The first is "total kWh" which describes the total technical capacity of a battery pack. The second is "usable kWh" which is the amount of energy that the vehicle OEM allows the EV to access during normal operation. The ratio between the "usable kWh" and "total kWh" is referred to as the depth-of-discharge (DoD). To estimate material demands in EV batteries, the "total kWh" specification published by OEMs is used whenever possible.

A list of the most popular EVs, their sales numbers, battery capacity and chemistry assumptions for each model for sales in 2017 can be found in Appendix I. There are two reliable sources for EV market demand. The first is the Bloomberg terminal, which has a quarterly update of all vehicle sales as part of its Bloomberg Intelligence service. The second,

referenced by consultancies such as Wood Mackenzie and Bloomberg New Energy Finance, is EV-Volumes.com. Data for this thesis has been primarily sourced from EV-Volumes.com.

The ten most popular BEVs sold in 2018 ranked by their contribution to LIB demand is found in

Table 3.2. The Tesla Model 3, Model S, and Model X have the most significant individual contributions to worldwide EV battery demand. Tesla is also the only automaker who uses the NCA chemistry at scale. Most other automakers use NMC, or if Chinese, LFP. However, China's EV market has recently started to move away from LFP and toward NMC.

Vehicle	2018 to July Sales	Battery Size	2018 Total kWhs	Chemistry
Tesla Model 3 (Long Range)	26,620	75	1,996,500	NCA
Tesla Model S	22,423	80	1,793,840	NCA
Tesla Model X	21,641	80	1,731,280	NCA
Nissan Leaf EV 2018+	41,775	40	1,671,000	NMC
BYD e5 450 (China)	16,626	61	1,014,186	NMC
BJEV EC180/200 EV (China)	39,906	22	877,932	LFP
Chevy Bolt	13,810	60	828,600	NMC
Renault Zoe	17,824	35	623,840	NMC
Geely Emgrand EV (China)	11,299	52	587,548	LFP
JAC iEV(7/s/e) (China)	17,556	30	526,680	LFP

Table 3.2 Global Sales for top 10 BEV models ranked by battery demand. Source: (EV-Sales, 2018, EV-Volumes.com, 2018, watter2buy.com, 2018) and manufacturer reports.

Plug-in hybrid vehicles use much smaller batteries, and it is not surprising that the most influential PHEV vehicles for battery demand do not meet even the battery demand of the tenth most influential BEV. BYD, the most successful PHEV manufacturer in 2018, announced in the previous year that all new PHEV vehicles would use NMC technology instead of LFP (Kou, 2018). This switch by BYD has contributed to the large loss in LFP market share in PHEVs from 2017 to 2018.

The average BEV sold in 2017 had a 35.7 kWh capacity battery the average PHEV sold in 2017 was 11.5 kWh. Sales data from the first half of 2018 suggests that BEV market share is holding steady at around 65% and that BEV battery sizes are creeping back up past 4 kWh per BEV up from 36kWh in 2016.

Vehicle	2018 to July Sales	Battery Size	2018 Total kWhs	Chemistry
BYD Song PHEV (China)	21,201	18.5	392,218	NMC
BYD Qin PHEV (China)	22,963	14	321,482	NMC
Toyota Prius Prime	24,767	9	222,903	NMC
Mitsubishi Outlander	17,494	12	209,928	LMO-NMC
Chevy Volt	10,819	18	194,742	LMO-NMC
SAIC Roewe eRX5 (China)	13,344	12	160,128	NMC
SAIC Roewe i6 (China)	15,190	9	136,710	NMC
Honda Clarity PHEV	7,361	17	125,137	NMC
BMW 530e	12,404	9.2	114,116.8	NMC
Volvo XC60	6,566	12	78,792	NMC

Table 3.3 Global sales for top 10 PHEV models ranked by battery demand. Source: (EV-Sales, 2018, EV-Volumes.com, 2018, watter2buy.com, 2018) and manufacturer reports.

Together, the average battery sizes for BEVs and PHEVs along with the powertrain market share for BEVs and PHEVs can be combined to model the total energy of batteries manufactured each year. It is crucial to separate BEVs and PHEVs not only because they lead to different quantities of battery demand, but because each application may use different cathode chemistries depending on design criteria such as the required power and energy ratio, safety, availability for battery cooling, energy density. The demand model generated in Phase I applies chemistry market share separately to the energy demand from PHEV and BEV applications.

Average EV kWh	2016	2017	2018
PHEV	16.1	11.5	11.7
BEV	40.7	35.7	40.9
% of EV as BEVs	60%	66%	64%
% Sales Categorized	89%	87%	81%

Table 3.4 Average battery size for BEV and PHEV vehicles. Source: (EV-Sales, 2018, EV-Volumes.com, 2018, watter2buy.com, 2018) and manufacturer reports.

3.4 Demand by Chemistry

There are two differences among the market share for chemistries in EV batteries: 1) the higher proportion of nickel-cobalt-aluminium (NCA) in BEV applications, and 2) increasing influence of nickel-manganese-cobalt (NMC) in PHEV applications (Figure 3.8). This section

will briefly introduce each commercially manufactured chemistry and discuss the relative advantages that contribute to their popularity in the EV battery market.

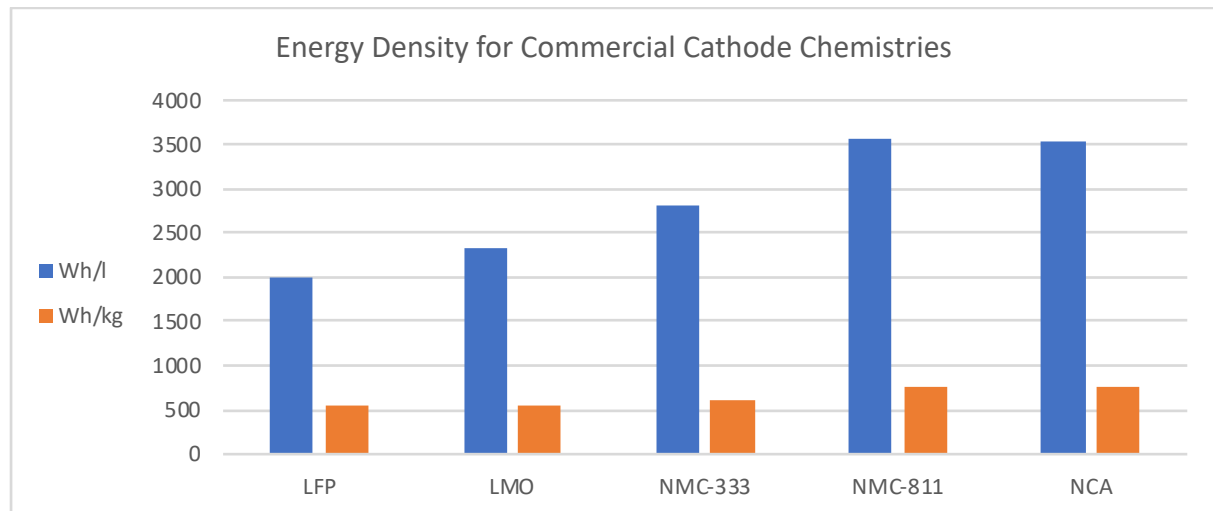


Figure 3.7 Energy Density for Commercial Cathode Chemistries (Nitta et al., 2015, Schmuch et al., 2018)

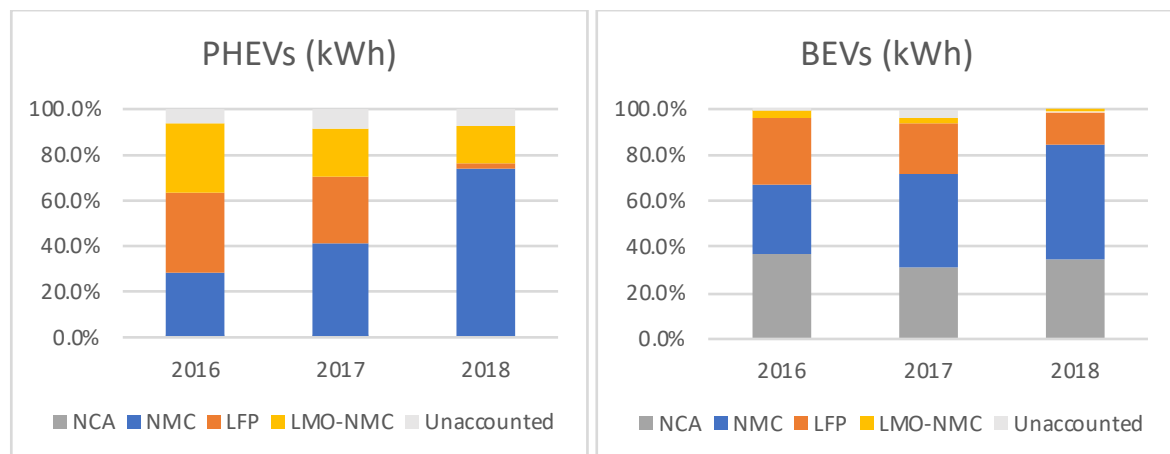


Figure 3.8 Comparison of PHEV and BEV battery chemistry market share of vehicles sold from 2016-2018. Source: (EV-Sales, 2018, EV-Volumes.com, 2018, watter2buy.com, 2018) & manufacturer reports

3.4.1 Lithium Manganese Oxide (LMO)

LMO is known as a low-cost LIB cathode chemistry option. Most notably, LMO was the cathode of choice for Nissan for its 24kWh battery packs for the Leaf and Renault Kangoo (AESC, 2013). However, as Nissan has released larger packs, they have switched the design to NMC (Frost, 2014). This is likely due to the consensus in Figure 3.9 that NMC is much more useful when energy density is a concern.

LMO is not the best choice in any category except cost, but other chemistries such as LFP and NMC perform equally well in cost and provide benefits in other categories such as safety, energy density and lifetime. The reliability of LMO packs may also be inferred by Nissan. When the Leaf is suspected to have switched technology from LMO to NMC, Nissan also improved the Leaf's warranty from 5 years / 60k miles for its 24kWh pack to 8 years / 100k miles for its 30kWh and 40kWh NMC packs (Nissan, 2018).

3.4.2 Lithium-Iron-Phosphate (LFP)

LFP demonstrates the lowest energy density (Figure 3.7) but is also one of the safest cathode choices. The Chinese market favours LFP because government subsidies were removed from some large NMC manufacturers in 2016. At that time, companies that produced NMC were mostly firms such as Samsung and LG who are based in South Korea (Deign, 2016). China would mostly subsidise EVs with LFP batteries until 2017 when domestic producers gained the ability to manufacturer NMC themselves (Reuters, 2017a).

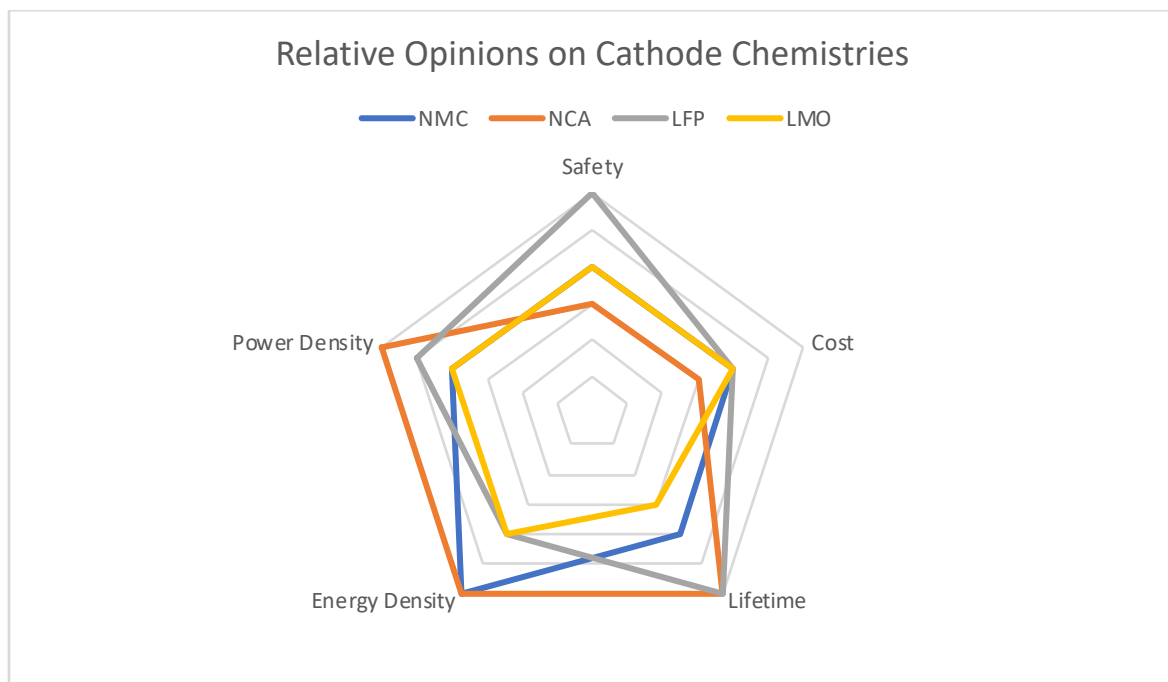


Figure 3.9 Consensus on cathode chemistry characteristics from independent reviews. (BCG, 2010, Cluzel & Douglas, 2012, IRENA, 2017, McKinsey, 2017, O'Donovan, 2017, Perner & Vetter, 2015)

The 2018 update to the Chinese subsidy program has shifted incentives to high range vehicles (Kou, 2018). Vehicles with an NMC or NCA chemistry require much less volume and mass than a vehicle designed with LFP (Figure 3.7). The resulting switch from LFP to NMC has dramatically reduced the market share of LFP among PHEVs sold from ~30% in 2017 to ~2%

in 2018. BYD, a large manufacturer of both LFP batteries and vehicles in China, announced in 2018 that all new PHEVs and all BEV passenger vehicles would start to use NMC in 2018 (Gasgoo, 2017). This choice by BYD is a major contributor to the market shift away from LFP.

3.4.3 Nickel Manganese Cobalt (NMC)

NMC is quickly gaining market share for all EVs from ~30% in 2016 to ~50% in 2018. Early versions of NMC with equal parts nickel, manganese and cobalt (NMC-333) probably assume a plurality of the market in between 2015 and 2020, but higher nickel blends together are more popular for new vehicle designs (Pillot, 2017).

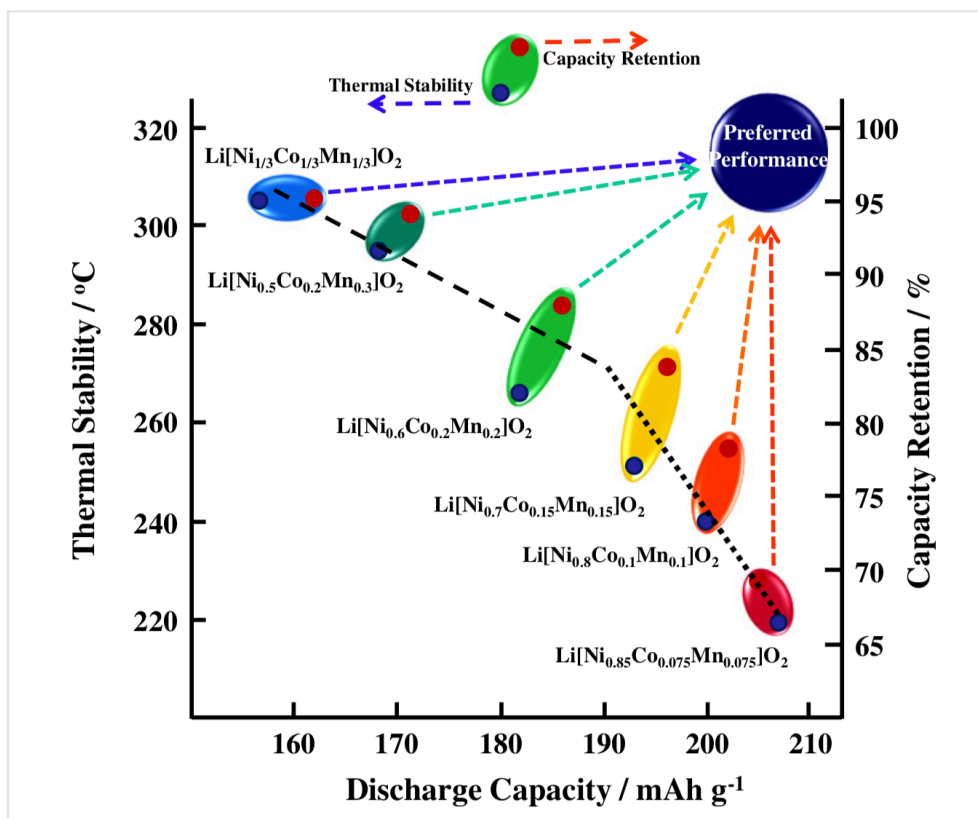


Figure 3.10 The relationship between NMC discharge capacity and thermal stability with nickel intensity. Reprinted from Noh et al. (2013). Copyright 2013.

As vehicle manufacturers build start to build EVs with larger batteries and at lower cost, high nickel NMC (622 or 811) may become more favoured due to both economic advantages in reducing the expensive metal cobalt, and engineering advantages due to higher charge capacity with higher levels of nickel. However, high-nickel NMC does demonstrate worse thermal stability and charge retention as shown in Figure 3.10 (Noh et al., 2013). As the

proportion of nickel in NMC increases, discharge capacity improves, capacity retention weakens, and normal operating temperatures are closer to the thermally stable threshold. Battery manufacturers Panasonic and LG Chem, as well as BMW, all have plans to commercialise high nickel NMC-811 between 2018 and 2021 (BMW, 2016, Lima, 2017, Reuters, 2017b).

3.4.4 Nickel Cobalt Aluminium (NCA)

The ~30% market share for NCA in BEVs in Figure 3.9 is exclusively due to demand for Tesla vehicles. NCA is a high-nickel chemistry with the ratio 0.85/0.15/0.05, which has high nickel and low cobalt proportions comparable to NMC-811.

NCA displays strong energy density but also poor thermal stability (Schmuck et al., 2018). Tesla manages this issue by applying advanced liquid-thermal-management to its battery packs, which add cost to their vehicles (Erriquez et al., 2017). Despite the poor thermal stability, or perhaps because of the advanced thermal management systems used in NCA vehicles, crowd-sourced data from vehicle owners suggest that luxury Model S and X vehicles keep 92% of their battery capacity after 100,000 miles (Steinbuch, 2018).

3.5 Thesis Demand Scenarios

The material demand projections defined in Chapter 4 of this thesis will depend on how much battery energy capacity is manufactured each year and the chemistry mix of those batteries. The demand scenarios are compared in Figure 3.11. However, detailed charts with the split of each scenarios' demand by BEV and PHEV by year can be found in Appendix II.

The following assumptions describe how the thesis demand scenarios forecast LIB chemistry demand from 2018 to 2030:

- The average size of BEV and PHEV batteries are held constant from 2018 for the “base” and “early action” scenarios, while the average battery sizes are increased by 25% for the “base plus” scenario;
- the chemistry share of BEV and PHEV batteries are held constant from 2018. However, within the NMC chemistry, higher-nickel formulas gain share within NMC;

- the “base” scenario forecasts that PHEVs become the dominant vehicle of choice by 2030 (30% BEV) and predicts a linear fall in BEV market share; and
- the “base plus” and “early action” scenarios forecast BEVs as the dominant vehicle of choice by 2030 (70% BEV) and predict a linear rise in BEV market share.

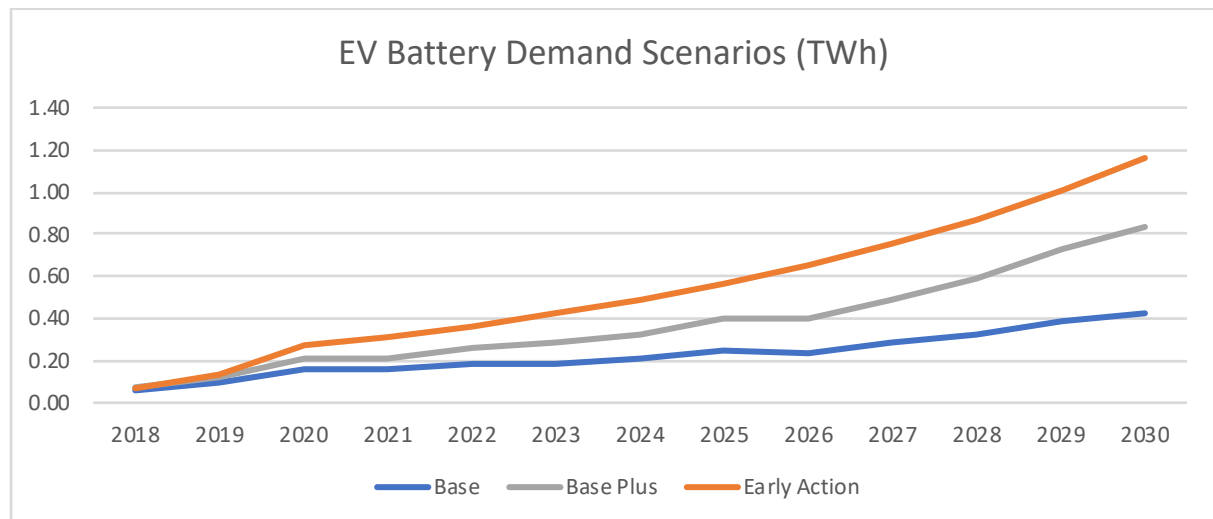


Figure 3.11 Forecasted battery demand across the NPS, “2022 Action” and “Early Action” scenarios

The “early action” scenario requires battery energy production to be double the “base” scenario by 2022. As well, the delayed “2022 Action” scenario requires 30% greater capacity than the “early action” scenario.

Compared to the “base” scenario, the “base plus” scenario is likely if consumers decide they need greater range. Consumers may prefer larger batteries if charging infrastructure does not develop quickly enough to support a dense network of fast chargers. With a well-developed future charging network, consumers may prefer smaller batteries which are satisfactory and cost less up front.

These scenarios can be considered underestimates over the next decade if:

- Average PHEV or BEV batteries sizes increase in size above 50kWh for BEVs or 15 kWh or PHEVs;
- the market share for BEVs rises above 70% for all EV sales; and
- EV sales exceed the scenarios defined in Figure 3.3.

3.6 Electric Buses

Beyond the growth of light-duty vehicles, electric buses (E-buses) account for a notable source of demand for EV LIBs due to their large size per bus of around 250kWh. The opportunity to save fuel and reduce price volatility for local governments make E-buses a popular choice for designing new public infrastructure. BNEF projects that 95% of E-buses purchased until 2025 will be bought in China (Rybczynska, 2018).

E-buses have application requirements that prefer high power density, low cost, and can afford reduced volumetric density. Therefore, it is little surprise that 90% of the E-Bus sales from 2015-2016 have been with models equipped with LFP cathode chemistries, which provide a very low cost per kWh despite having a larger specific volume than those with nickel-based ternary cathodes (O'Donovan, 2017).

E-buses are probably more interesting for dynamics in demand for fuel (either electricity consumed or oil displaced) than battery demand due to their high rate of utilisation compared with personal vehicles. Even with their high popularity in China, and despite their larger battery sizes, E-Buses are predicted to only assume ~10 GWh of annual battery demand throughout the 2020s (O'Donovan, 2018).

4. The Battery Commodity Model (Phase II)

This thesis will use two methods of cost forecasting. The first, bottom-up cost modelling, examines the significant costs in LIBs and can incorporate information on possible improvements in technology. LIBs are a sophisticated technology with many interrelated engineering design choices. In this chapter, the battery performance and cost model (BatPaC) developed by Argonne National Lab is examined as an open model to be adapted. The battery commodity model (BCM) developed for this thesis does five things:

1. Simplifies BatPaC;
2. Calculates the commodity cost of LIBs;
3. Extends temporal effects (2020-2030);
4. Allows for detailed commodity price input; and
5. Informs material inputs in kg/kWh terms for popular LIB chemistries.

Chapter 0 will use a top-down experience curve model to forecast the fall in LIB batteries over the next decade for each doubling in cumulative production. The results from the BCM and the work in chapter 5 will inform the fundamental cost floors that should be considered in the top-down cost forecasting method.

4.1 Bottom-Up Cost Modelling Overview

Analysing technology by its subcomponents provides advantageous insights. A bottom-up cost model starts from the fundamental features of a technology to estimate how it will adapt to changes in prices or innovation. This way, a cost trend does not need to be observed, and sensitivities in the parameters of a technology can be studied (Gross et al., 2013). Bottom-up cost models inform the material projections for the later phases of this thesis.

4.2 The BatPaC Model

Argonne National Laboratory in Chicago, Illinois first published BatPaC in 2012 as a tool for academics and industry to model the characteristics of EV LIBs (Nelson et al., 2012). BatPaC is designed to be flexible and supports BEVs, PHEVs, as well as hybrid vehicles and micro-hybrid vehicles which do not plug-in to the electricity grid.

In 2012, Element Energy evaluated the LIB market in a report for the Committee on Climate Change and concluded that while the ANL BatPaC model was the most trusted open model at the time, it lacked a temporal component (Cluzel & Douglas, 2012). BatPaC is primarily designed to simulate the cost of batteries in the year 2020 which limits its use in forecasting cost past 2020. Furthermore, only one temporal set of commodity price data is available to use in BatPaC which limits its use in simulating the cost of LIBs over time as input prices change.

BatPaC simulates battery design at the cell engineering level and simulates the effect of manufacturing cost by scaling factory volume. This can make BatPaC tedious to edit and challenging to use. This thesis is interested in the costs of scale on the commodity inputs into the manufacturing process and is not primarily concerned with particular manufacturing methods and therefore will use BatPaC as a reference for its modelling.

4.3 The Battery Commodity Model

The battery commodity model (BCM) has been developed over the course of this masters' thesis as an extension for BatPaC to simplify the techno-economic analysis of lithium-ion batteries when temporal pricing with commodities are prioritised over the optimised design of a battery pouch cell. Simplicity will inevitably lead to more generalised approximations for the analysis of a battery pack. The BCM is designed to be applied after a battery chemistry and pack has been designed. The BCM not designed to be applied to hypothetical battery chemistries or designs. In practice, a select number of calculations from BatPaC are applied to the BCM. This is because the recursive battery design functions of BatPaC are best run standalone as an initialisation of the BCM.

The process of determining the mass of materials in a specific battery chemistry involves analysing the properties of the materials that can vary between different LIB types. Generally, the electrode chemistries and form factor will vary among different lithium-ion batteries. However, in determining the material required for the active material in the battery electrodes, the battery's form factor is not a significant variable (Nelson et al., 2012).

The functional components of a LIB to store charge are the anode and cathode. Table 4.1 compares the characteristics of popular LIB cathode materials and Table 4.2 for LIB anode materials. The chemistry of cathode and anode determines both the voltage potential across each electrode referenced to the electrolyte as well as the current

capacity (mAh/g) in the cathode and anode. A material with a high current capacity would imply that less material would be necessary to store charge and therefore contribute to a lighter battery.

Cathode Comparison	NMC-111	NMC-622	NMC-811	NCA	LFP
Current Capacity (mAh/g)	155.00	175.00	200.00	200.00	150.00
Molar Mass (g)	93.93	94.38	94.72	96.09	157.76
Potential against Li⁺ (V)	3.8	3.9	3.9	3.8	3.4
Li g/g active	0.08	0.08	0.08	0.07	0.04
Ni g/g active	0.20	0.35	0.47	0.49	-
Mn g/g active	0.19	0.11	0.06	-	-
Co g/g active	0.20	0.12	0.06	0.09	-
Al g/g active	-	-	-	0.01	-
Fe g/g active	-	-	-	-	0.35
P g/g active	-	-	-	-	0.20

Table 4.1 Cathode Chemistry properties. OCV and Current Capacity from Nelson et al. (2012)

While the cathode generally is sized to meet 100% of the cell charge, the anode is oversized between 1.1 – 1.25 times to prevent lithium plating on the graphite during charging (Nelson et al., 2012). Even with this anode oversizing factor (called the “negative-to-positive ratio” or the “N/P ratio”), the cathode generally contributes more to the cell’s mass because graphite anodes have a higher current capacity of 360 mAh/g while the range of popular cathode materials is between 150-200 mAh/g. Graphite commands a vast majority of the LIB anode market. Figure 4.1 outlines the process to estimate the amount of active material in the cathode and anode.

Anode Comparison	Graphite	LTO	Gr & 5% Si
Current Capacity (mAh/g)	360.00	170.00	477.00
N/P Ratio	1.25	1.10	1.25
Molar Mass (g)	12.00	459.11	12.81
Potential against Li⁺ (V)	0.1	1.5	0.2
Mass for 1Ah (g)	3.47	6.47	2.62
C g/g active	1.00	-	0.95
Li g/g active	-	0.06	-
Ti g/g active	-	0.52	-
Si g/g active	-	-	0.05

Table 4.2 Comparison of anode chemistry properties (Dash & Pannala, 2016, Nelson et al., 2012)

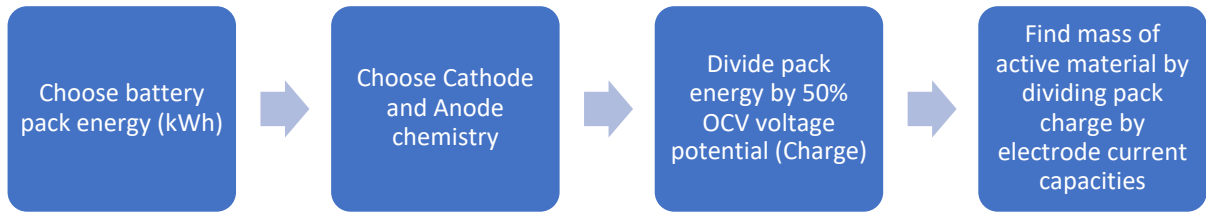


Figure 4.1 Process to determine the quantity of active material necessary in a LIB

For example, to find the active material in a 1kWh battery with LFP cathode and graphite anode it is worth remembering the electrical definition of power which is voltage times current:

$$3.4 \text{ (LFP vs. Li}^+) - 0.1 \text{ (Gr vs. Li}^+) = 3.3 \text{ V}$$

$$\frac{1\text{kWh (Energy)}}{3.3 \text{ V (OCV)}} = 303 \text{ Ah (Cell)}$$

$$\text{Cathode Material} = \frac{303 \text{ Ah (Cell)}}{150 \frac{\text{Ah}}{\text{kg}} \text{ (LFP CC)}} = 2.02 \text{ kg LFP}$$

$$\text{Anode Material} = \frac{303 \text{ Ah (Cell CC)}}{360 \frac{\text{Ah}}{\text{kg}} \text{ (Graphite CC)}} * 1.25 \text{ (Graphite N/P Ratio)} = 1.05 \text{ kg Graphite}$$

Equation 4.1 Calculating the mass of active battery material based on cell chemistry and energy.

Converting material mass into individual metal involves using the constants calculated in Table 4.1 and Table 4.2, which convert active material mass into the mass of the individual metals.

$$\text{Lithium Mass} = 2.02 \text{ kg LFP} * \frac{0.04 \text{ kg Li}}{\text{kg Active Material}} = 0.08 \text{ kg of Li}$$

$$\text{Iron Mass} = 2.02 \text{ kg LFP} * \frac{0.35 \text{ kg Fe}}{\text{kg Active Material}} = 0.71 \text{ kg of Fe}$$

$$\text{Phosphorus Mass} = 2.02 \text{ kg LFP} * \frac{0.20 \text{ kg P}}{\text{kg Active Material}} = 0.40 \text{ kg of P}$$

$$\text{Mass} = 1.05 \text{ kg Graphite} * \frac{1.05 \text{ kg C}}{\text{kg Active Material}} = 1.05 \text{ kg of C}$$

Equation 4.2 Calculating the elements in LIB materials based on the material mass

4.4 Forecasting LIB Commodity Demand

The goal of Phase II is to derive EV sector demand for the valuable metals that make up LIBs. The EV sales forecasts from Phase I are first separated into BEV and PHEV sales segments applying any change in BEV market share over time. A series of examples that work through this process with the “early action” scenario is shown in this section. The “early action” scenario is the most aggressive EV sales forecast. Figure 4.2 splits EV sales by vehicle type from 2018 to 2030.

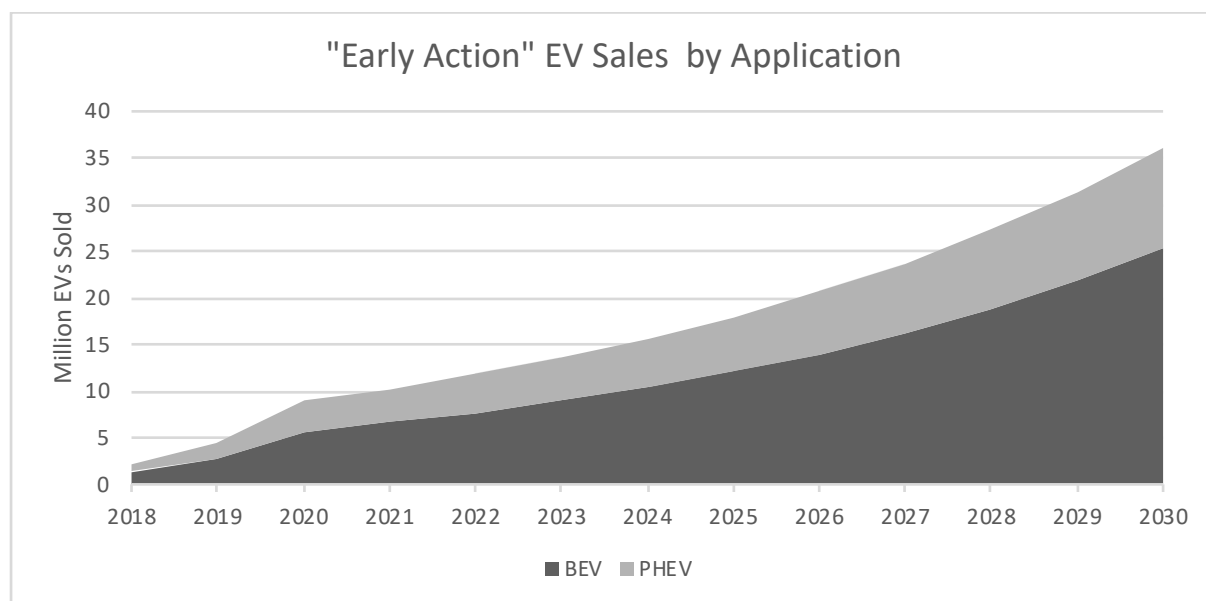


Figure 4.2 Early Action EV Sales split by application from 2018 -2030. BEV share slowly increases to 70%

In the “early action” scenario, 70% of EVs sold are BEVs. The high quantity of EVs sold and the high market share for BEVs translate into high projections for LIB production. The average BEV sold has a 41kWh battery while the average PHEV sold has an 11.7 kWh battery.

Next, average battery sizes for BEVs and PHEVs in 2018 are applied to the sales forecasts to 2030. Battery sizes should increase if one assumes that lower battery cost will increase consumer appetite for vehicle range. However, battery size assumptions should decrease if high-power charging infrastructure proliferates and consumers instead prefer to minimise vehicle cost. Due to the uncertainty, this thesis has chosen to model the status quo by holding BEV and PHEV market share for 2018 is constant to 2030.

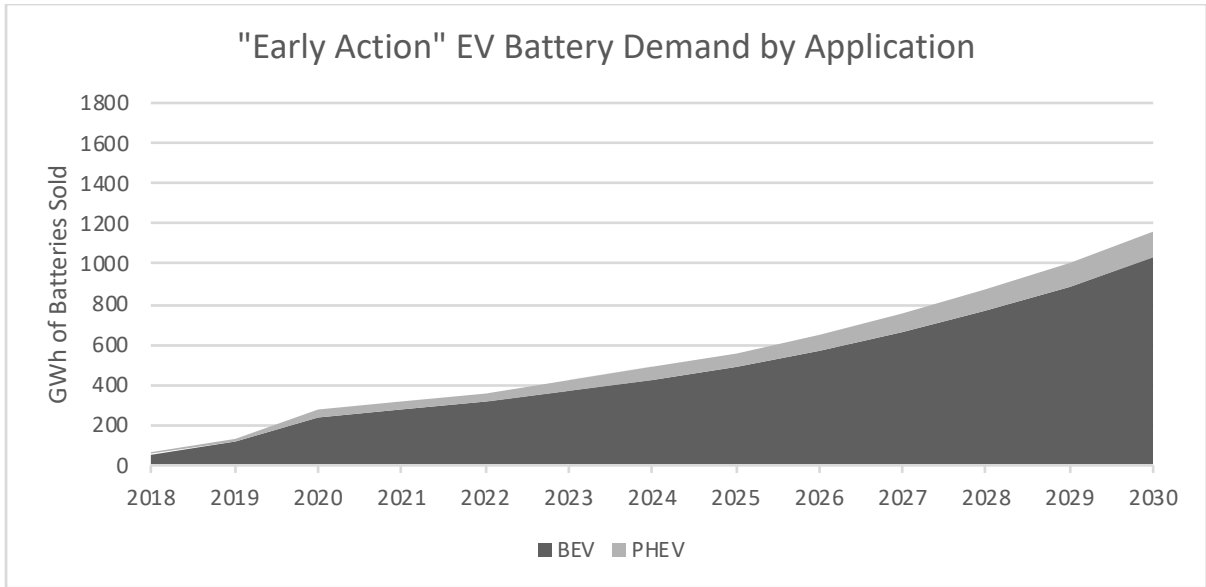


Figure 4.3 Early Action EV battery demand (GWh) by application from 2018 – 2030

By applying the market share for NMC, NCA, and LFP for each GWh of BEV or PHEV, demand for each chemistry can be forecast which together adds up to the demand of BEVs and PHEVs.

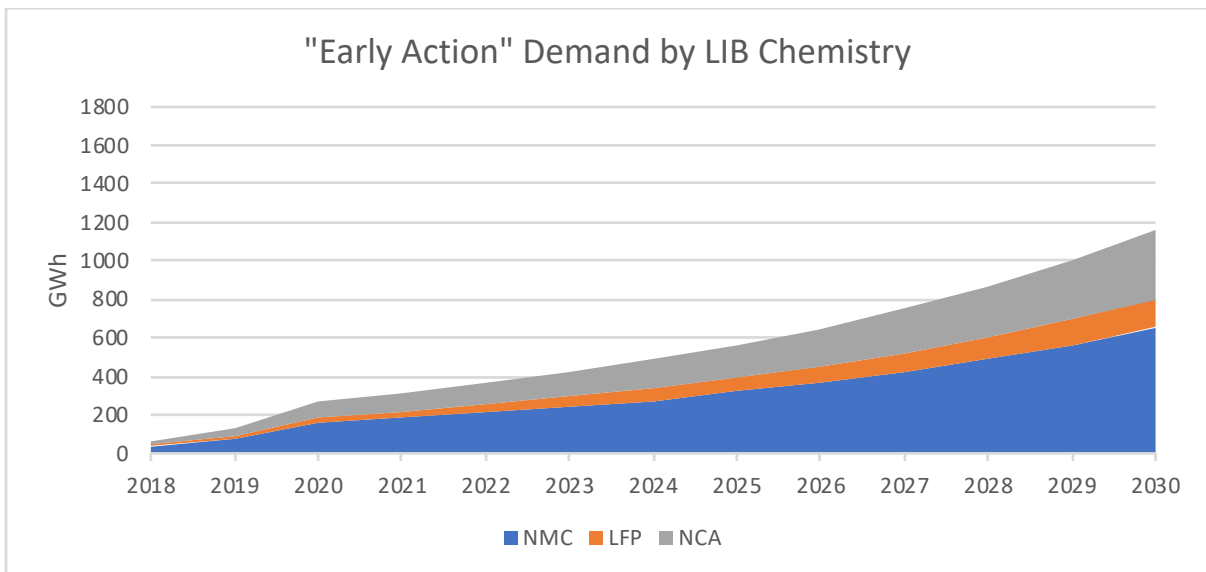


Figure 4.4 "Early Action" scenario EV LIB demand by LIB Chemistry

The BCM forecasts that NMC is the most popular chemistry in 2030. However, NMC is a general family of sub-chemistries, each with different intensities of metal. Data to segment the NMC market into NMC-333, NMC-622, and NMC-811 variants is challenging to find. However, Wood Mackenzie believes the split in 2018 is even between NMC-333 and NMC-622. NMC-811 is the most energy-dense and advanced variant, but it has stability issues, and it is not

yet clear whether manufacturers will solve these challenges. Therefore, NMC-622 is projected in this thesis to become the main NMC variant in 2030.

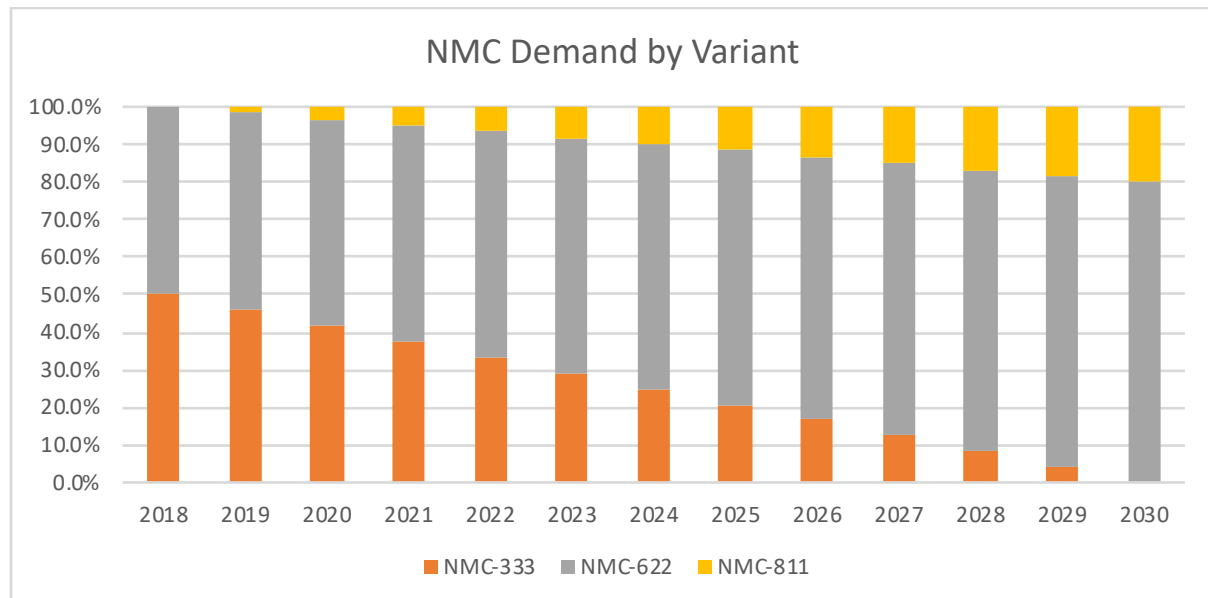


Figure 4.5 NMC Demand by Variant (333, 622, or 811) from 2018 – 2030

Finally, metal intensity constants derived from the BatPaC model are applied over energy demand for each chemistry from 2018 to 2030. Crucially, a year of demand lag is implemented in the model to simulate lag in the supply chain. This means that material demand will be projected from 2017 to 2029 for EV demand modelled from 2018 to 2030.

Cathode/Anode (g/kWh)	Li	Ni	Co	Graphite
LFP/C	113	0	0	1047
NMC 333/C	141	348	349	975
NMC 622/C	119	551	184	955
NMC 811/C	111	622	172	959
NCA/C	107	655	137	972

Table 4.3 Material Intensity by commercial cathode/anode combinations

Figure 4.6 shows the growth in demand for each of the valuable elements studied for this thesis: lithium (LCE), nickel, cobalt, and graphitised carbon. Graphite is the most affected material, with over 1,000 kTons demanded by EVs in 2029. This growth in demand is not a surprise since commercialised anodes are almost entirely made from carbon, while the cathodes are mixtures of lithium and various other metals such as nickel and cobalt.

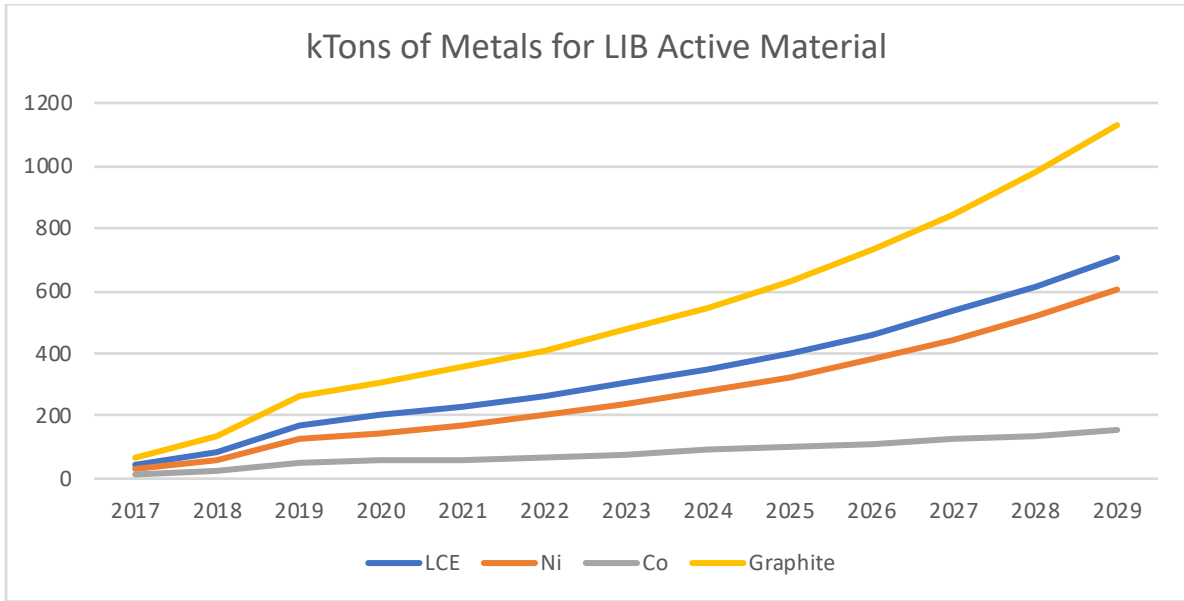


Figure 4.6 "Early Action" Metal Demand for LIBs 2017-2029 (kTons)

Figure 4.7 suggests that while the sales of EVs in the "early action" scenario are expected to grow 16 times from 2018 – 2030, only lithium and graphite follow that demand trend. Nickel grows much faster, and cobalt grows much slower. This disparity in cobalt and nickel growth is a derivative of the assumption that high nickel cathode chemistries like NMC-622 and NMC-811 become more prevalent late in the decade. It is also important to note that lithium demand is measured in LCE terms. There is 0.189 kg of lithium per kg of LCE.

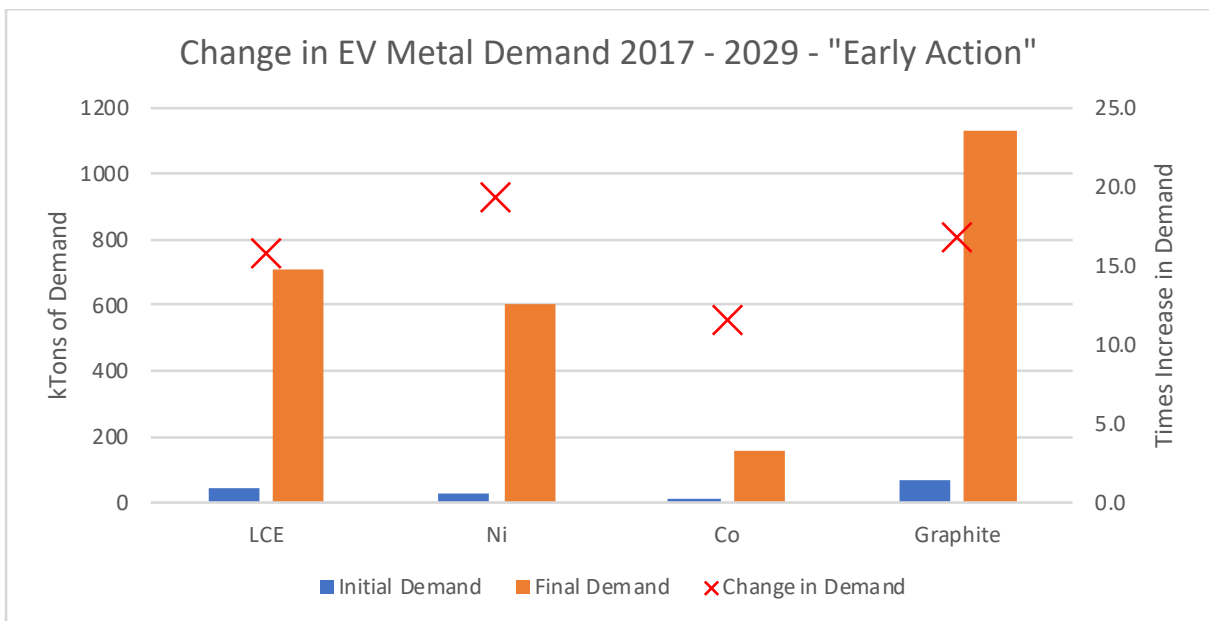


Figure 4.7 Early Action Change in EV Metal Demand 2017-2029

4.5 LIB Material Forecasts by Commodity

Wood Mackenzie’s metals and mining group has projected lithium carbonate, cobalt, nickel, and graphite demand over the next decade for non-EV sectors. While demand for each of these resources is expected to grow naturally, extra demand from EVs will substantially increase demand for lithium, cobalt, nickel, and graphite.

For the next chapter, supplementary metal demand for EVs is considered to project the supply-demand balance over the next decade and forecast incentive prices.

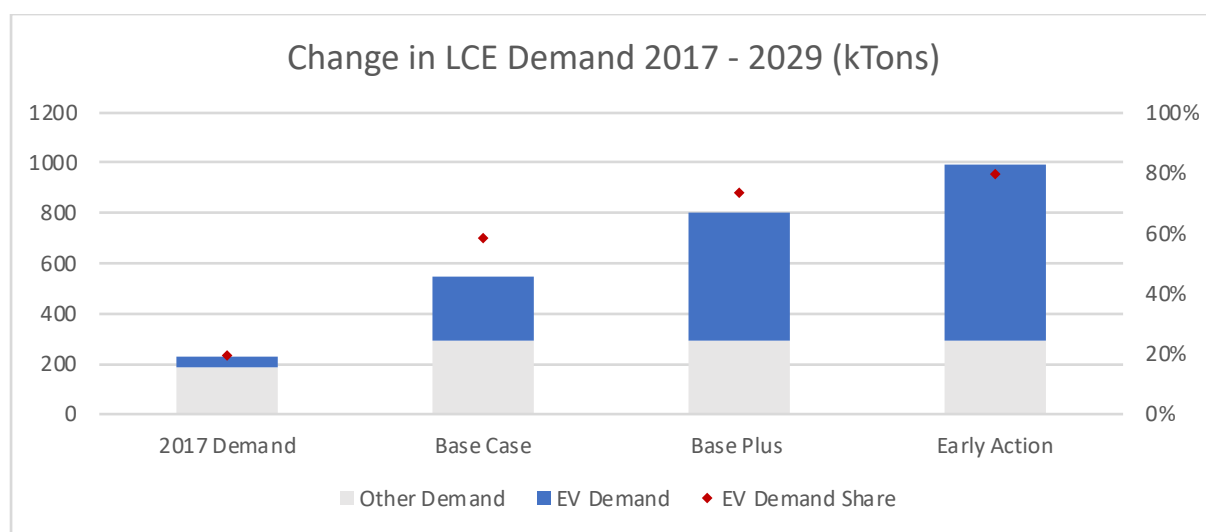


Figure 4.8 change in LCE Demand from 2017 to 2029

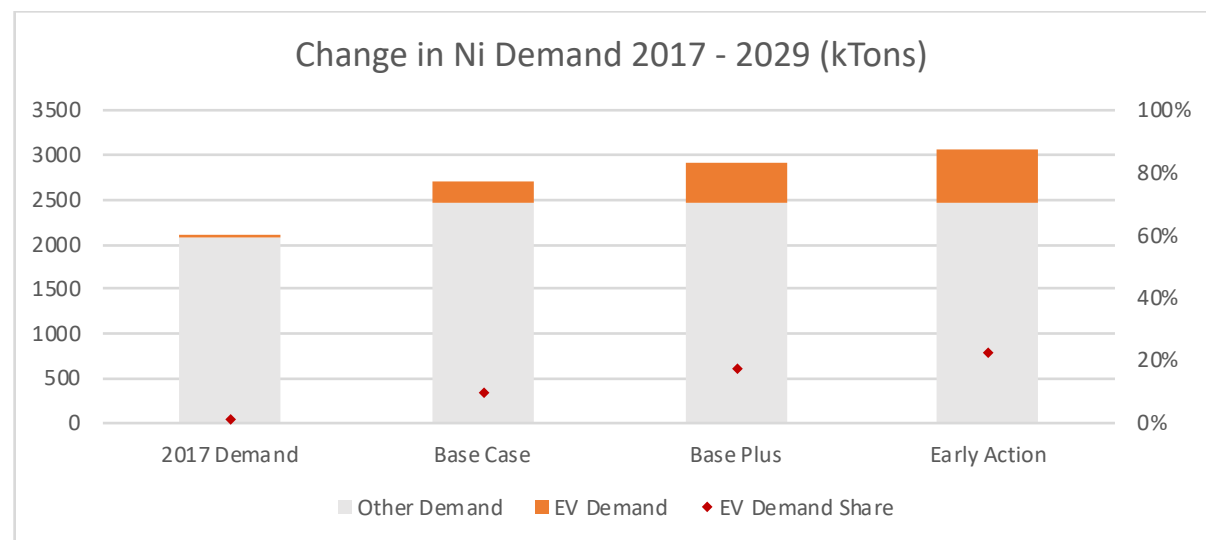


Figure 4.9 Change in nickel demand from 2017 - 2029

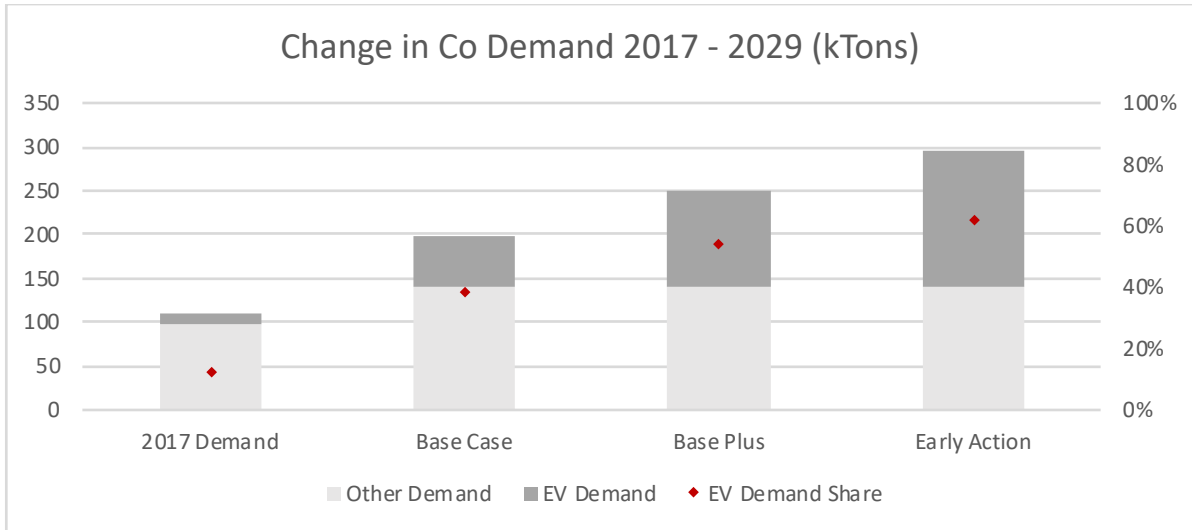


Figure 4.10 Change in cobalt demand from 2017 – 2029

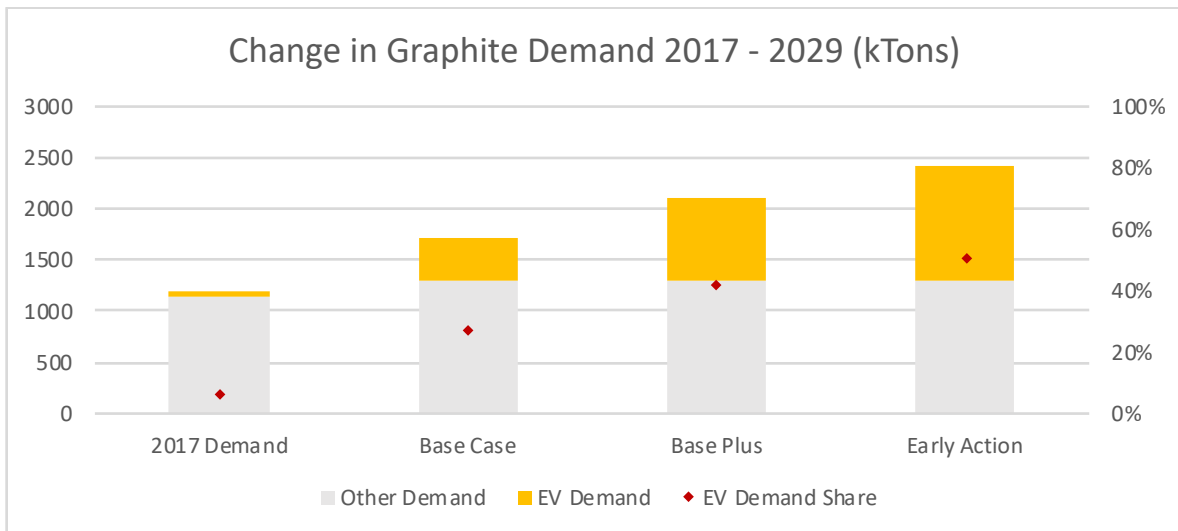


Figure 4.11 Change in graphite demand from 2017 - 2029

5. Supply and Demand for LIB Materials (Phase III)

This chapter will discuss the commodities used in the production of LIBs in detail and will include historical price trends and descriptions of production techniques. Distinctions will be made between the price of a material commodity and any derivatives of that material that may be used as a value-added feedstock that is a more desirable precursor for LIB production.

5.1 Commodity Review

The primary commodities used in LIB cells are graphite, nickel, lithium, cobalt, copper and aluminium assuming a majority NMC or NCA mix. This section will summarise the market dynamics behind each one and discuss any relevant value-added derivatives that are popular for battery manufacturing processes.

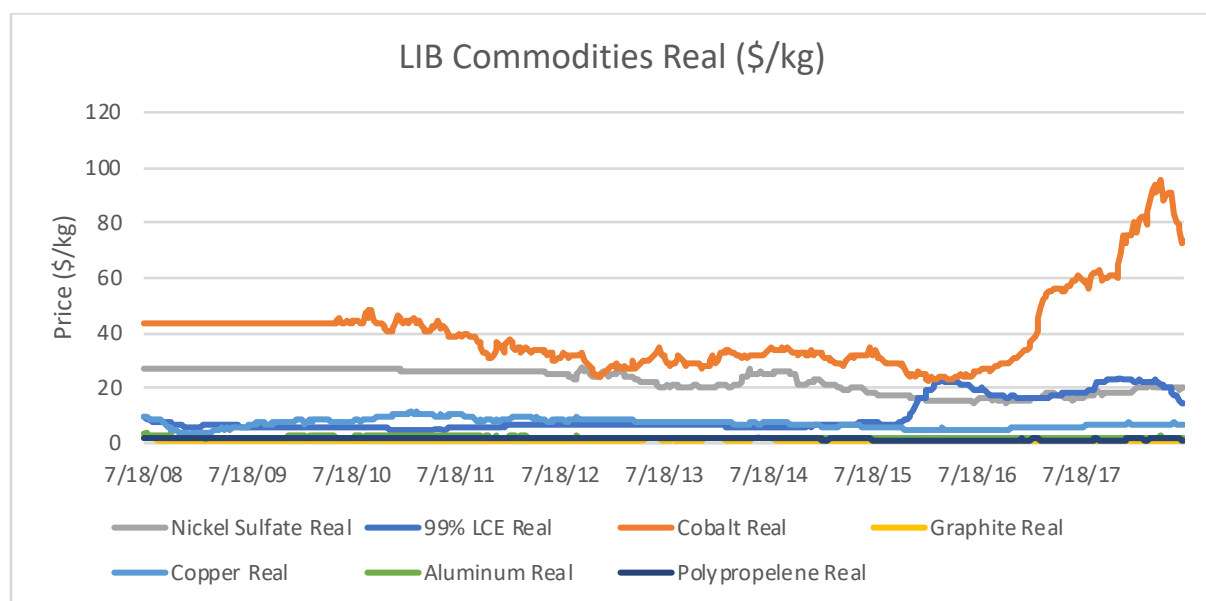


Figure 5.1 LIB Commodity prices in USD per kg from 2008 to 2018 (Bloomberg, 2018)

5.1.1 Lithium

Lithium is typically measured in terms of lithium-carbonate equivalent (LCE). Lithium carbonate has the form Li_2CO_3 , which contains 18.9% lithium. The precursors for cathode preparation are often lithium carbonate or lithium hydroxide of the form $\text{LiOH}\cdot\text{H}_2\text{O}$. Lithium carbonate is preferred for solid-state reactions while lithium hydroxide is preferred for wet mixing and coprecipitation (Liang & MacNeil, 2012).

LCE increased in price from 6.69 \$/kg in 2014 to 13.9 \$/kg in 2017 (USGS, 2018). However, a review of recent lithium supply studies has found that, despite the accelerating growth in demand, there is probably enough lithium in the world to meet an increase in EV demand powered by LIBs (Jaffe, 2017). The current lithium supply could last 431 years, which is much longer than other popular metals such as copper (39) or nickel (31) (Gait, de Floris & Absolon, 2016).

There are two main categories of lithium mines: brine and hard-rock extraction. Of the two, brine extraction has much lower costs to produce battery-grade lithium (Wood Mackenzie, 2018c). Only two of the ten most significant brine deposits in the world are currently producing (McEwen, 2017).

Gait, de Floris & Absolon (2016) of Bernstein Research believe that lithium is experiencing a ‘Schumpeterian moment’: the idea that technological innovation will lead to lower prices for buyers if there is no constraint in supply. Innovation in hard-rock lithium extraction can expand supply and can convert expensive mines into resources. For example, Lithium Australia (2018) uses the Sileach process, which it claims costs a third of traditional hard-rock mines and less than some brine operations. The expansion of lithium supply is compared to the situation in which copper prices fell in the 1990s when previously unsalvageable scrap copper oxide was inexpensively processed with the commercialisation of the solvent extraction and electrowinning process (Gait, de Floris & Absolon, 2016).

Lithium is a geographically concentrated commodity and is mostly supplied from 4 countries: Australia, Chile, Argentina, and China. In 2017, most lithium was mined from 3x spodumene (hard-rock) mines in Australia as well as 2x brine operations each in Argentina and Chile (USGS, 2018).

Country	2017 Production (k US tons)	Reserves (k US tons)	Resources (k US tons)
Chile	14	7,500	8,400
China	3	3,200	7,000
Australia	18.7	2,700	5,000
Argentina	4.4	2,000	9,800
U.S.	Withheld	35	6,800

Table 5.1 Lithium reserves by the top 4 countries in terms of production (USGS, 2018)

5.1.2 Cobalt

Jaffe (2017) has highlighted cobalt as a “serious and potentially unsolvable” problem and has suggested emphasising research on cathode designs which do not use it. In 2018, the price of cobalt rose to 95 \$/kg, its highest level since 2008 and up over 3x from a low of 23 \$/kg in 2016 (LME, 2018). Just under half of cobalt consumption in the United States is used for super-alloys, primarily for efficient aircraft engines and thus it plays a critical role in enabling technology for national security (USGS, 2018). Cobalt’s value in technological applications is derived from its size as a relatively small ion for its electron cloud configuration and therefore enables applications where density is desirable (Olivetti et al., 2017).

Cobalt miners are unlikely to be stimulated by price signals since most cobalt is mined as a by-product. 50% of cobalt production is co-mined with nickel, 35% is co-mined with copper, and only 15% is attributed to primary production (Vaalma et al., 2018). Wood Mackenzie (2017c) observes that copper or nickel economics set cobalt economics. For example, Cobalt can account for 2% of the revenue of the by-product of a nickel miner. However, a simultaneous increase in nickel possibly due to EV demand for nickel-based cathode materials could shift industry from Nickel Pig-Iron (NPI) to Nickel-Cobalt projects and recycling is planned to attract more attention as supply is strained (Wood Mackenzie, 2017c). Some researchers worry that an economic downturn could reduce nickel demand in stainless steel which would lead to reduced cobalt production as a by-product (King, 2018).

Supply of cobalt is also heavily concentrated. 49% of global reserves and 63% of cobalt mined in 2017 is in the Democratic Republic of Congo (DRC) (Wood Mackenzie, 2017c). The “Central African Copper Belt” is in a politically unstable region with significant reported human rights abuses (Vaalma et al., 2018). Cobalt refining, the next step in the process after mining, is also geographically concentrated in China with 80% of Chinese cobalt consumption used for LIBs (Olivetti et al., 2017). Despite its history as a by-product, “pure-play” cobalt facilities do exist particularly near the Ben Azzer in Morocco (King, 2018).

Country	2017 Production (k US tons)	Reserves (k US tons)	Primary Product
Congo	64	3,500	Cu
Australia	5	1,200	Ni, Ni-Cu
Cuba	4.2	500	Ni
Total		7,100	

Table 5.2 Cobalt production, resources, and reserves (USGS, 2018)

The world reserve for Cobalt is considered to be 25M US-tons. However, the reserve grows to 120M US-tons if one considers the cobalt located in manganese nodules on the ocean floor (USGS, 2018). The Tesla Gigafactory will require 6-7 metric-tonnes of cobalt per year which will be supplied by Panasonic via Sumitomo. Cobalt-free LIBs such as LFP and LMO are declining in popularity. However, some beyond-lithium-ion chemistries such as lithium-air or lithium-sulphur do not contain any cobalt (Wood Mackenzie, 2017c).

5.1.3 Graphite

Graphite is the most popular anode chemistry in LIBs. It is made of highly-ordered carbon rings, each containing six carbon atoms. If the structure is not ordered (crystallised) then it is considered non-graphitic. The heat treatment of solid phase material creates non-graphitic carbon, whereas graphitising carbon is derived from gas and liquid phase material (Winter & Besenhard, 1999).

Over half of graphite demand comes from the steel industry, where it is used to make electrodes for arc furnaces. Batteries currently consume use 8-10% of global supply (Hayes, 2016). The USGS (2018) notes that 65% of graphite is mined in China and that only Brazil and Turkey are known to have more abundant graphite reserves. Natural graphite is unique to other commodities in that it is not traded on a spot market since most buyers procure directly from the mines (Hayes, 2016). Some new graphite producers will vertically integrate the value-added process to supply value-added product directly to EV LIB manufacturers (Syrah Resources, 2015)

5.1.3.1 *How is Synthetic Graphite produced?*

Synthetic graphite is produced from a mixture of petroleum coke and coal-tar pitch, whose availability and pricing are linked to trends in the coal and steel industry (Jäger et al., 2012). Petroleum coke is the residue from the petroleum distillation process where petroleum pitch is heated in a nitrogen atmosphere (Nishio & Furukawa, 1999). The coke is finely ground, kneaded with coal-tar pitch, formed, and then heated to very high temperatures above 2000°C to create synthetic graphite (Jäger et al., 2012).

5.1.3.2 *How is Natural Graphite produced?*

Graphite is mined as flakes and categorised in a series of grades called meshes. A mesh number is the count of how many openings there are in a square inch of the screen used to filter graphite (Netafim, 2018). Syrah Natural Resources (2017) reports a plan to supply 40% of the natural graphite market by 2020. Their process uses a fine -100 mesh graphite to refine into battery grade graphite product. This means that the graphite particles used are the ones that filter through the 100-mesh screen and are less than 150 microns in diameter.

After the natural graphite is filtered, it is ground to a more uniform size of 10 microns. This phase of the process can have a yield of roughly 30% (Hayes, 2016, USGS, 2018). This product is called uncoated spherical graphite. Coating spherical graphite with carbon can reduce the irreversible capacity of the anode (Nozaki et al., 2009). Minimising the irreversible discharge in a LIB is desirable because it reduces the amount of anode material that must be oversupplied to match a battery cell's designed charge capacity (Nelson & Gallagher, 2014). For these reasons, coating graphite with carbon is a key value-add process to enable coated spherical graphite (CSG) to be used for the battery manufacturing process.

5.1.3.3 *How do Synthetic and Natural Graphite differ?*

Synthetic graphite is thought of to be of a higher purity for battery manufacturing because its process of formation can be controlled (Hayes, 2016). For this reason, value-added coated spherical graphite derived from synthetic means sells at a 40-50% premium to natural graphite, but this also provides an economic incentive to supply high-purity CSG derived from natural sources (Verner, 2018).

Avicenne Energy, a consultancy focused on the battery market, has predicted that the prices for natural graphite will fall from 15 \$/kg to 5 \$/kg and synthetic graphite from 20 \$/kg to 10 \$/kg between 2010 to 2025 (Pillot, 2017). The cost premium for synthetic graphite stems from the energy intensity in forming graphite in a high-temperature furnace.

5.1.4 *Nickel*

Most EVs use batteries with cathodes that have high intensities of nickel (typically NMC or NCA formats). According to Wood Mackenzie (2017b) EV demand for nickel is expected to grow over 400% from 2016 levels to 220k metric-tonnes in 2025 even though half of global

nickel products are not suitable for batteries. Battery manufacturers prefer nickel in sulphate form (NiSO_4). McKinsey (2017) distinguishes Class 1 nickel as the only type of refined nickel that can be used as a precursor for nickel sulphate and notes that it has in the past traded at a 35% premium to pure nickel briquettes on the London Metals Exchange (LME) (Figure 5.2). Class I nickel is a nickel product that is at least 99.8% pure (NiPERA, 2018).

New projects may focus on producing nickel intermediates that are better precursors for nickel sulphate and also produce Cobalt.

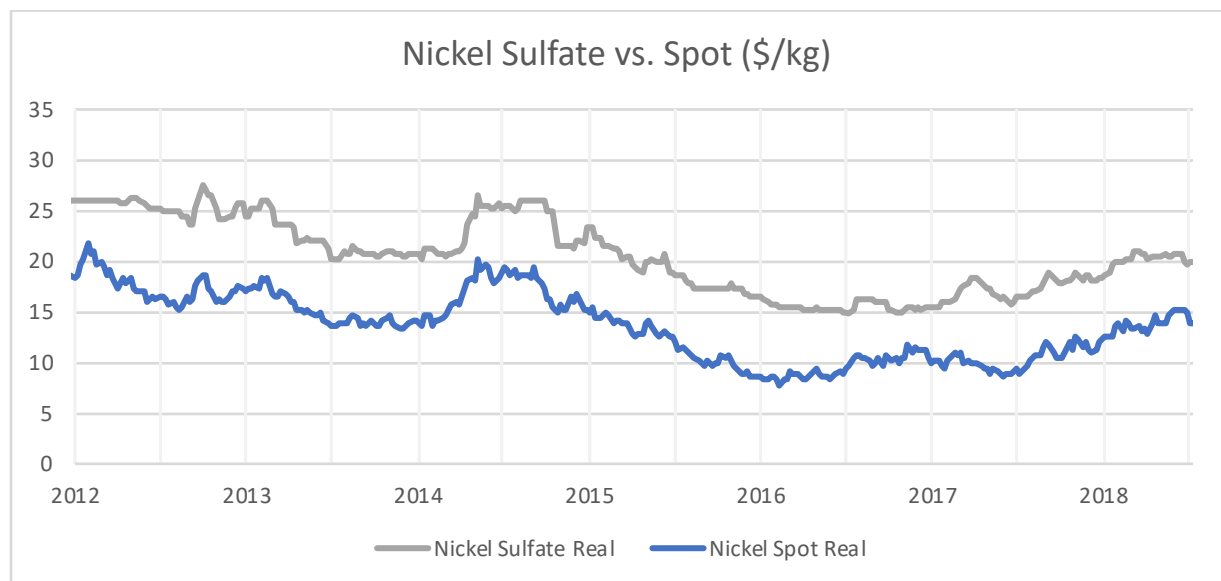


Figure 5.2 Comparison of nickel sulfate and nickel metal spot prices from the LME (Bloomberg, 2018)

5.2 LIB Cell Commodity Costs by Chemistry

Weekly commodity spot prices for the past ten years have been collected through data published on the Bloomberg Terminal. These prices were then standardised into \$/kg-of-metal modulating the spot price by the rate of inflation in 2018 terms by the Bloomberg US GDP deflator. The prices were then multiplied by the metal intensities for the three variants of NMC focused on for this study (333, 622, and 811) and charted weekly for the past ten years in Figure 5.3.

The commodity costs normalised by energy capacity Figure 5.3 show that varying the chemical compositions of LIB active materials have effects on price volatility. While high nickel NMC chemistries are being developed to increase LIB energy density, they also have the

effect of reducing the impact of volatile cobalt prices. In 2018, as cobalt experienced a short price spike, the commodity costs of NMC-333 rose to a 50% premium over NMC-811.

	Nickel Sulfate	99% LCE	Cobalt	Graphite	Copper	Aluminium
Bloomberg Ticker	N3CNFRQV	L4CNVHTQ	LMCODY	GPCNEPOF	LMCADY	LMAHDY
NMC333	0.35	0.74	0.35	0.98	0.27	0.10
NMC622	0.55	0.63	0.18	0.95	0.26	0.10
NMC811	0.62	0.58	0.08	0.96	0.26	0.10

Table 5.3 Bloomberg commodity tickers and metal intensity for battery cell commodity cost analysis.

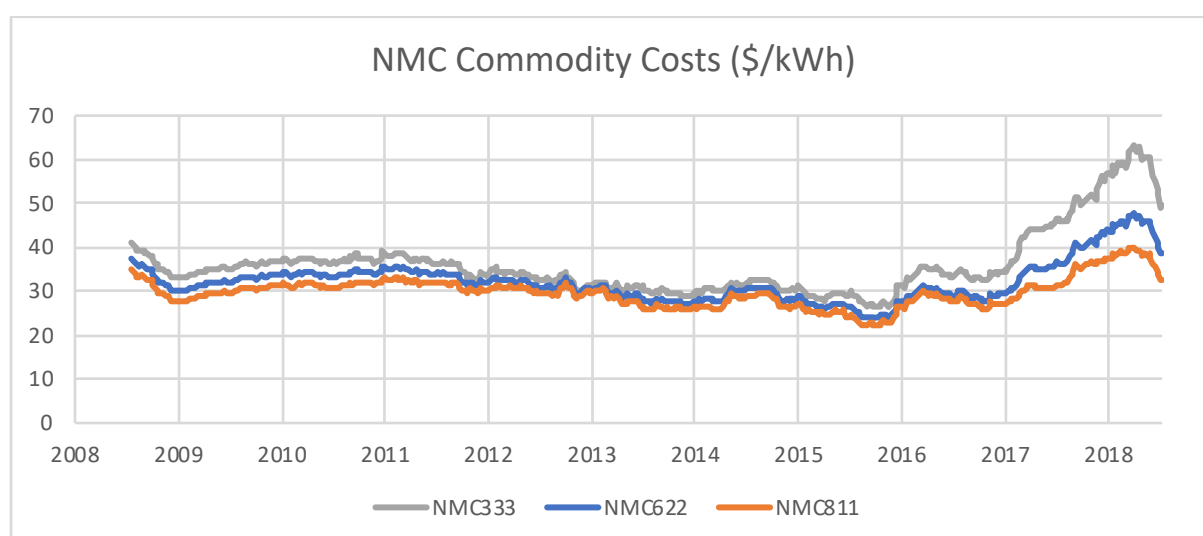


Figure 5.3 Commodity costs for NMC cathode chemistries from 2008 to 2018 (Bloomberg, 2018)

5.3 Supply-Demand Balance for LIB Materials

Wood Mackenzie has provided forecasts on global lithium, cobalt, and nickel supply up until 2030. Forecasts for graphite were not provided, but graphite is also treated differently since it can be synthesised easily apart from natural graphite extraction. Based upon their knowledge of existing and planned mining projects and the economics of the metals market, Wood Mackenzie categorises future metals supply into “base case”, “probable”, and “possible” categories. The projects in the “possible” category have the highest risk or most expensive costs.

The supply-demand balance figures in this section will chart the projected market supply for the commodities studied and compare them with all sector demand for the metal including

demand from the EV sector. Demand from other sectors is assumed to be consistent through each scenario for these figures. However, scenarios with higher commodity demand, such as the “early action” scenario, might suppress demand from other sectors due to higher commodity costs and potential product substitution.

Wood Mackenzie forecasts long-term incentive prices based on their proprietary analyses of mine and project costs (Wood Mackenzie, 2017d). They will adjust prices based on business conditions such as country risks, competitive rates of return and the forecasted supply gap. However, price forecasts revert to a constant trend after ten years since they believe that is a threshold for predicting market conditions. The underlying assumption in these price models is that supply and demand match over a long-term equilibrium.

Incentive price modelling compares the internal costs of known and potential sources of product supply along a curve. A theoretical example of such a curve is shown in Figure 5.4. The incentive price for the market is set by the incentive price of the marginal firm required to meet market demand. In the example, the left side shows it is possible for producers with lucrative by-products to have a negative incentive price (implying a cost to the firm not sell the product). It is also possible to have producers with very high incentive prices that act as ceilings on the market. For metals, this could represent production from difficult to access resources such as subsea nodules for cobalt or seawater for lithium (Speirs et al., 2014, USGS, 2018)

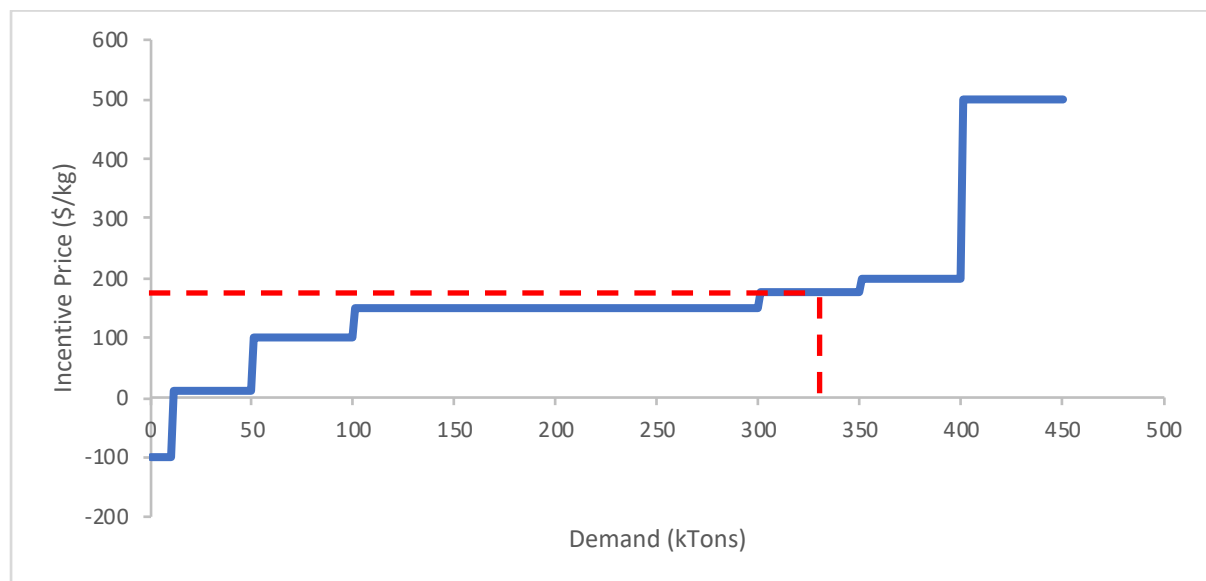


Figure 5.4 Theoretical incentive price curve (Speirs et al., 2014)

5.3.1 Lithium

The lithium supply is expected to double from 400kT per year in 2017 to 800kT per year in 2021. Furthermore, demand forecasts from this thesis do not predict riskier sources of supply until at least 2026 for the climate-constrained scenarios. The lithium supply-demand balance for the “base’ and “base plus” EV demand forecasts rely only upon base-case supply throughout the next decade.

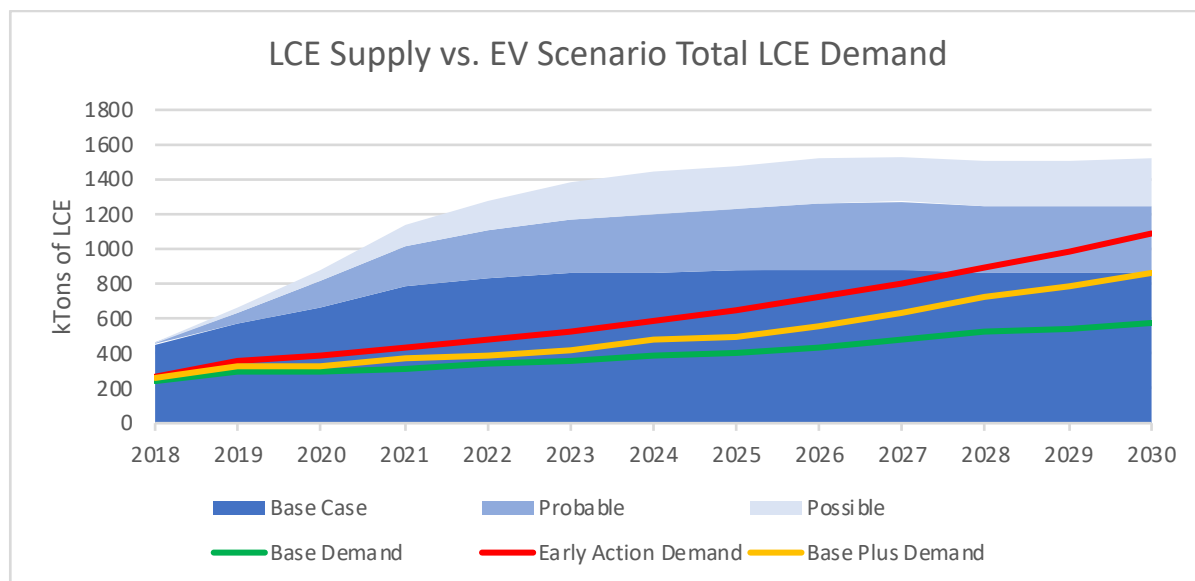


Figure 5.5 Lithium supply-demand balance from 2017 to 2030 (Wood Mackenzie, 2018a)

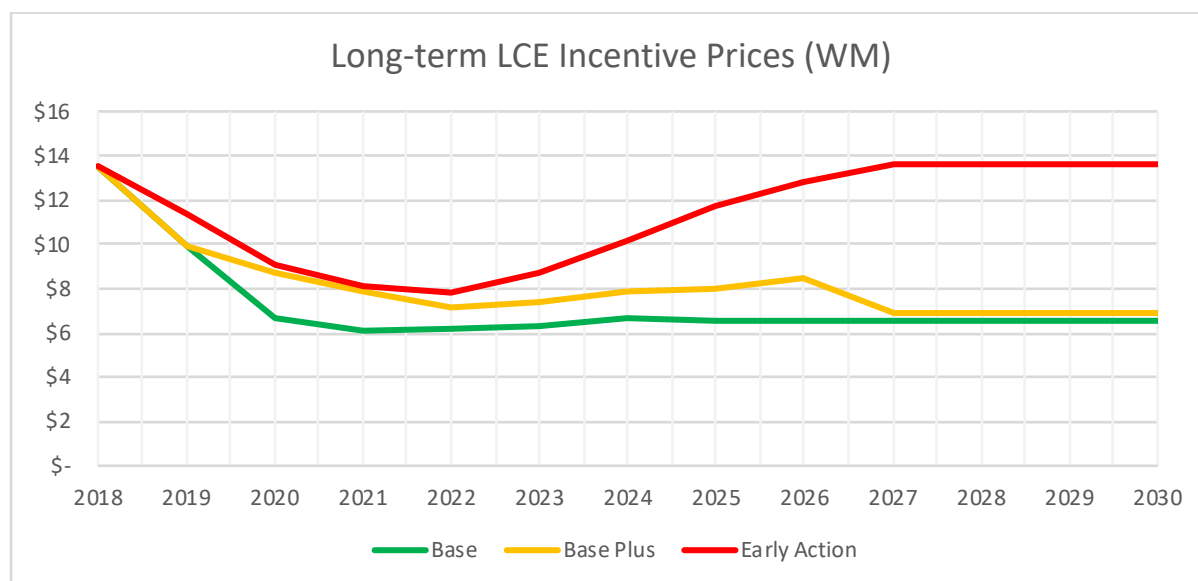


Figure 5.6 LCE long-term incentive prices (Wood Mackenzie, 2018a)

A situation where lithium supply will outpace demand may favour lithium buyers over the next decade. Oversupply of lithium may lead to a price crash from \$14/kg in 2018 to just over \$7/kg in real 2018 terms. SQM, a Chilean producer who has the capacity to supply an eighth of the market, warned investors that prices would fall in 2018 (Sanderson, 2018). Deflation in the lithium price in the short term is predicted in all three modelled scenarios. Only in the “early action” scenario is lithium expected to rebound to prices experienced recently.

5.3.2 Nickel

The nickel supply must move beyond its base supply starting in 2021 in order to meet demand by EVs. Although EV nickel demand is projected to be a small proportion of total nickel demand relative to other EV metals, primary nickel mine production is projected to decrease over the next decade on top of growing EV supply.

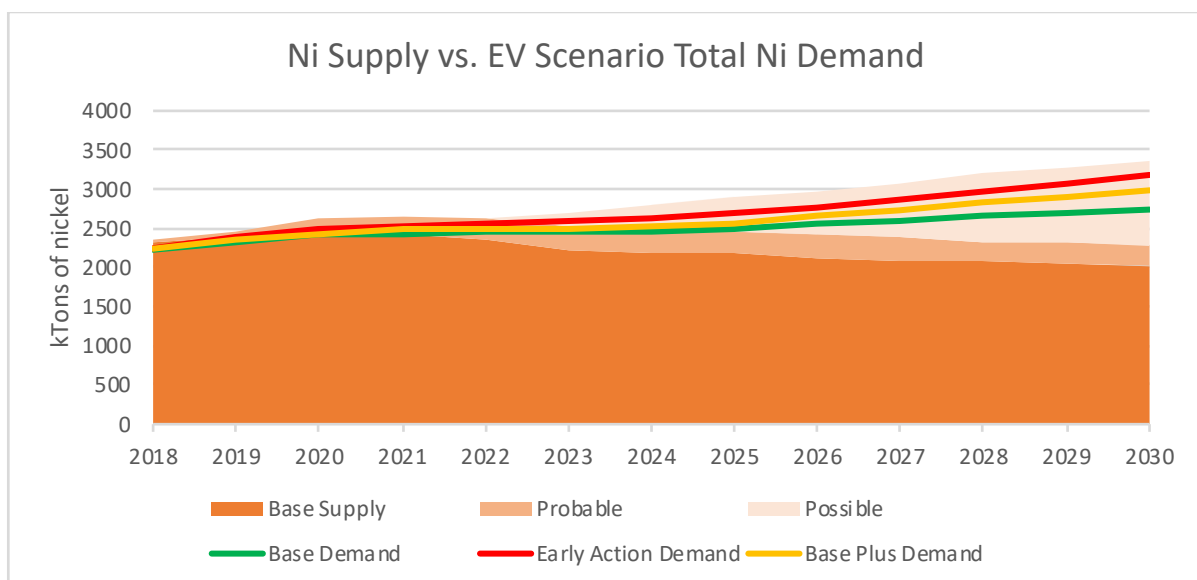


Figure 5.7 Nickel supply-demand balance from 2018 – 2030 (Wood Mackenzie, 2018a)

Wood Mackenzie notes that the average capital intensity of nickel production is estimated at \$50,000 per tonne of nickel per year (Wood Mackenzie, 2018b). Between the “base” and “early action” cases there is 700 to 1,100 kilotons of incremental demand over the base supply case implying that US\$50 billion of nickel projects may need to be financed by the end of the next decade to keep supply and demand in balance.

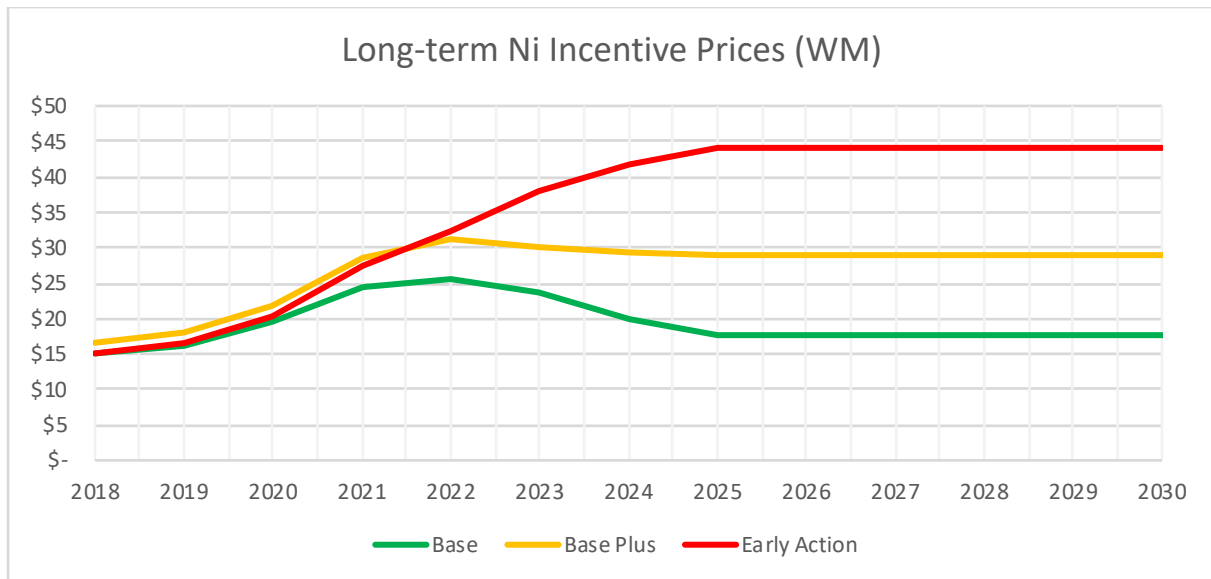


Figure 5.8 Long-term Ni incentive prices (Wood Mackenzie, 2018a)

There is no shortage of nickel, the USGS (2018) accounts for 74,000 kilo-tons of nickel reserves globally. However, Wood Mackenzie is not aware of any expansion plans from major non-Chinese nickel producers (Wood Mackenzie, 2018b). With new assets requiring up to ten years to come online, it is possible that there will be a supply shortage in the mid-2020s.

5.3.3 Cobalt

Cobalt has serious supply concentration issues as a majority of the metal is sourced from the DRC (USGS, 2018). Considering all potential supply including that categorised as “probable,” the cobalt supply may double by 2022. Unfortunately, cobalt demand is expected to exhaust the cumulative output of projects known to Wood Mackenzie by 2025 in the climate-constrained scenarios. Even if demand is limited to the IEA NPS forecast with EV sales weighted toward low-capacity PHEVs instead of high-capacity BEVs, cobalt supplies will still need to rely upon risky and expensive “possible” projects by 2030.

A complicating factor for the cobalt supply is the relationship between incentive prices and new production. Since cobalt is typically a by-product, mines that have low cobalt concentrations will be set by the economics of the primary metal. For cobalt, the primary metal may be copper or nickel. As the previous section on nickel argues, nickel production may need to be expanded to meet EV demand. It will be useful to observe over the next decade whether plans for new nickel production include cobalt co-extraction.

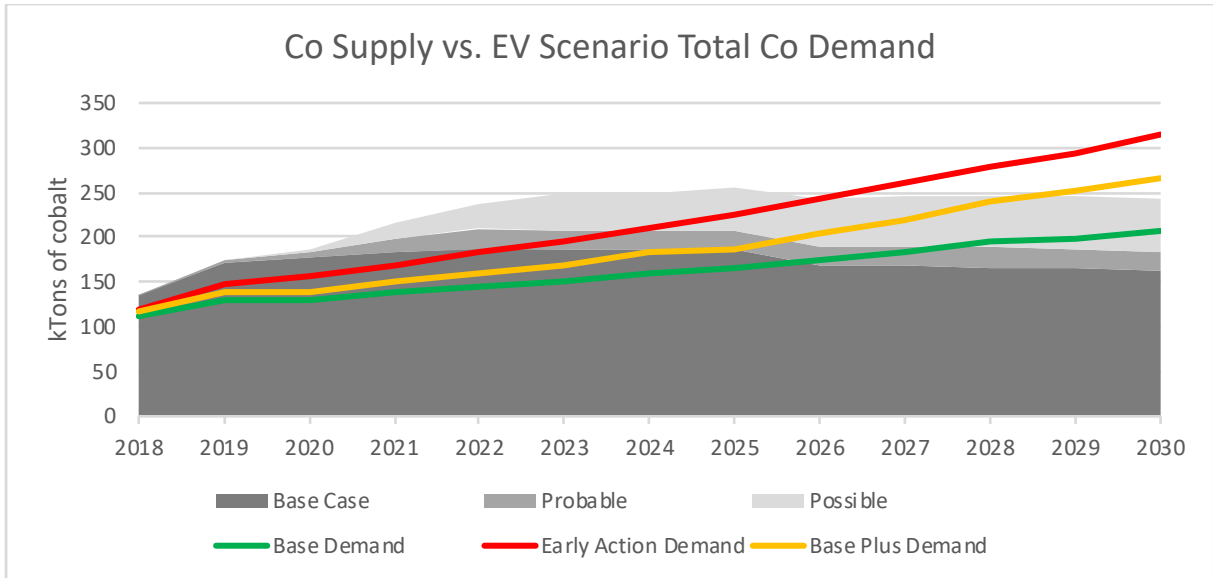


Figure 5.9 Cobalt supply-demand balance from 2018 to 2030 (Wood Mackenzie, 2018a)

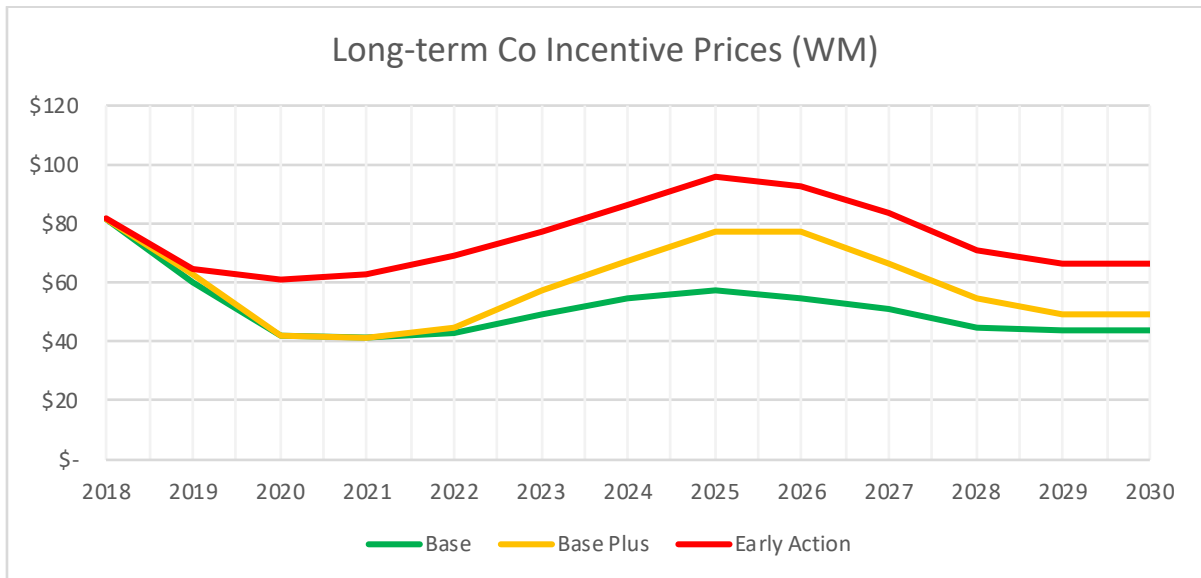


Figure 5.10 Long-term cobalt incentive prices (Wood Mackenzie, 2018a)

5.4 LIB Commodity Price Forecasts by Scenarios

By weighting each price forecast to the element intensities in Table 5.3, indexed price forecasts for long-term incentive prices can be calculated for 2018 – 2030 and are found in Figure 5.11. The curves shown for each scenario are averages of each LIB chemistry studied weighted to the market share of cathodes in 2018. The assumptions made to inform the average “market” prices are found in Appendix III. An in-depth spread of each cathode chemistry price forecast can be found in Appendix IV.

This thesis has found a diverging spread for predicted cathode prices over the next decade. The only difference in metal demand in all three scenarios is demand from the EV battery sector. However, the Wood Mackenzie incentive price models may account for product substitution based on commodity prices, especially in the nickel model where demand from other sectors is more significant than EV demand. While commodity prices may stay near historical levels in the “base plus” scenario, they fall slightly in the “base” scenario and rise to a 92% premium over the “base” level in the “early action” scenario.

The two major trends to consider through each scenario is whether lower lithium prices can offset low rises in nickel prices or whether extremely elevated nickel prices will coincide with elevated lithium prices. Cobalt will likely stay at levels first witnessed in late 2017. However, the trend in LIB chemistries is to reduce the amount of cobalt in NMC or NCA to reduce short-term price volatility and ethical issues associated with its extraction in the DRC.

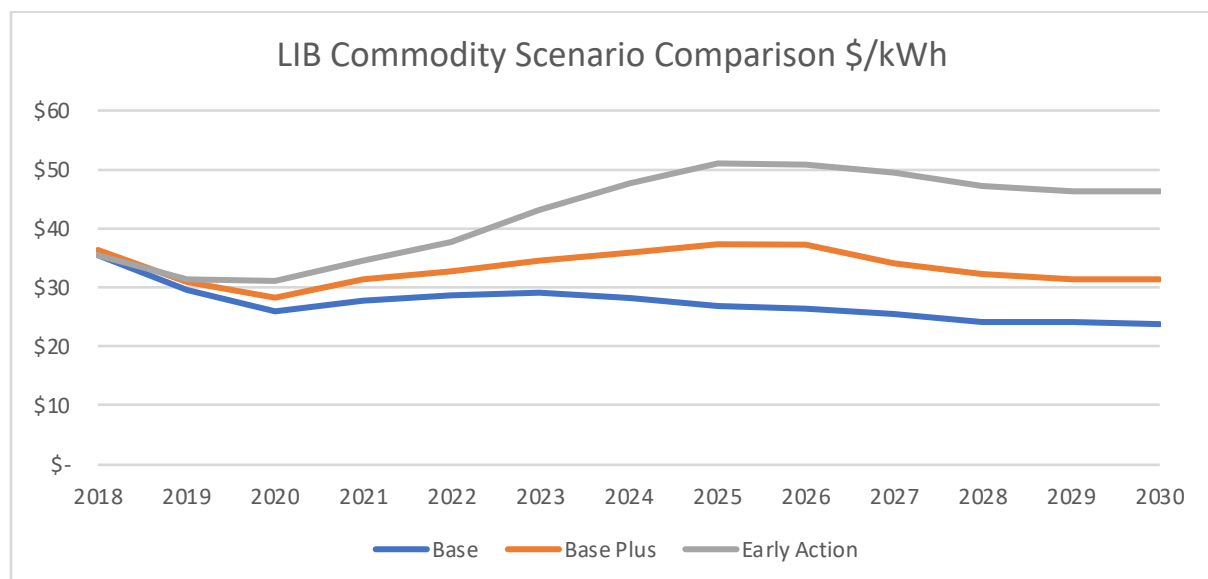


Figure 5.11 LIB commodity price forecasts through the Base, Base Plus, and Early Action scenarios

6. LIB Cost Forecasting with Commodity Price Floors (Phase IV)

This chapter will overview “top-down” technological price forecasting methods and project the cost of LIBs by applying experience curves. Data for the experience curve will be informed by the battery demand projected by Phase I as well as the commodity prices from Phase III. The fundamental costs of LIBs will be introduced as a commodity price floor to estimate the reductions in the “value-added” cost of a LIB EV pack. Finally, LIB pack price forecasts are developed for each scenario modelled in this thesis to understand the effect of EV demand on the cost competitiveness of EVs.

6.1 Forecasting with Experience

Cost reductions in technology by scale originate from Wright’s (1936) observations in the aircraft industry which showed that material and labour costs decrease as a factor of accumulated output. Decreases in cost in a single product or process is called a learning curve. Moore (1959) observed that processes in many different industries exhibit the “0.6 power rule” which observes that the rate at which capital costs grow through scaling manufacturing is comparable to how the surface area of a sphere grows as its volume grows to the $2/3$ power. In simple terms, the capacity of a container grows at a much faster rate than the area of material to build the container. This implies that processes that scale-up are inherently more efficient than those that are very small.

Henderson (1968), the founder of the Boston Consulting Group, distinguished the experience curve as a macroeconomic tool that can consider effects beyond simple labour and production costs in a particular industry and can include phenomena such as the loss of more expensive competition as consumers choose the most optimal products. After introducing the concept of the experience curve, Henderson (1973) observed that the most reliable measure of cost for experience curves are total organisational cash flows, implying that costs separate to the production process such as overhead and management are essential. By tracking technology cost by production, the experience curve model incorporates a mix of different effects of scaling manufacturing and efficient techniques that can be communicated across the industry.

Applying experience curves has been a principal argument in favour of investing in the sustainable energy industry. Rick Swanson, the founder of SunPower, observed that the photovoltaic industry exhibits a modest 20% cost fall for every doubling in production in a phenomenon called “Swanson’s Law” by The Economist (2012).

6.2 Learning Rates applied to LIBs

In 2017, BNEF published a LIB price survey which predicted LIB costs out to 2030 using a Wright's law learning curve (Figure 6.1) (Frith, 2017). In the report, Bloomberg predicted that LIBs would reach the \$100 mark, which suggests cost-competitiveness with ICEVs, by 2025-26. However, BNEF also predicted that a step-change in chemistry would be required for LIBs to reach any further cost reductions beyond then (Frith, 2017). While BNEF does not publish their methodology, the calculation of their experience curve can be replicated if the LIB prices and volumes in 2011 and 2017 are treated as endpoints, and the experience rate is calculated between them. This method generates a learning rate of 18.6% (Table 6.1) on the LIB pack with an R² value of 0.9156 (Table 6.2).

$$\frac{\text{Log (new price)} - \text{Log (old price)}}{\text{Log(new deployment)} - \text{Log (old deployment)}} = \text{Learning Curve Gradient}$$

Equation 6.1 Wright's Law Equation for Learning Curve Gradient (Frith, 2017)

$$1 - 2^{\text{Learning Curve Gradient}} = \text{Learning Rate}$$

Equation 6.2 Wright's Law Equation for the Learning Rate (Frith, 2017)

If the same endpoint method is applied to the five most recent data points, a learning rate of 26% is calculated with an R² value of 0.9510, but only an R² value of 0.8646 to the entire data set. This recent increase in the learning rate suggests that LIB pack prices have been falling more aggressively in recent years. This also demonstrates that learning rates can be arbitrarily defined by the chosen endpoints in the endpoint estimation method.

Kittner et al. (2017) have argued that a recent surge in LIB deployment has coincided with an increase in LIB patenting, and has demonstrated that a two-factor learning curve can help explain the recent steepening of the curve in falling cell costs. LIBs are also a modular technology used in many applications from consumer electronics to stationary energy storage.

Broad learning rate estimations should be applied carefully. Long-term experience curve projections can theoretically reach a cost of zero. Schmidt et al. (2017) remarked that electrical energy storage (EES) technologies such as LIBs should be careful not to use top-down cost forecasting approaches too liberally and that they should generally consider cost floors that can be independent of technological learning.

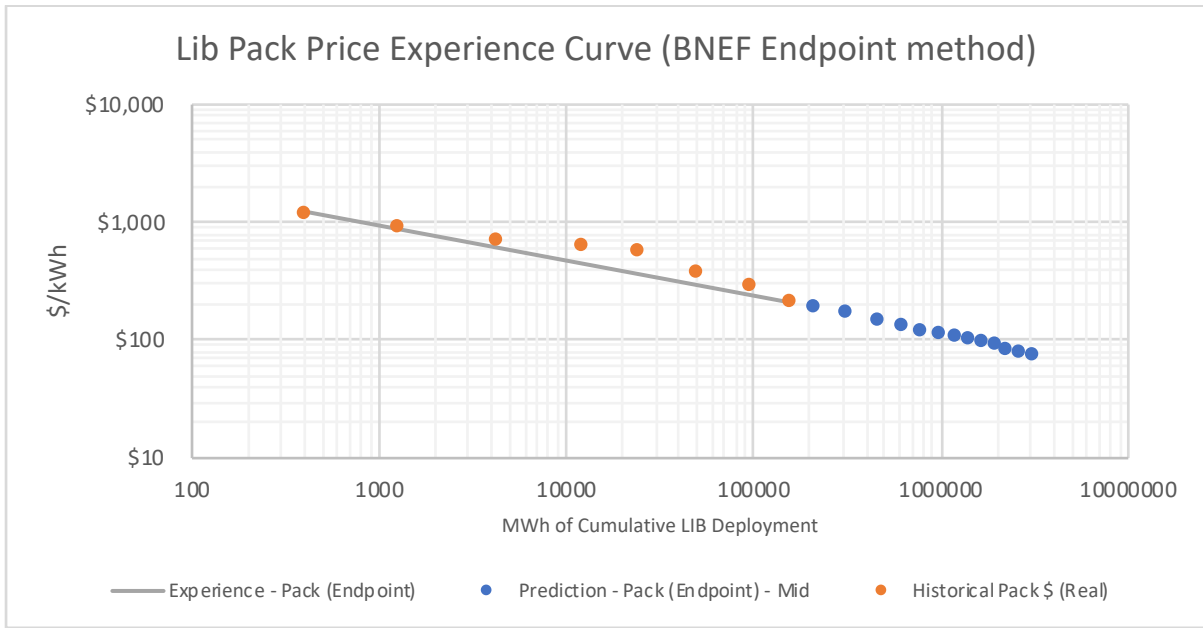


Figure 6.1 Log experience curve of LIB prices out to 2030. Source: (Frith, 2017)

The average of LIB commodities (lithium, nickel, graphite, cobalt, copper, and aluminium) in 2018 dollars indexed to the weighted market share of EV LIB chemistries is shown in Figure 6.2. A close examination shows that the average commodity price of LIB commodities has oscillated about \$30/kWh while the LIB price survey from BNEF (Figure 6.2) reported that prices had plunged 80% since 2010.

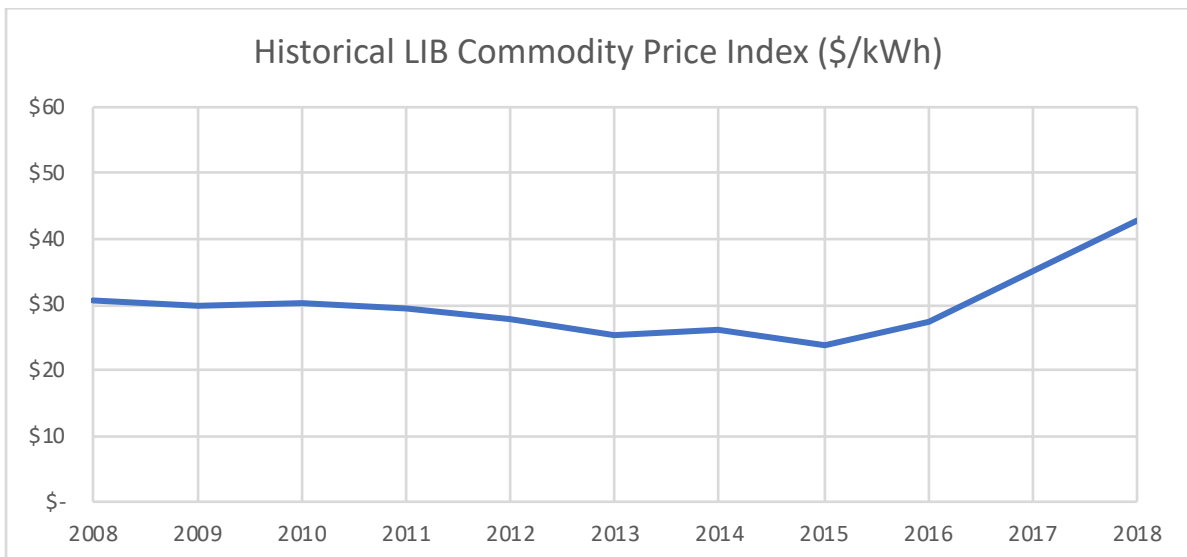


Figure 6.2 Historical LIB commodity price index (\$/kWh) (Bloomberg, 2018)

As pack prices for LIBs have decreased since 2010, the relative proportion of commodities in the active material of a LIB cell has been increasing relative to the cost of the battery pack. In 2017, the cost of LIB commodities per kWh of battery pack reached nearly 20% of total pack costs (Figure 6.3).

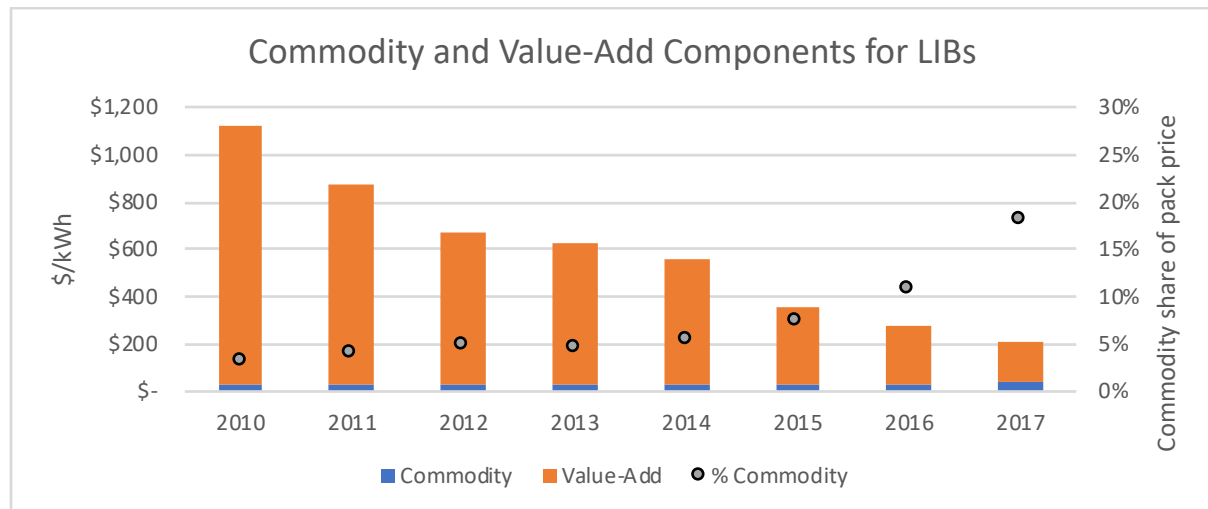


Figure 6.3 Commodity and Value-Add Components for Lithium-Ion Batteries. Source: (Frith, 2017)

Using learning rates to forecast LIB prices based on whole pack price data is more feasible if the ratio of commodity prices is small relative to the value-added cost of the manufacturing process. However, as the price of LIBs converges towards the cost of its input materials, the cost of those materials should be carefully considered.

6.3 Re-calculating Experience Curves

This section will explain the methodology for re-calculating LIB experience curves both by examining the most appropriate fit of the curve through a least-squares technique and by removing the cost of LIB commodities to approximate the learning in the manufacturing process better. Removing the cost of LIB materials from the total pack price results in a portion of the pack cost which will be referred to as “value-add” cost throughout this section.

The learning rate for the “value-add” component should be larger than the total pack learning rate. This is because the price of the “commodity” component (Figure 6.2) has been relatively steady over the past decade and recent price improvements have been attributed to improved economies of scale in LIB manufacturing. Indeed, if a learning rate analysis with the endpoint method is applied to the total pack price, a pack learning rate of 18.6% is calculated. However, when the commodity price is removed from the pack price, the learning rate increases to

19.4%. While removing commodity prices does result in a higher learning rate for the “Value-Add” component, this does not suggest that LIB pack prices will fall more quickly. The forecasted commodity component must be added back. The process of adding back input costs acts as a floor to future LIB pack prices.

The endpoint method for calculating an experience curve, as employed by BNEF, can be calculated by arbitrarily picking two points. The method inherently assumes that prices observed by their LIB price survey are reflective of the costs of production. However, fitting the data through a linear regression model would consider information from all data points and maximise the fit of the model.

A least-squares calculation of battery pack price data using the LINEST function in excel over the log of LIB pack price data and the log of cumulative battery deployment calculates a learning rate with a higher R² fit of .942 compared with .932 calculated in the endpoint method (Table 6.2). The difference in predictions is significant. While BNEF reported a weighted average pack price of \$209/kWh in 2017, the endpoint model would predict a battery price of \$190/kWh in 2018 while the least-squares model would predict prices revert to a higher price of \$240/kWh or plateau until industrial learning can catch-up to the market. The experience curve calculated with the least-square method in Figure 6.4 would suggest that the price observed in 2017 may be a local minimum rather than evidence of an accelerating experience curve. One possible explanation for this behaviour is that manufacturers may be competing for market share by selling their batteries at a price lower than their cost of production.

Learning Rates		
Method	Least Squares	Endpoint
Whole Pack	16.6%	18.6%
Commodity Floor	17.8%	19.4%

Table 6.1 Calculated learning rates for LIB pack prices using a whole pack and commodity floor methods

R ² Fit		
Method	Least Squares	Endpoint
Whole Pack	94.2%	93.2%
Commodity Floor	93.4%	92.6%

Table 6.2 Calculated R-squared fit of LIB pack learning rates of whole pack and commodity floor methods

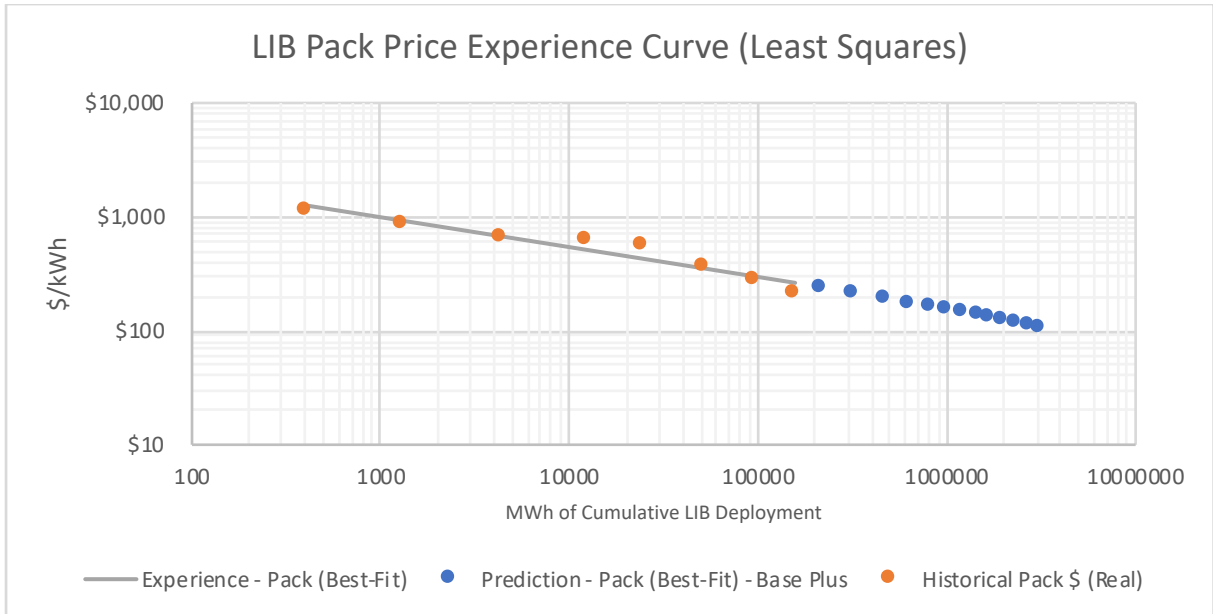


Figure 6.4 LIB experience curve modelled with a best-fit method across two endpoints and by considering the entire pack price

The commodity floor method of calculating the experience curve removes the LIB commodity price index from the reported pack price of lithium-ion batteries and performs a least-squares fit of the resulting “value-added” cost. The “value-added” cost subsequently develops at a faster learning rate while the commodity costs vary only by the balance of the market. Figure 6.5 shows how this method predicts that commodities may reach up to 25% of the price of a LIB pack. Unlike the BNEF model which predicts that LIBs will breach the \$100/kWh threshold by 2026, the “commodity floor” method predicts that this does not occur in the next decade.

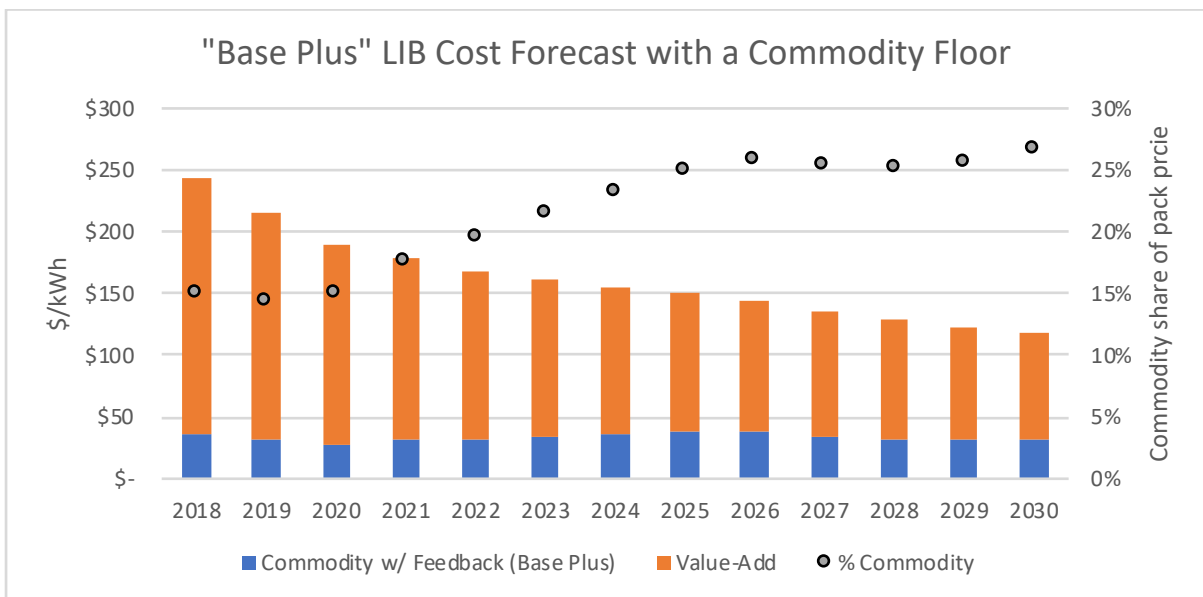


Figure 6.5 “Base Plus” scenario yearly LIB pack price calculated by the least-squares commodity floor method compared with the share of pack price for commodities.

6.4 Comparing Experience Cost Forecasts for Different Scenarios

This thesis has calculated a least-squares experience curve for each EV market scenario. Intuitively, the Early Action scenario sees LIB costs improving much more quickly over time as more EV battery capacity is demanded over the next decade. By 2030, the difference results that an aggressive EV scenario may see a 20% improvement in the “value-added” pack cost over the “Base” scenario (Figure 6.6).

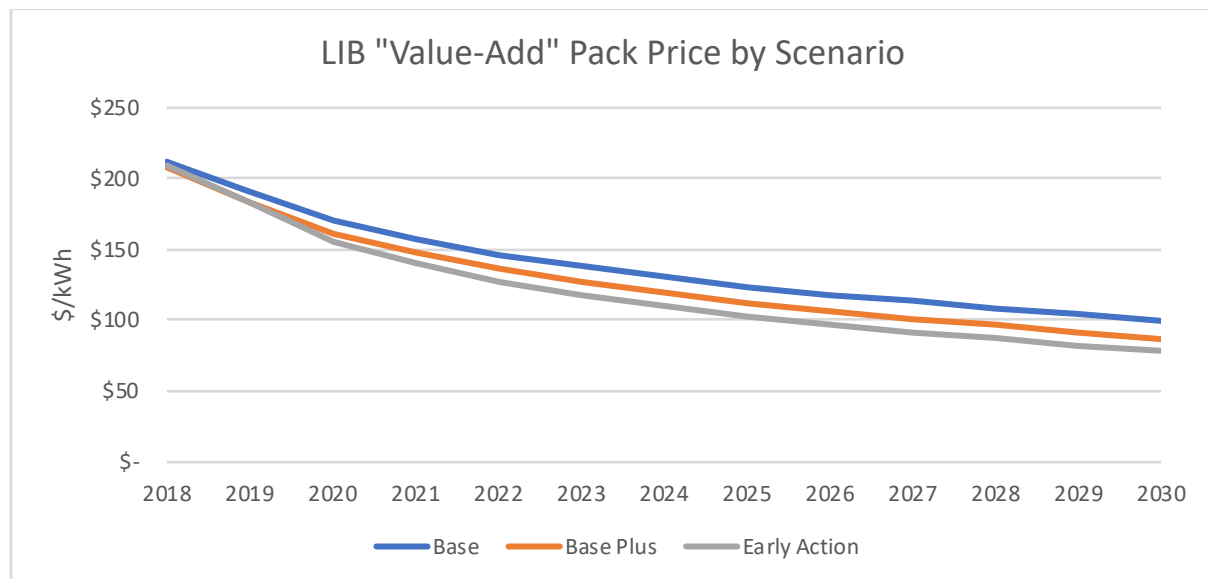


Figure 6.6 LIB "Value-Add" price forecast compared by scenario from 2018 to 2030

Finally, the forecasted average price for LIB commodities in each scenario is added in to calculate the final LIB pack price predicted by the “commodity-floor” model. Surprisingly, this model predicts that EV pack prices may be insensitive to varying scenarios of EV market demand. High EV demand scenarios improve LIB development but increase LIB commodity prices while low EV demand scenarios lack sufficient industrial learning but can take advantage of more favourable LIB commodity prices. Segmented total LIB pack price forecasts for each scenario can be found in Appendix V.

It is important to note that these findings say more about the reaction of future LIB prices as a function of EV market demand than they do about the exact date EVs become cost competitive with ICEVs. If the recent steepening of the experience curve from 2014 – 2017 are genuine rather than artificial, then LIBs for EVs may reach \$100/kWh by 2028. Otherwise, it is possible that cost competitiveness will not occur soon. LIB pack prices should be carefully monitored in the near term to determine which case is most likely.

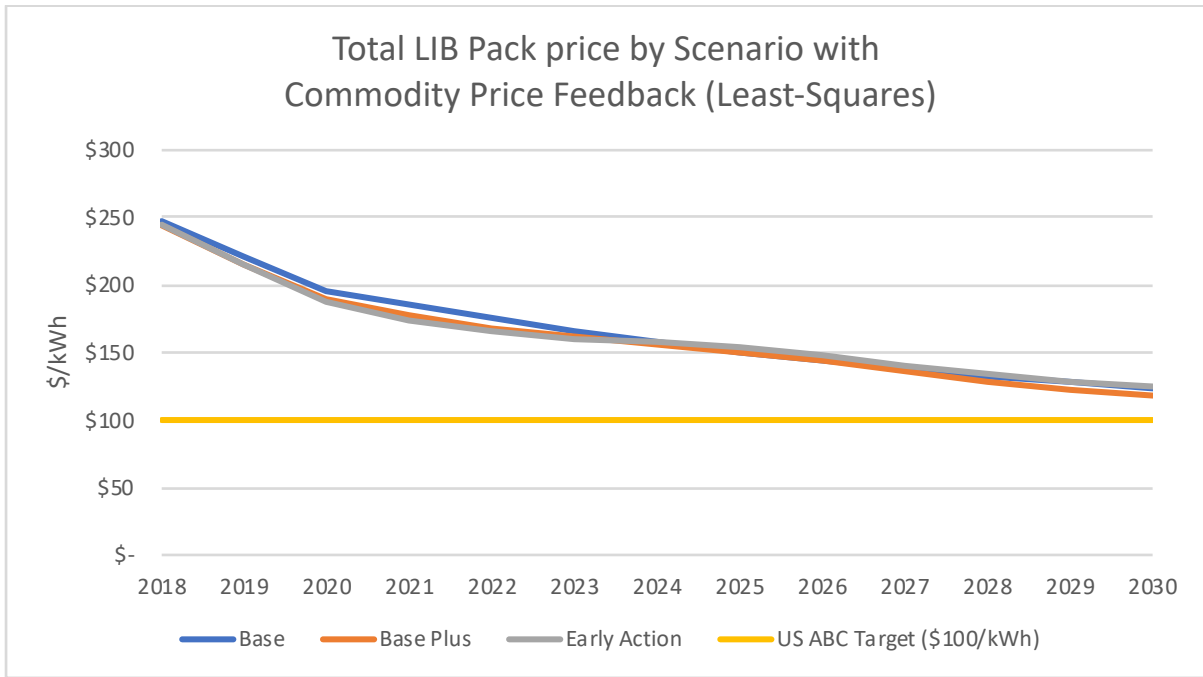


Figure 6.7 Total LIB pack price forecast by scenario with commodity price feedback from 2018 to 2030 using the least-squares method

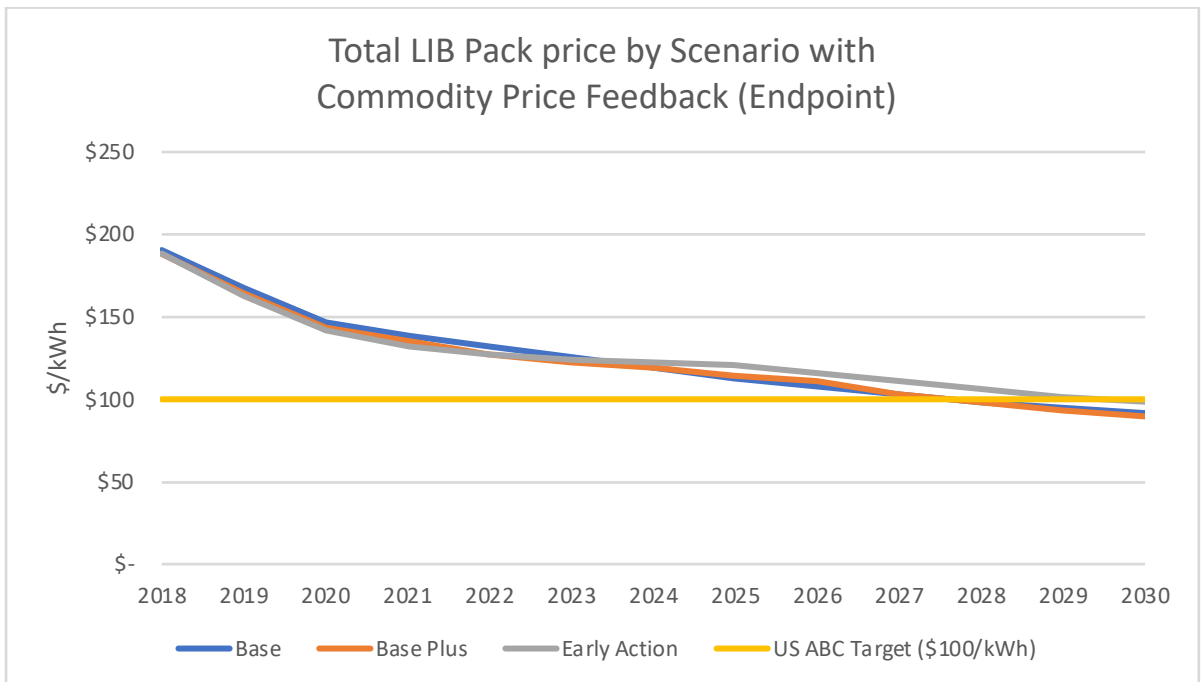


Figure 6.8 Total LIB pack price forecast by scenario with commodity price feedback from 2018 to 2030 using the endpoint method

7. Discussion

In this chapter the findings of the thesis on forecasted EV LIB costs and their impact on the affordability of EVs will be discussed. Battery materials which may overcome the supply bottlenecks identified will be recommended. Finally, the supply challenges facing EVs will be compared to the situation experienced by the crystalline silicon photovoltaic (CSPV) industry in the mid-noughties.

7.1 Results of the Thesis

The forecasts in the final phase of this project suggest that varying magnitudes of EV demand may have a muted impact on the ultimate cost-competitiveness of EVs. Reductions in technology costs as a function of a battery demand seem to counteract rises in input costs due to metal demand. If EVs need to be cost-competitive with ICEVs on a purchase price basis and not just in terms of their total cost of ownership, these findings would predict that market stimulation efforts to increase EV demand might not have their intended effect. While demand side promotion would increase the stock of EVs, it might also increase the cost of valuable commodities used in many other sectors of the economy.

To reduce the cost of EVs, it will become important to focus resources on the supply of critical EV materials such as cobalt, lithium, and especially nickel. The “Early Action” EV case which represented an optimistic climate-constrained EV demand scenario reached a demand-driven value-added component cost of 78 \$/kWh by 2030. With high commodity costs of nearly 50 \$/kWh by the late decade, it will become challenging to reduce LIB costs below the target of 100 \$/kWh. However, if commodity cost prices could reach levels obtained in the low demand “base” scenario, purchase-cost-competitive EVs may become possible.

If the average identified LIB pack price of the three scenarios, \$122/kWh, is the applicable cost for EV manufacturers in 2030, then the powertrain cost for a vehicle with a battery capacity of 60 kWh would fall by nearly \$5,000 (30%). Assuming that the costs of ICEV powertrains will rise over the next decade by 3% annually to reach emissions targets (BofAML, 2017) and that the non-LIB EV powertrain costs do not change, the cost of a VW golf would still be \$2,000 less than a mid-range EV such as the Chevy Bolt. Due to commodity price feedback effects, increasing EV demand as a cost-reduction tool may not lower LIB prices. However, not considered are learning effects for non-LIB powertrain components which presumably could improve most under an “early action” type scenario.

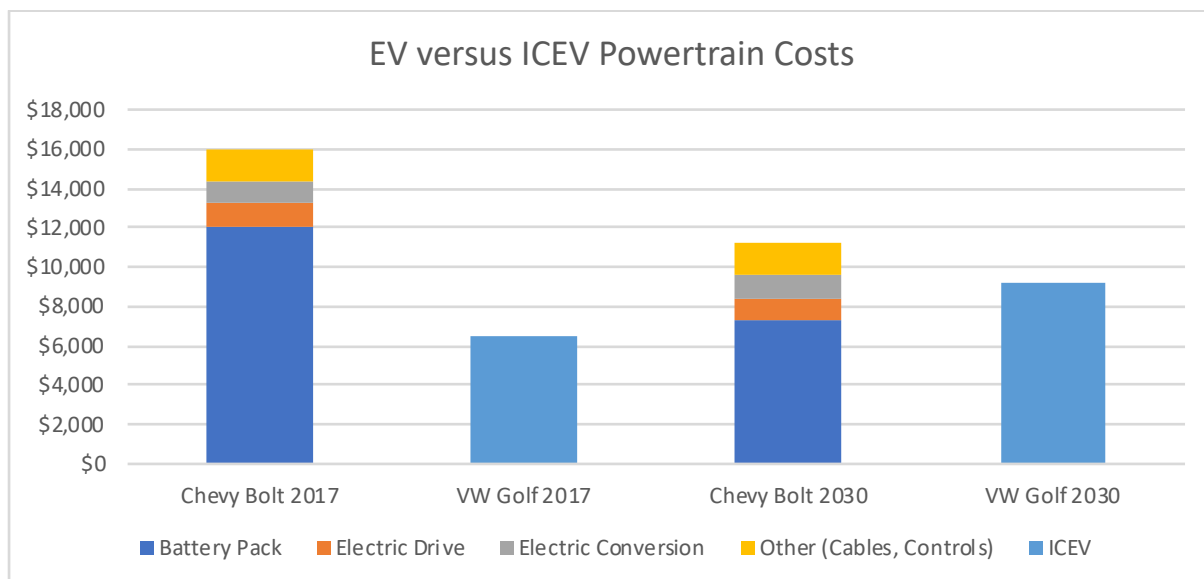


Figure 7.1 Comparison of comparable EV and ICEV powertrain costs in 2017 and 2030 (BofAML, 2017, UBS, 2017)

Drivers would likely see lower costs of ownership from both a reduction in maintenance and fuel costs.

Table 7.1 shows a simplified cost analysis between the costs modelled in Figure 7.1 including assumptions about the price of fuel and vehicle energy efficiency. If fuel is considered the most visible cost to consumers, the EV-ICEV price gap for the U.S. market in 2017 would be overcome after fuels savings over 135,000 miles, while the gap in 2030 would require only 50,000. In Europe, where petrol prices are much higher than in the US, the gap drops from 50,000 miles to 20,000 by 2030. With fuel prices as low as they are in the U.S., EVs may require more cost reductions to be widely considered economically competitive.

One possibility to reduce the cost of LIB commodities would be to switch to cathodes which use fewer valuable metals. As the EV industry is moving towards higher concentrations of nickel in LIB cathodes (Tesla-Panasonic, which has a third of the battery market, already uses a very high nickel NCA chemistry), nickel production will become heavily constrained. While high nickel NMC cathodes have a higher energy density, and require less overall material, switching 60 \$/kg cobalt to use 45 \$/kg nickel may prove to be a counterproductive activity.

This project suggests that nickel-intense cathodes while providing excellent cycle life, performance, and energy density, may be a good solution for the high-end EVs but would not provide economic appeal for a mass-market vehicle. It would be advantageous to develop chemistries that use lower cost elements such as manganese or iron instead of nickel or

cobalt. Suitable alternatives include a layered lithium-manganese oxide (as opposed to the spinel LMO) or advanced lithium-iron-phosphate or lithium-manganese-phosphate olivines (Bakenov & Taniguchi, 2012, Schmuch et al., 2018).

	U.S. 2017	U.S. 2030	Europe 2017	Europe 2030
Electricity Price (\$₂₀₁₇/kWh)	0.12	0.12	0.24	0.24
Petrol Price (\$₂₀₁₇/gallon)	2.5	2.5	6	6
ICEV eff. (MPG)	25	40	25	40
EV eff. (Wh/mile)	250	200	250	200
EV-ICEV Powertrain Gap (\$₂₀₁₇)	9,500	2,000	9,500	2,000
\$/mi ICEV	0.10	0.06	0.24	0.15
\$/mi EV	0.03	0.02	0.06	0.05
Miles to Gap	135,714	51,948	52,778	19,608

Table 7.1 ICEV and EV fuel cost comparison (BofAML, 2017, UBS, 2017)

7.2 Lessons from the Polysilicon Shortage

The price of crystalline-silicon photovoltaic modules stalled from 2004 to 2009. Despite two decades of steady price decreases, the cost per watt-peak of CSPVs held at around 4.5 \$/Wp (Figure 7.2). As solar module production rose due to demand stimulation policies in Europe, the polysilicon became a resource bottleneck for the continuation of its learning curve.

Polysilicon for CSPVs is produced by the Siemens process which involves the reduction of trichlorosilane (SiHCl₃) with hydrogen into silicon and gaseous compounds on a heated silicon rod (Gambhir, Gross & Green, 2014). CSPVs require high-quality polysilicon from 5 nines

(99.999%) to 10 nines of purity. The large scale and complexity of polysilicon plants resulted in lead-times of two to five years to begin production and an additional year to ramp-up. Before 2000, more than 80% of polysilicon was consumed by the semiconductor industry. Recently the balance has shifted: the primary consumer for polysilicon is now the CSPV market (90% in 2016) suggesting that PV demand now sets polysilicon economics (Sandor et al., 2018).

Polysilicon production is considered sensitive to supply-demand imbalances because the production facilities have little flexibility to respond quickly to market conditions. Plants are either run at a high utilisation rate (>80%) or shut down (Sandor et al., 2018). This fragility was tested by feed-in tariff policy implementations in Germany and Spain when a quick increase in demand in 2007 caused the price of polysilicon from 50 \$/kg to 500 \$/kg (Gross et al., 2013).

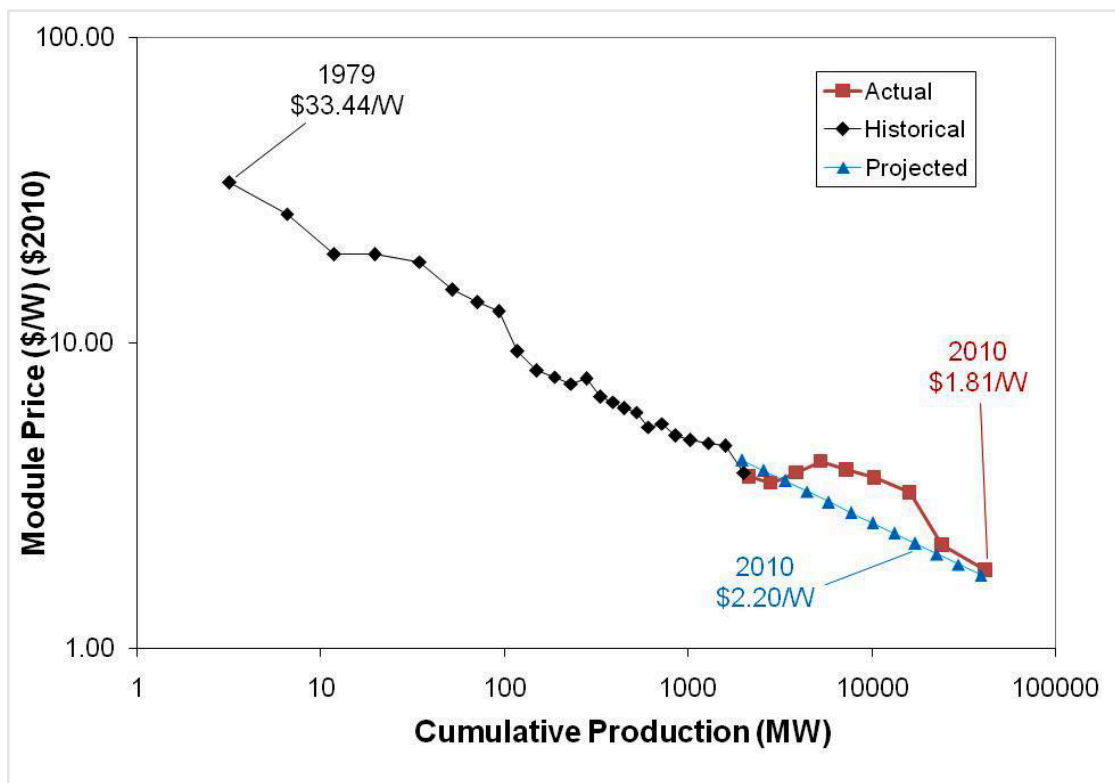


Figure 7.2 CSPV cost improvement by cumulative production projected versus actual 1979 to 2010. Reprinted from Swanson (2011)

Hence, the elevated price of polysilicon stalled the price decreases in CSPV modules. Swanson (2011), the founder of Sunpower, estimated that solar consumers spent \$17 billion more than the historical trend suggested they would have paid. This is due to the shortage of polysilicon as higher polysilicon prices translated into higher CSPV module prices.

The polysilicon shortage demonstrates that price reductions in technology are not guaranteed. Despite well-meaning demand stimulation policies, scarce materials can restrict production from the supply-side to limit cost improvements. New firms emerged to exploit the high prices of polysilicon. Solyndra, a manufacturer of silicon-less thin-film technology, received support from the U.S. government. When the price of polysilicon returned to low levels, Solyndra could not compete and filed for bankruptcy in 2011.

A situation similar to the stalling of crystalline silicon photovoltaic module pricing in the late noughties may occur for EV LIBs if commodity prices rise faster than LIB costs fall. While the price of silica for solar cells is much less expensive than that of cobalt, nickel, or even lithium used in LIBs, the shortage of refined silicon precursor played a significant supply-chain disruption over the life of the CSPV experience curve. Over five years, price signals were able to incentivise new production of refined polysilicon, and the experience curve was able to catch-up to its long-term trend.

However, the analogy breaks down under scrutiny. Polysilicon is a value-added precursor of silica which is derived from sand. The supply chain risk for LIBs is the availability of the fundamental minerals and not necessarily their refined products, although those manufacturing precursors would also be affected. Lead-times for new mining production can be up to ten years while new manufacturing capacity in the CSPV industry only required two to five to start a new polysilicon plant. With LIB demand projected to accelerate, it will be interesting to observe whether commodity price signals act with enough foresight to incentivise sufficient future production. High prices may also act to stifle future demand.

8. Conclusions

This thesis has studied the active materials in LIBs and evaluated the availability of their feedstock metals. Of these metals, nickel has the most uncertain future supply and will likely increase the most in price over the next decade assuming current trends in LIB design. As battery technologies such as NMC are expected to increase in nickel content from equal parts nickel, manganese, and cobalt to majority-nickel compositions, the EV industry is placing greater reliance on the metal.

Metal price forecasts from Wood Mackenzie developed with the EV demand scenarios from this thesis suggest that nickel prices will rise with EV demand. Projections for the commodity costs of LIB active materials suggest that commodities will be 20 to 40% of LIB pack costs by 2030. The experience curve model was adapted to separate commodity costs and “value-added” cost to account for commodity price floors that limit experience curves. The model in this thesis predicts that increased EV demand over the next decade should reduce the “value-added” costs of LIBs through industrial experience. However, these price improvements will also be offset by higher commodity prices.

Future work on this topic should consider alternative non-commercial LIB chemistries such as LMR-NMC, advanced LFP or LMnP. These chemistries minimise the amount of nickel and cobalt in LIB and therefore could reduce commodity price risk. The supply chains for manganese, iron, and phosphorus should be scrutinised in the same detail as lithium, nickel, and cobalt were for this thesis.

The decarbonisation of transportation requires the encouragement of low-emissions vehicles. Unaffordable options will delay the transition, and it is imperative that EVs provide value when compared with ICEVs. The LIB price forecasts for this thesis suggest that commodity feedback effects will prevent EV LIB packs reaching \$100/kWh by 2030, which would make EVs purchase price competitive with ICEVs. To reach this price without a fundamental change in battery technology will require an expansion of the supply of lithium, nickel, and cobalt, particularly in high EV demand scenarios.

Appendix I: Global EV Sales in 2017

Vehicle	2017 Sales	Battery Size (kWh)	2017 Total kWhs	Chemistry	BEV	PHEV
BJEV EC180/200 EV (China)	78,079	22	1717738	LFP	x	
Tesla Model S	54,798	80	4383840	NCA	x	
Toyota Prius Prime	50,833	9	457497	NMC		x
Nissan Leaf EV 2016+	47,211	30	1416330	NMC	x	
Tesla Model X	46,688	80	3735040	NCA	x	
Zhi Dou D2 (China)	42,342	18	762156	NMC	x	
Renault Zoe	31,535	35	1103725	NMC	x	
BMW i3	31,431	27	848637	NMC	x	
BYD Song PHEV 2017 (China)	30,920	18.5	572020	LFP		x
Chevy Bolt	27,982	60	1678920	NMC	x	
Chery eQ (China)	27,444	22	603768	LFP	x	
Chevy Volt (USA + Canada)	26,291	18	473238	LMO-NMC		x
JAC iEV(6/s/e) (China)	25,741	26	25741	LFP	x	
Mitsubishi Outlander	25,530	12	306360	LMO-NMC		x
BYD e5 300 (China)	23,632	48	1134336	LFP	x	
Geely Emgrand EV Old (China)	23,324	41	956284	LFP	x	
BYD Qin PHEV Old	20,776	13	270088	LFP		x
BMW 330e PHEV (2016/2018 - US+EU)	19,815	7.6	150594	NMC		x
SAIC Roewe eRX5 PHEV (China)	19,510	12	234120	NMC		x
BAIC EV-200	18,814	30.4	571945.6	NMC	x	
Hyundai Ioniq	17,241	28	482748	LMO-NMC	x	
VW E-Golf	17,065	36	614340	NMC	x	
Zotye E200 (China)	16,751	24.5	410399.5	NMC	x	
JMC E100 (China)	15,491	15	232365	NMC	x	
BYD Tang PHEV (China)	14,592	18.4	268492.8	LFP		x

Table A.1 Top selling electric vehicles for 2017 including Sales, Battery Size, Battery Chemistry and Application type. Source: (EV-Sales, 2018, EV-Volumes.com, 2018, watteV2buy.com, 2018) and manufacturer reports.

Appendix II: EV Battery Demand by Scenario

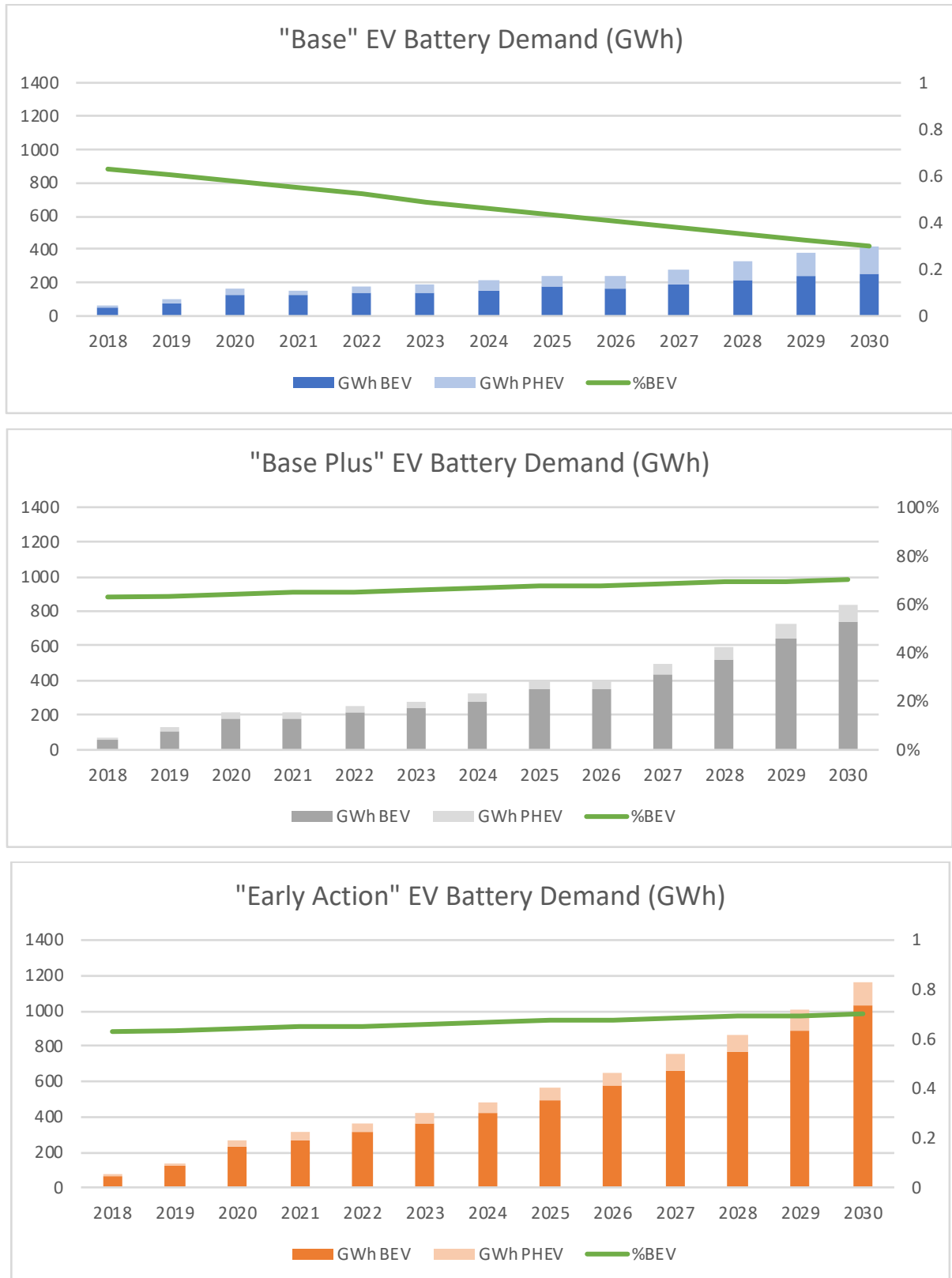


Figure A.2 Comparison of the "Base", "Base Plus", and "Early Action" Battery Demand Scenarios

Appendix III: EV LIB Cathode Market Share Assumptions

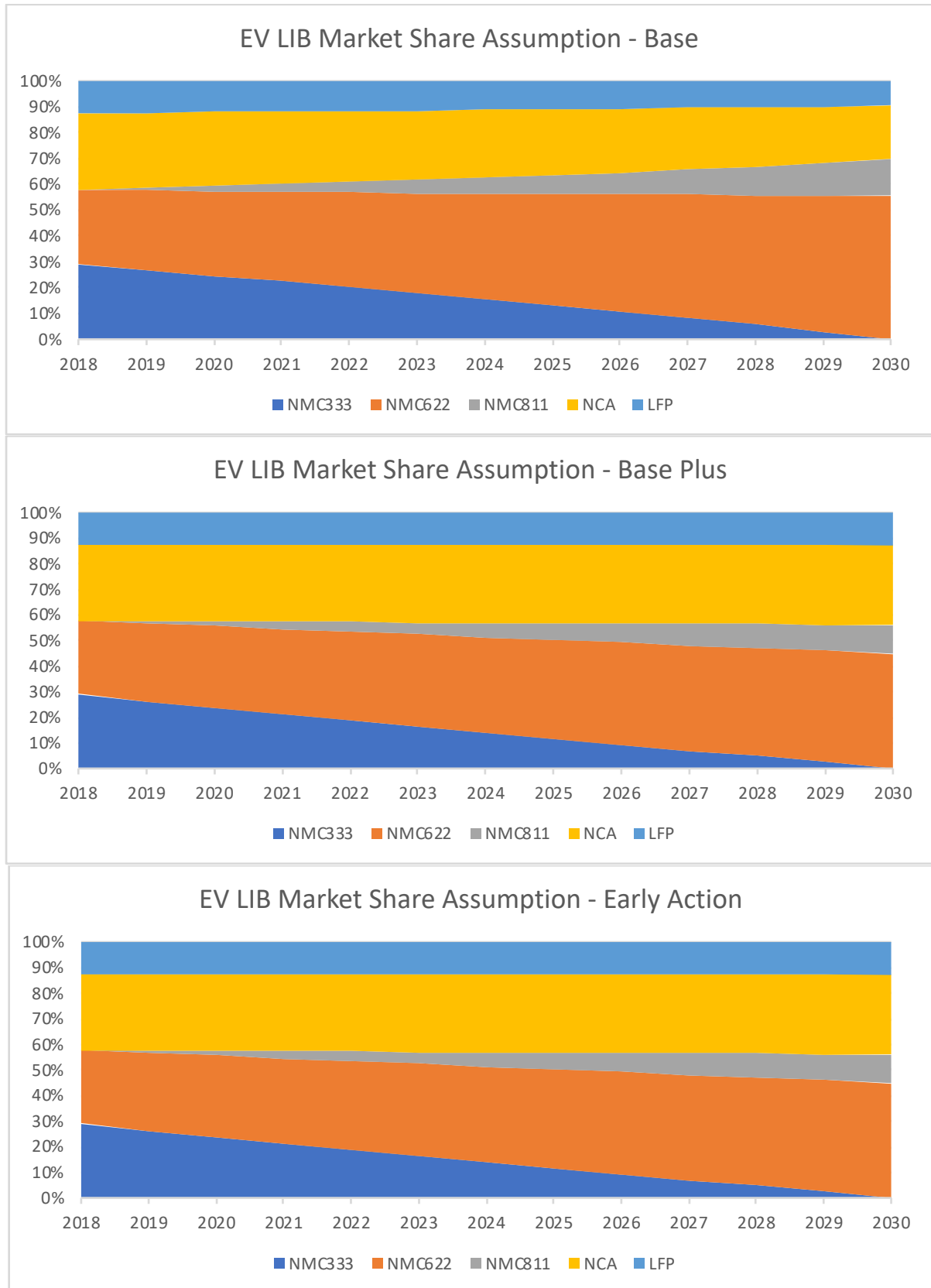


Figure A.3 EV LIB cathode market share assumptions from 2018 to 2030

Appendix IV: EV LIB Commodity Price Forecasts by Scenario

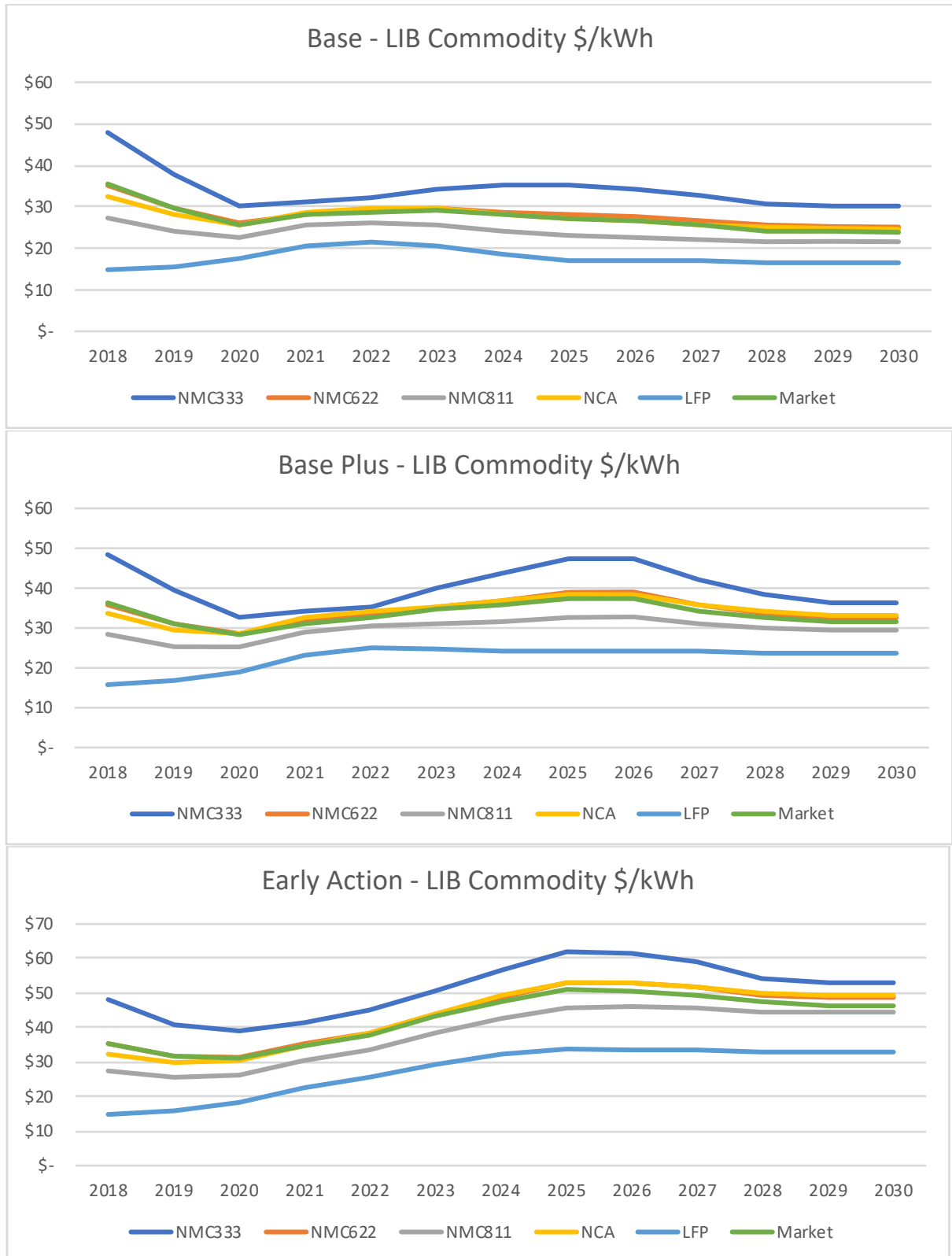


Figure A.4 Comparison of the “Base”, “Base Plus”, and “Early Action” Price Forecast Scenarios

Appendix V: LIB Cost Forecast by Scenario

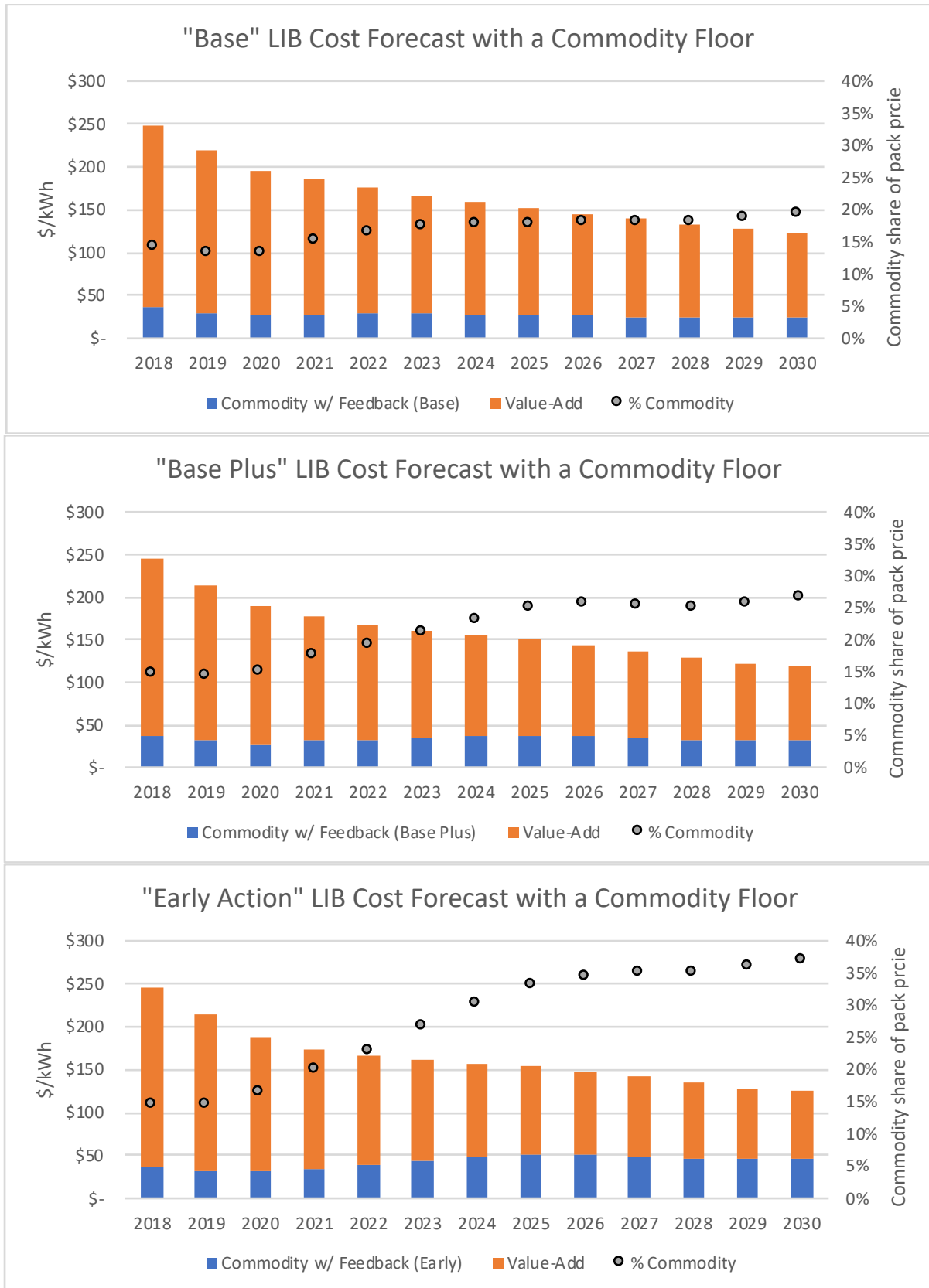


Figure A.5 EV LIB pack price forecasts by scenario with commodity price floor

References

- AESC. (2013) *Cell, Module, and Pack for EV Applications*. Available from: http://www.eco-aesc-lb.com/en/product/liion_ev/ [Accessed Jun 8 2018].
- Albertus, P., Babinec, S., Litzelman, S. & Newman, A. (2018) Status and challenges in enabling the lithium metal electrode for high-energy and low-cost rechargeable batteries. *Nature Energy*. 3 (1), 16-21. Available from: doi: 10.1038/s41560-017-0047-2.
- Bakenov, Z. & Taniguchi, I. (2012) Cathode Materials for Lithium-Ion Batteries. In: Yuan, X., Liu, H. & Zhang, J. (eds.). *Lithium-Ion Batteries Advanced Materials and Technologies*. , CRC. pp. 51-96.
- BCG. (2010) *Batteries for Electric Cars: Challenges, Opportunities and the Outlook to 2020*.
- Bloomberg. (2018) *Bloomberg Professional*. Available from: Subscription Service [Accessed July 10, 2018].
- BMO. (2018) *The Lithium Ion Battery and the EV Market: The Science Behind What You Can't See*.
- BMW. (2016) *BMW Group Technology Workshops - E-Mobility*. Available from: https://www.bmwgroup.com/content/dam/bmw-group-websites/bmwgroup_com/ir/downloads/en/2016/BMWGroup_TechnologyWorkshops_Automated_Driving_Digitalization_Mobility%20Services.pdf.
- BNEF. (2018) *Electric Vehicle Outlook 2018*. Bloomberg New Energy Finance. Available from: <https://about.bnef.com/electric-vehicle-outlook/>.
- BofAML. (2017) *Global Electric Vehicle Primer: Fully Charged by 2050*. Bank of America - Merrill Lynch.
- CEM-EVI. (2017) *EV30@30 campaign*. International Energy Agency. Available from: <https://www.iea.org/media/topics/transport/3030CampaignDocumentFinal.pdf>.
- Cluzel, C. & Douglas, C. (2012) *Cost and performance of EV batteries*. Element Energy. Available from: http://www.element-energy.co.uk/wordpress/wp-content/uploads/2012/06/CCC-battery-cost_-Element-Energy-report_March2012_Finalbis.pdf.
- Curry, C. (2017) *Lithium-ion Battery Costs and Market*. Bloomberg New Energy Finance Available from: <https://data.bloomberglp.com/bnef/sites/14/2017/07/BNEF-Lithium-ion-battery-costs-and-market.pdf>.
- Dash, R. & Pannala, S. (2016) Theoretical Limits of Energy Density in Silicon-Carbon Composite Anode Based Lithium Ion Batteries. *Scientific Reports*. 6 (1), 27449. Available from: doi: 10.1038/srep27449.
- Deign, J. (2016) *South Korea Battery Makers Face a Surprising Challenge in China*. Available from: <https://www.greentechmedia.com/articles/read/South-Korean-Battery-Makers-Face-a-Surprise-Challenge-in-China#gs.CW7Yv2Y> [Accessed August 10th, 2018].

Deutsche Bank. (2016) *F.I.T.T for Investors: Charging the Car of Tomorrow*.

Erickson, E. M., Schipper, F., Penki, T. R., Shin, J., Erk, C., Chesneau, F., Markovsky, B. & Aurbach, D. (2017) Review—Recent Advances and Remaining Challenges for Lithium Ion Battery Cathodes. *Journal of the Electrochemical Society*. 164 (1), A6348. Available from: doi: 10.1149/2.0461701jes.

Erriquez, M., Morel, T., Mouliere, P. & Schafer, P. (2017) *Trends in Electric-Vehicle Design*. McKinsey. Available from: <https://www.mckinsey.com/industries/automotive-and-assembly/our-insights/trends-in-electric-vehicle-design>.

EV-Sales. (2018) *EV Sales*. Available from: <http://ev-sales.blogspot.com> .

EV-Volumes.com. (2018) *EV Volumes*. Available from: <http://www.ev-volumes.com> [Accessed June 27, 2018].

Frederick T. Moore. (1959) Economies of Scale: Some Statistical Evidence. *The Quarterly Journal of Economics*. 73 (2), 232-245. Available from: doi: 10.2307/1883722.

Frith, J. (2017) *2017 Lithium-Ion Battery Price Survey*. Bloomberg New Energy Finance.

Frost, L. (Sep 15, 2014) Exclusive: Nissan faces battery plant cuts as electric car hopes fade. *Reuters*. Available from: <https://www.reuters.com/article/us-renault-sa-nissan-batteries-exclusive/exclusive-nissan-faces-battery-plant-cuts-as-electric-car-hopes-fade-idUSKBN0HA0CA20140915> [Accessed Jun 8, 2018].

Gaines, L. & Cuenca, R. (2000) *Costs of lithium-ion batteries for vehicles*. United States, US Department of Energy (US).

Gait, P., de Floris, M. & Absolon, J. (2016) *Global Metals and Mining - Lithium: The Big Short*. Bernstein.

Gambhir, A., Gross, R. & Green, R. (2014) *The impact of policy on technology innovation and cost reduction: a case study on crystalline silicon solar PV modules*.

Gasgoo. (Dec 06, 2017) BYD power battery production to reach 16 GWh this year. Gasgoo. Available from: http://autonews.gasgoo.com/new_energy/70012136.html .

Gross, R., Heptonstall, P., Greenacre, P., Candelise, C., Jones, F. & Castillo Castillo, A. (2013) *Presenting the Future* . UKERC.

Hayes, T. (2016) *Graphite for batteries*. Edison Investment Research. Available from: <https://www.edisoninvestmentresearch.com/?ACT=19&ID=17404&dir=sectorreports&field=19>.

Helms, H., Kämper, C. & Lambrecht, U. (2015) 2 - Carbon dioxide and consumption reduction through electric vehicles. In: Anonymous *Advances in Battery Technologies for Electric Vehicles*. [e-book] , Elsevier Ltd. pp. 17-34.

Henderson, B. (1968) *The Experience Curve*. Boston Consulting Group. Available from: <https://www.bcg.com/en-gb/publications/1968/business-unit-strategy-growth-experience-curve.aspx>.

Henderson, B. (1973) *The Experience Curve - Reviewed (Part II)*. Boston Consulting Group. Available from: <https://www.bcg.com/publications/1973/corporate-finance-strategy-portfolio-management-experience-curve-reviewed-part-ii-the-history.aspx>.

Howell, D. (2017) *VTO Electrochemical Energy Storage Research and Development Overview*. OEERE VTO.

IEA. (2017) *Global EV Outlook 2017*.

IEA. (2018) *Global Electric Vehicle Outlook 2018*.

IPCC. (2014) *Climate Change 2014: Mitigation of Climate Change*.

IRENA. (2017) *Electricity Storage and Renewables: Costs and Markets to 2030*.

Jaffe, S. (2017) Vulnerable Links in the Lithium-Ion Battery Supply Chain. *Joule*. 1 220-228.

Jäger, H., Frohs, W., Banek, M., Christ, M., Daimer, J., Fendt, F., Freidrich, C., Gojny, F., Hiltmann, F., Reckendorf, R. M. z., Montimny, J., Ostermann, H., Muller, N., Wimmer, K., Sturm, F. v., Wege, E., Roussel, K. & Handl, W. (2012) Carbon, 4. Industrial Carbon . In: Anonymous *Ullmann's Encyclopedia of Industrial Chemistry*. Weinheim, Wiley-VCH. pp. 731-770.

Jürgen, J. & Zeier, W. G. (2016) A solid future for battery development. *Nature Energy*. 1 Available from: DOI: 10.1038/NENERGY.2016.141.

Kim, H. C., Wallington, T. J., Arsenault, R., Bae, C., Ahn, S. & Lee, J. (2016) Cradle-to-Gate Emissions from a Commercial Electric Vehicle Li-Ion Battery: A Comparative Analysis. *Environmental Science & Technology*. 50 (14), 7715. Available from: <http://www.ncbi.nlm.nih.gov/pubmed/27303957>.

King, A. (2018) Battery builders get the cobalt blues. *The Royal Society of Chemistry*. Available from: <https://www.chemistryworld.com/news/battery-builders-get-the-cobalt-blues/3008738.article>.

Kittner, N., Lill, F. & Kammen, D. M. (2017) Energy storage deployment and innovation for the clean energy transition. *Nature Energy*. 2 (9), 17125. Available from: doi: 10.1038/nenergy.2017.125.

Kou, N. (2018) *China Changes Its Electric Vehicle Subsidy Program*. Bloomberg New Energy Finance.

Liang, G. & MacNeil, D. D. (2012) State-of-the-Art Production Technology of Cathode and Anode Materials for Lithium-Ion Batteries. In: Yuan, X., Liu, H. & Zhang, J. (eds.). *Lithium-Ion Batteries Advanced Materials and Technologies*. , CRC Press. pp. 327-393.

Lim, B., Myung, S., Yoon, C. S. & Sun, Y. (2016) Comparative Study of Ni-Rich Layered Cathodes for Rechargeable Lithium Batteries: Li[Ni_{0.85}Co_{0.11}Al_{0.04}]O₂ and Li[Ni_{0.84}Co_{0.06}Mn_{0.09}Al_{0.01}]O₂ with Two-Step Full Concentration Gradients. *ACS Energy Letters*. 1 (1), 283-289. Available from: doi: 10.1021/acsenerylett.6b00150.

Lima, P. (2017) *LG Chem will introduce NCM 811 battery cells for EVs next year*. Available from: <https://pushevs.com/2017/09/08/lg-chem-will-introduce-ncm-811-battery-cells-evs-next-year/> .

Lithium Australia. (2018) *Investing in a Vertically Integrated Lithium Company*. Available from: <https://lithiumau.wpengine.com/wp-content/uploads/2016/11/30042018-General-Meeting-presentation.pdf>.

LME. (2018) *Cobalt Historical Price*. Available from: <https://www.lme.com/en-GB/Metals/Minor-metals/Cobalt> [Accessed April 4, 2018].

Mackenzie, K. (2017) *Why IEA scenarios should be treated with extreme caution*. Available from: <https://ftalphaville.ft.com/2017/05/24/2189189/guest-post-why-iea-scenarios-should-be-treated-with-extreme-caution/> [Accessed June 14, 2018].

Manthiram, A., Yu, X. & Wang, S. (2017) Lithium battery chemistries enabled by solid-state electrolytes. *Nature Reviews Materials*. 2 (3), 16103. Available from: doi: 10.1038/natrevmats.2016.103.

McEwen, B. (2017) *Lithium and Tesla: Electric Shock?* .

McKinsey. (2017) *The Future of Nickel: A Class Act*.

Mims, C. (Mar 18, 2018) *The Battery Boost We've Been Waiting for Is Only a Few Years Out*. *Wall Street Journal*. Available from: <https://www.wsj.com/articles/the-battery-boost-weve-been-waiting-for-is-only-a-few-years-out-1521374401> .

Nelson, P. A. & Gallagher, K. G. (2014) *Manufacturing Costs of Batteries for Electric Vehicles*.

Nelson, P. A., Gallagher, K. G., Bloom, I. D. & Dees, D. W. (2012) *Modeling the Performance and Cost of Lithium-Ion Batteries for Electric-Drive Vehicles - SECOND EDITION*. United States, USDOE Office of Energy Efficiency and Renewable Energy (EERE).

Netafim. (2018) *Mesh vs. Micron Comparison Chart*. Available from: <http://www.netafimusa.com/wp-content/uploads/2016/10/Mesh-vs-Micron.pdf>.

Neubauer, J. (2013) *Analysis of Electric Vehicle Battery Performance Targets*.

Neubauer, J., Pesaran, A., Bae, C., Elder, R. & Cunningham, B. (2014) Updating United States Advanced Battery Consortium and Department of Energy battery technology targets for battery electric vehicles. *Journal of Power Sources*. 271 614-621. Available from: doi: 10.1016/j.jpowsour.2014.06.043.

NiPERA. (2018) *Nickel Producing Industries*. Available from: <http://www.nipera.org/en/WorkplaceGuide/ProductionAndUse/NickelProducingIndustries.aspx> .

Nishio, K. & Furukawa, N. (1999) Practical Batteries. In: Besenhard, J. O. (ed.). *Handbook of Battery Materials*. Weinheim, Germany, Wiley-VCH Verlag GmbH. pp. 19-61.

Nissan. (2018) *Nissan Warranty*. Available from: <https://www.nissan.co.uk/ownership/nissan-car-warranties.html> [Accessed 8 June 2018].

Nitta, N., Wu, F., Lee, J. T. & Yushin, G. (2015) Li-ion battery materials: present and future. *Materials Today*. 18 (5), 252-264. Available from: doi: 10.1016/j.mattod.2014.10.040.

Noh, H., Youn, S., Yoon, C. S. & Sun, Y. (2013) Comparison of the structural and electrochemical properties of layered $\text{LiNi}_x\text{Co}_y\text{Mn}_z\text{O}_2$ ($x + y + z = 1/3, 0.5, 0.6, 0.7, 0.8$ and 0.85) cathode material for lithium-ion batteries. *Journal of Power Sources*. 233 121-130. Available from: doi: //doi.org/10.1016/j.jpowsour.2013.01.063.

Nozaki, H., Nagaoka, K., Hoshi, K., Ohta, N. & Inagaki, M. (2009) Carbon-coated graphite for anode of lithium ion rechargeable batteries: Carbon coating conditions and precursors. *Journal of Power Sources*. 194 (1), 486-493. Available from: doi: 10.1016/j.jpowsour.2009.05.040.

Nykqvist, B. & Nilsson, M. (2015) Rapidly falling costs of battery packs for electric vehicles. *Nature Climate Change*. 5 329. Available from: <http://dx.doi.org/10.1038/nclimate2564>.

O'Donovan, A. (2017) *The Global Electric Bus Market Gets Into Gear (Part 1 of 2)*. Bloomberg New Energy Finance.

O'Donovan, A. (2018) *The Global Electric Bus Market Gets Into Gear (Part 2)*. Bloomberg New Energy Finance.

Olivetti, E. A., Ceder, G., Gaustad, G. G. & Fu, X. (2017) Lithium-Ion Battery Supply Chain Considerations: Analysis of Potential Bottlenecks in Critical Metals. *Joule*. 1 229-243.

Patel, P. (2015) Improving the Lithium-Ion Battery. *ACS Central Science*. 1 (4), 161-162. Available from: doi: 10.1021/acscentsci.5b00223.

Perner, A. & Vetter, J. (2015) Lithium-ion batteries for hybrid electric vehicles and battery electric vehicles. In: Scrosati, B., Garche, J. & Tillmetz, W. (eds.). *Advances in Battery Technologies for Electric Vehicles*. pp. 173-190.

Pillot, C. (2017) *The rechargeable battery market 2016-2025*.

Plötz, P., Funke, S. A., Jochem, P. & Wietschel, M. (2017) CO₂ Mitigation Potential of Plug-in Hybrid Electric Vehicles larger than expected. *Scientific Reports (Nature Publisher Group)*. 7 1-6. Available from: doi: 10.1038/s41598-017-16684-9.

Reuters. (Jan 23, 2017a) China approves first list of green car models for subsidies this year. *Reuters*. Available from: <https://www.reuters.com/article/us-china-autos-electric-idUSKBN15712I> .

Reuters. (Aug 31, 2017b) S.Korea's SK Innovation starts production of batteries with more nickel. *Reuters*. Available from: <https://www.reuters.com/article/southkorea-skinnovation-battery/s-koreas-sk-innovation-starts-production-of-batteries-with-more-nickel-idUSL4N1LH25Y> .

Rybczynska, A. (July 6, 2018) China Responsible for 95% of Global E-Bus Sales to 2025: BNEF. *Bloomberg*.

- Sanderson, H. (August 24, 2018) SQM warns on lithium prices after following sector share slump. *Financial Times*. Available from: <https://www.ft.com/content/72ebf94c-a7b5-11e8-926a-7342fe5e173f> [Accessed August 26, 2018].
- Sandor, D., Fulton, S., Engel-Cox, J., Peck, C. & Peterson, S. (2018) System Dynamics of Polysilicon for Solar Photovoltaics: A Framework for Investigating the Energy Security of Renewable Energy Supply Chains. *Sustainability*. 10 (1), 160. Available from: doi: 10.3390/su10010160.
- Schmidt, O., Hawkes, A., Gambhir, A. & Staffell, I. (2017) The future cost of electrical energy storage based on experience rates. *Nature Energy*. 2 17110. Available from: <http://dx.doi.org/10.1038/nenergy.2017.110>.
- Schmich, R., Wagner, R., Horpel, G., Placke, T. & Winter, M. (2018) Performance and cost of materials for lithium-based rechargeable automotive batteries. *Nature Energy*. 3 267-278. Available from: <http://media.daimler.com/marsMediaSite/en/instance/ko/The-Mercedes-Benz-B-Class-Electric-Drive-Electric-driving-without-compromises.xhtml?oid=9905257>.
- Speirs, J., Gross, R., Contestabile, M., Candelise, C., Houari, Y. & Gross, B. (2014) *Materials availability for low-carbon technologies: An assessment of the evidence*. UK Energy Research Centre.
- Steinbuch, M. (2018) *Tesla Model S battery degradation data*. Available from: <https://steinbuch.wordpress.com/2015/01/24/tesla-model-s-battery-degradation-data/> [Accessed June 8, 2018].
- Stettler, M. (2018) *SEF09: Sustainable Transport Lecture 1*.
- Swanson, R. (2011) *The Silicon Photovoltaic Roadmap*. Stanford University Available from: <https://energy.stanford.edu/events/solar-energy-mini-series-silicon-photovoltaic-roadmap>.
- Syrah Resources. (2015) *Syrah Announces Internal Economic Assessment for Coated Spherical Graphite*.
- Syrah Resources. (2017) *Sales and Marketing*. Available from: http://www.syrahresources.com.au/application/third_party/ckfinder/userfiles/files/sales-and-marketing-presentation-april-2017.pdf.
- Thackeray, M. M., Wolverton, C. & Isaacs, E. D. (2012) Electrical energy storage for transportation—approaching the limits of, and going beyond, lithium-ion batteries. *Energy & Environmental Science*. 5 (7), 7854-7863. Available from: doi: 10.1039/c2ee21892e.
- The Economist. (2012) *Sunny Uplands*.
- UBS. (2017) UBS Evidence Lab Electric Car Teardown - Disruption Ahead? .
- UNFCCC. (2015) *Adoption of the Paris Agreement*.
- US DOE. (2017) *Cost and Price Metrics for Automotive Lithium-Ion Batteries*.
- US EIA. (2018) *Autonomous Vehicles: Uncertainties and Energy Implications*.
- USGS. (2018) *Mineral Commodity Summaries 2018*. Reston, Va, Dept.

Vaalma, C., Buchholz, D., Weil, M. & Passerini, S. (2018) A cost and resource analysis of sodium-ion batteries. *Nature Reviews: Materials*. 3 (18013), 1-11.

Verner, S. (2018) *Syrah Resources: In Production, Focussed on Value*.

Vidal, J. (Sep 22, 2015) The rise of diesel in Europe: the impact on health and pollution. *The Guardian*. Available from: <http://www.theguardian.com/environment/2015/sep/22/the-rise-diesel-in-europe-impact-on-health-pollution> .

wattev2buy.com. (2018) *Watt EV 2 Buy*. Available from: <https://wattev2buy.com> [Accessed June 27, 2018].

Winter, M. & Besenhard, J. O. (1999) Lithiated Carbons. In: Anonymous *Handbook of Battery Materials*. [e-book] Weinheim, Germany, Wiley-VCH Verlag GmbH. pp. 383-418.

Wood Mackenzie. (2017a) *Battery Demand Model*.

Wood Mackenzie. (2017b) *The challenges of nickel supply in an EV world*.

Wood Mackenzie. (2017c) *EV exuberance - tightening the cobalt supply chain*.

Wood Mackenzie. (2017d) *Lenders Report for Cobre Panama Project*. Wood Mackenzie.

Wood Mackenzie. (2018a) *Battery Raw Material Service - Long-Term Outlook: Demand - H1 2018*. Wood Mackenzie.

Wood Mackenzie. (2018b) *Global nickel long-term outlook*. Wood Mackenzie.

Wood Mackenzie. (2018c) *Lithium Multi-Client Study*.

Wright, T. P. (1936) Factors Affecting the Cost of Airplanes. *Journal of the Aeronautical Sciences*. 3 (4), 122-128. Available from: doi: 10.2514/8.155.

Yoshino, A. (2014) Development of the Lithium-Ion Battery and Recent Technological Trends. In: Anonymous *Lithium-Ion Batteries : Advances and Applications*. pp. 1-20.

Zimmermann, N. (Feb 26, 2018) Move is on to ban diesel cars from cities. *DW*. Available from: <https://p.dw.com/p/2tMSR> .